UNIVERSITY OF SOUTHAMPTON

FACULTY OF MEDICINE, HEALTH AND LIFE SCIENCES

Biomolecular Sciences

Liver Fatty Acid Binding Protein; Relating Structure to Function

by

Robert Mark Hagan

Thesis for the degree of Doctor of Philosophy

September 2004

DECLARATION OF AUTHORSHIP

I, Robert Mark Hagan declare that the thesis entitled 'Liver Fatty Acid Binding Protein; Relating Structure To Function' and the work presented in it are my own. I confirm that:

- This work was done wholly or partly while in candidature for a research degree at this University;
- Where any part of this thesis has been submitted for a degree or any other qualification at this University or any other institution, this has been clearly stated;
- Where I have consulted the published work of others, this is always clearly attributed;
- Where I have quoted from the work of others, the source is always given. With the exception of such quotations, this thesis is entirely my own work;
- I have acknowledged all main sources of help;
- Where the thesis is based on work done by myself jointly with others, I have made clear exactly what was done by others and what I have contributed myself;
- Parts of this work have been published as:

Hagan, R.M.; Davies, J.K. and Wilton, D.C.; Mol Cell Biochem (2002) **239** (1-2); 55-60
Davies, J.K.; Hagan, R.M. and Wilton, D.C.; J Biol Chem (2002) **277** (50); 48395-48402

Signed.....

Date.....

Acknowledgements

I would like to acknowledge the following:

Prof. David Wilton as supervisor of this project

University of Southampton for funding

Neville Wright and Paul Skipp for assistance with Mass Spectrometry analysis

Jane Worner-Gibbs for providing data from urea-tryptophan mutants unfolding studies, and for production of the portal region tryptophan mutants

Prof. Mike Gore for use of the CD machine

Dr.Joanne Davies for providing the single and double charge reversal mutants

All of the members of Prof David Wilton's research group past and present; namely Dr. Stephen Beers, Dr. Andrew Buckland, Dr. Suzanne Edwards, Dr. Niroshina Silva and Charles Birts

UNIVERSITY OF SOUTHAMPTON

ABSTRACT

FACULTY OF MEDICINE, HEALTH AND LIFE SCIENCES
BIOMOLECULAR SCIENCES

Doctor of Philosophy

LIVER FATTY ACID BINDING PROTEIN; RELATING STRUCTURE TO FUNCTION

By Robert M. Hagan

Liver Fatty Acid Binding Protein (LFABP) is a member of a family of small (14 kDa) intracellular proteins that reversibly bind fatty acids. This binding greatly enhances their aqueous solubility and thus facilitates their transport. The Fatty Acid Binding Proteins (FABPs) are characterized by a β-barrel containing the binding cavity of the protein and a helix-turn-helix motif that caps the protein.

LFABP is known to bind to anionic phospholipid vesicles under conditions of low ionic strength, resulting in ligand release from LFABP. The interaction of LFABP with anionic phospholipid vesicles involves K31 of α-helix II. Studies on adipocyte and heart FABP that had previously identified the α-helical region as being important for electrostatic interactions between these proteins and the phospholipid interface.

In this investigation the involvement of cationic α-helical residues (K20, K31 and K33) in ligand binding and residues contributing to the positive surface charge of the protein (K36, K47 and K57) in ligand binding and interaction with phospholipid vesicles has been studied by using charge reversal mutagenesis to convert these residues to glutamate. It was found that the three residues that made the largest contribution in terms of ligand binding and in regards to the protein's interaction with phospholipid vesicles were K31, K36 and K57. These residues are positioned around the hypothesized portal region of LFABP.

The tryptophan insertion mutants of LFABP, L28W, Y54W and M74W, were produced. Ligand binding studies highlighted L28W as a mutant that demonstrated dramatically enhanced fluorescence on fatty acid binding. Detailed studies of the mutant made it possible to show co-operative binding of oleic acid to LFABP and to carry out direct competition assays between oleic acid and oleoyl CoA. These competition assays found that these two ligands have similar affinities in terms of binding to LFABP, a result that is important in assigning the role of LFABP within the cell. A further tryptophan mutant Y7W, has been used to investigate the conformational change at the protein's N-terminal region. Complementing previous studies with the mutant F3W.

The binding of lithocholic acid derivatives to charge reversal and tryptophan containing mutants allowed the orientation of conjugated bile acids within the binding cavity to be determined.

Contents

List of Figures

Chapter Seven – General Summary and Future Work

List of Tables

Chapter 1 - Introduction

1.Introduction

1.1 Fatty Acid Binding Protein

Fatty acid binding protein (FABP) was first reported by Ockner *et al.* over 25 years ago [1]. Since the initial discovery around twenty of these proteins that can reversibly and non-covalently bind fatty acids have been identified. This binding greatly enhances their aqueous solubility and thus facilitates their transport. The intracellular fatty acid binding proteins are one of the most widely studied classes of proteins used for investigating protein-lipid interactions. They are low molecular mass cytosolic proteins that bind fatty acids amongst other non-polar ligands. Although there are many polypeptides capable of interacting with lipids, the FABPs differ from these other proteins by way of their conserved β-barrel fold, a four exon-three intron gene motif, and their molecular association with monoacyl lipids such as fatty acids. FABPs are the major component of a larger group of proteins known as the intracellular binding proteins that also include retinol, retinoic acid and bile acid binding proteins. Intracellular lipid binding proteins (iLBPs) typically have a sequence of about 130 residues and a molecular mass of around 14kDa. These proteins have been found in eukaryotes as diverse as sharks [2] and chickens [3]. These proteins enhance the uptake of their respective ligands from the extracellular medium.

The FABP β-barrel, displayed in **Fig 1.1**, is made up by an arrangement of ten

β-strands identified as βA through to βJ, these strands vary in length from four to ten amino acids. The strands are connected by tight turns except for the first two where they are separated by a helix-turn-helix motif. Each of these strands is in an antiparallel arrangement and each strand forms hydrogen bonds to the two adjacent strands to form a

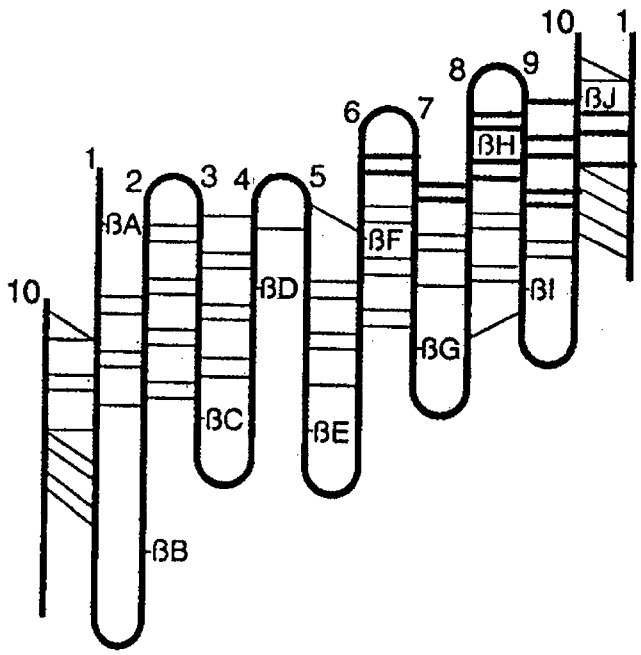

Fig 1.1 The LBP β barrel, showing the 10 β strands of a typical iLBP
Strands 1 and 10 are repeated so that the closing of the β barrel is also depicted. Hydrogen bonds linking the labeled β strands are indicated by the horizontal lines (Banaszak *et al*) [4]

contiguous β sheet. Thus, strand x forms hydrogen bonds with both strand (x+1) and strand (x-1). Each strand forms between ten and seventeen hydrogen bonds. One assumption is that the hydrogen bonding framework found in the mainchain is co-operative. The β-barrel description is not perfectly accurate as the hydrogen-bonding network is interrupted between strands D and E, as shown in **Fig 1.2**. The distance here is too great for hydrogen bonding to occur. Instead the side chains intercalate to form a closed system in combination with ordered water molecules. In the tertiary structure the

first and tenth β strands of FABP also hydrogen bond to form a β-barrel with a characteristic twist. The first and tenth β-strands are able to bind because of a bulge in βA. The cylinder is closed off at one end by a helix-turn-helix motif that exists between β-strands A and B. The helix-turn-helix motif is believed to be the structure that caps the protein. FABPs typically have dimensions of 25x35x40Å giving them a more flattened appearance. This flattened appearance explains why the proteins are also commonly referred to as β-clams. This β-clam structure remains in the absence of ligand and in this case the ligand is replaced in the central cavity by six ordered water molecules.

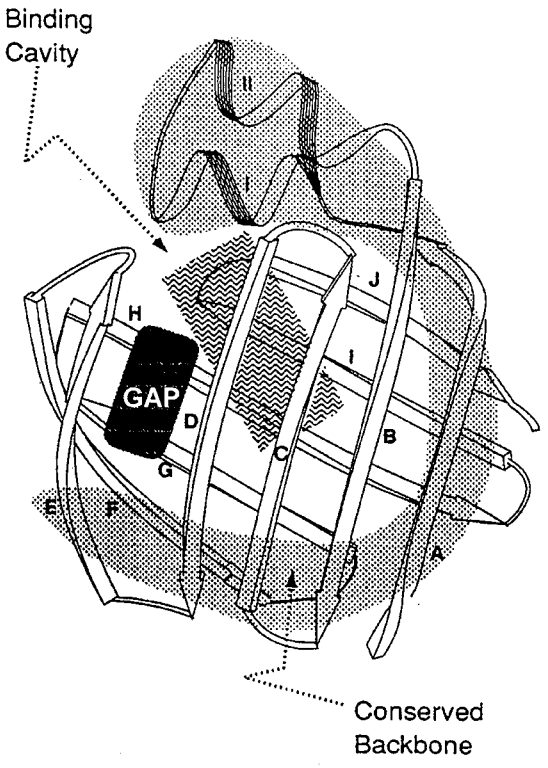

Fig 1.2 A representation of the iLBP conformation. The secondary structural components of iLBPs are represented by that of ALBP (Adipocyte LBP), with arrows for β structure and a coil for α helices. The two α helices (I and II) are near the amino terminus. Strands are labeled from A to J. Three important structural features are also highlighted: the gap between β strands D and E, the internal binding cavity, and the "backbone", where most of the conserved amino acids are located. Banaszak *et al.* [4]

iLBPs bind the hydrophobic ligand in a cavity rather than a cleft. FABP has a large interior cavity, in all known iLBPs this cavity is filled by ordered and disordered water molecules. This cavity is lined by a series of polar and hydrophobic amino acids; the side chains of these residues extend into the cavity. The specific amino acids that line this cavity are highly varied between members of the iLBP family, this variability is consistent with the low conservation of amino acid residues throughout FABPs (20-70%). The cavity volume can vary from 300 to 700 $Å^3$ between different forms of FABP. Variations in the size of the β-barrel are due to differences in length and number of β-strands as well as the size of the individual amino acids making up each strand. The cavity occupies a mere 5% of the entire protein volume. So although these proteins are characterised as β-barrels their actual interior volume is quite small. A typical ligand for this family of proteins occupies between one half and one third of the total binding cavity volume.

FABPs have ordered water molecules within the cavity, some of which are within van der Waal's contact distance of the bound fatty acid. Upon ligand binding there occurs a loss of typically disordered but not ordered water molecules from the binding cavity. The cavity is not connected to the solvent by any obviously large opening. Helix α-II and loops connecting the β-strands C/D and E/F, form a small opening that allows ligand to enter the cavity, this opening is referred to as the portal region. The current model for ligand binding to the FABPs envisages this portal at the top of the barrel opening, allowing a hydrophobic ligand to enter the cavity.

In all crystallographic studies undertaken so far, the polar head group of the lipid is positioned deep at the bottom of the cavity in the holoprotein. All existing evidence points to the binding cavity and the poorly delimited 'portal' region as defining the specific function of each individual member of the FABP family. It is the local structure within the cavity that appears to be the major factor determining binding affinity and specificity for the lipid.

In general, enthalpic considerations outweigh the entropic contributions when considering ligand binding to FABP. It is common that 60-80% of the total binding energy is derived from enthalpic factors. Enthalpic factors arise from a combination of electrostatic interactions at the head group and van der Waal's forces along the acyl chain [5].

Liver FABP (LFABP) shares an amino acid identity with other iLBPs of between 18% for epidermal fatty-binding protein (E-FABP) and 38% for intestinal fatty acid binding protein 2 (IFABP2), liver FABP having the lowest sequence identity amongst the FABP family. LFABP was originally isolated from rat liver cytosol and has been identified in numerous cell and tissue types. These include the stomach, pancreas, adipose deposits, myocardium, small and large intestine and kidney. LFABP is expressed in hepatocytes, jejenul and ileal enterocytes, colonocytes and proximal tubules of the kidney. In the small intestine LFABP is expressed in particularly high concentrations in the tips of the villi where it can account for up to 5% of the soluble protein. In the liver LFABP comprises 5% of the cytoplasmic proteins. The tissue expression of FABP is

normally specific to a single tissue or cell type, LFABP along with Heart FABP (HFABP), is unusual in that it displays multi-tissue expression. The structure of LFABP in the presence of ligand (the holoprotein) has now been solved at low resolution [6]. A comparison of LFABP with the crystal structures of the other members of the FABP family reveals the same basic skeleton. LFABP is 127 amino acid residues in length including the initiating N-formyl-methionine and the protein has a mass of 14, 272 Da. LFABP is the member of the FABP family that has been investigated most thoroughly in terms of ligand-binding properties. LFABP is unique amongst the FABP family in that it is capable of binding fatty acid ligand in a stoichiometry of two moles of fatty acid to just one mole of protein (see **Fig 1.4** and **Fig 1.5**).

1.2 The Structure of LFABP

LFABP is found in a wider range of tissue but has a very similar overall structure to the other members of the FABP family. The LFABP structure displays (a) an anti-parallel β-barrel with an internal cavity; (b) a gap between β-strands D and E; (c) a lid or portal to the cavity for ligand entry, this is formed by the hairpin turns connecting β-strands C and D, D and E, G and H and a helix-turn-helix; (d) a cavity lined with polar and nonpolar residues and filled with water.

In all other existing FABP family members a comparison of hydrogen bonds shows that ten β strands form the β-barrel, LFABP is an exception with eleven β strands [7]. LFABP has a second gap in the hydrogen bonding network as shown in **Fig 1.3**, this

is found between βF and βG. At least four interstrand hydrogen bonds are absent and this causes βF to be assigned two βstrands, βF' and βF" instead of one. Furthermore the

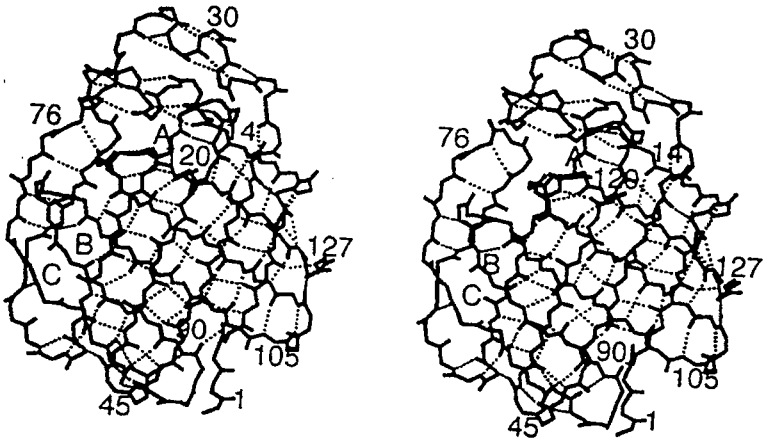

Fig 1.3 The stereodiagram shows the β-barrel framework with mainchain hydrogen bond as observed in the crystal structure of L-FABP. The hydrogen bonds are represented by the dotted connections and the stick model contains only mainchain atoms. The letter 'A' is placed in the stereodiagram in the approximate region of the portal. The letter 'B' is the gap found in all of the iLBP family members between βD and βE. 'C' marks a smaller gap only present in LFABP. (Thompson *et al.*) [8]

neighbouring β-turn joining βG and βH is two residues shorter than average for the iLBP family. The function of this gap is unknown; it does not add any significant volume to the cavity, but it may allow for increased conformational motion.

The binding cavity is well described as an empty vessel. The volume of this vessel is defined as either the van der Waal's surface of all the component atoms or more commonly as the space available to be filled by other atoms, such as fatty acids in the case of the iLBP cavity (shown in Fig 1.4). For iLBP the first definition gives a value that would be double a value given by the latter.

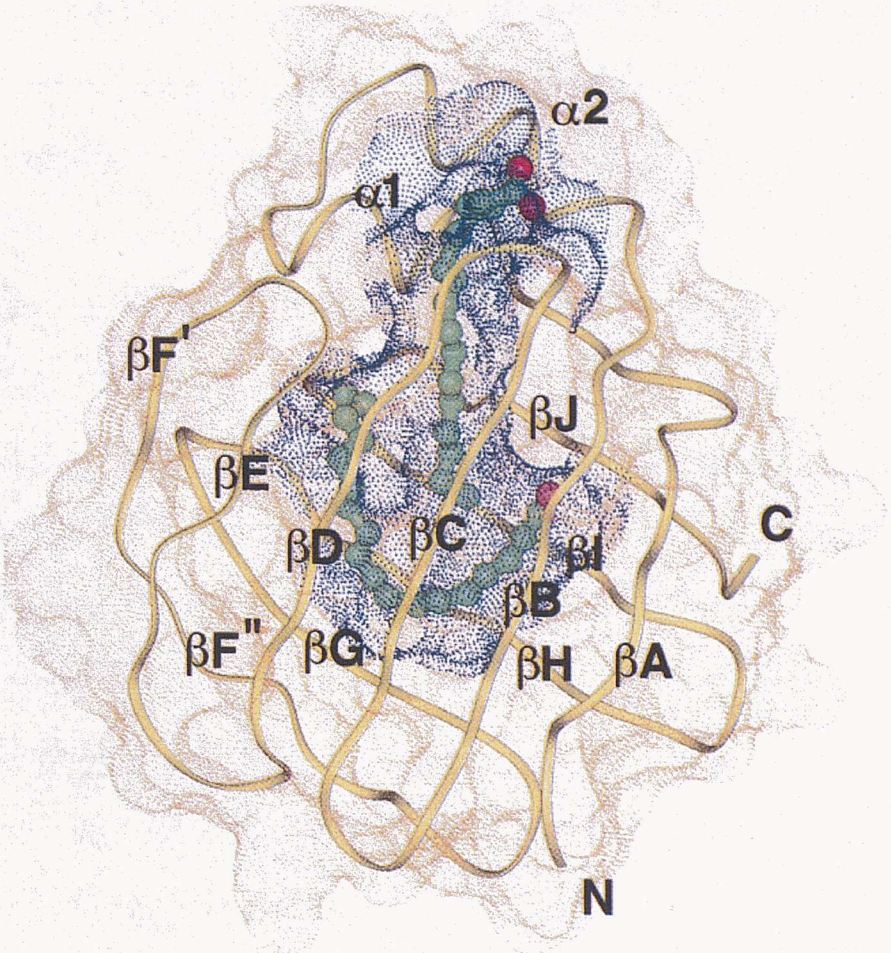

Fig 1.4 The crystal structure and cavity location of LFABP. The mainchain conformation of LFABP is shown by the yellow tube-like representation. Each of the elements of secondary structure is labeled. The blue dot surface is generated by illustrating every LFABP atom within 4.5 Å of any atom in either of the bound oleate molecules. The surface that was not identified as in close contact to oleate is shown as a buff to brown dot surface, illustrating the exterior of the molecule. The two oleic acid molecules bound to LFABP in the crystal structure are shown by the green and red spheres. [9]

A combination of the protein molecules and a series of ordered and disordered cavity water molecules construct the lipid-protein interface[9]. The weak bonding of the water molecules to each other means that it is possible for the protein to have a high degree of internal flexibility. The effect of this water combined with the van der Waal's interactions between methylene carbons is likely to make a significant contribution to the

enthalpy associated with ligand binding. These two factors may also account for the lack of specificity in lipid binding by FABPs that have a wide variety of non-polar ligands, such as LFABP.

The side chains within the cavity are not all hydrophobic, indeed in LFABP only 48% of the cavity is believed to be hydrophobic residues, 52% are charged polar amino acids [8]. Such a situation is however explainable. Charged atoms are not necessarily in physical contact with the bound ligand's hydrocarbon tail because even ionisable side chains have methylene carbons. The LFABP ligand binding site is more hydrophobic than the other lipid binding proteins. The side chains must also be involved in forming the water networks. A combination of the water molecules and side chains in the cavity are likely to be important in determining ligand specificity, defining lipid conformation and contributing to the overall binding energy.

The cavity is the lipid binding site and in all crystallographic studies the polar head group of the fatty acid was found to reside at the bottom of the cavity in the holoprotein. ^{13}C NMR had shown this is not the case for both ligands in LFABP, where the carboxylate group of one of the fatty acids has a normal pK_A and is exposed to the solvent. This was confirmed by the crystal structure of LFABP with two oleic acid molecules bound. Further to this, fluorescence quenching studies using 2-bromopalmitate have shown that a fatty acid carboxylate is close to the tryptophan residue in the mutant LFABP protein F18W [10].

The presence of a portal near the helical lid to allow ligand entrance has been suggested by the crystal structure of LFABP that is available. Such a portal may have a major role in defining the different functions of the FABP family members. This portal has been visualised as a small opening in the molecular surface in the region of αI, αII and the turns βC-βD and βE-βF. A fluorescence change in an F3W LFABP mutant protein showed that the βA chain has the potential to be destabilised to a small degree, before the rest of the β-clam structure and the α-helical portal domains unfold. The latter step was also evident at F18W (portal) and C69W (β-clam) regions. The following reaction scheme was proposed [10]:

Native → Intermediate 1 (β-A chain) → Intermediate 2 (Portal & βclam)

→ Unfolded

The hypothesised preferential portal described above would regulate fatty acid passage to and from the cavity. The amino acid residues that define the opening in rat LFABP are Leu-28 and Lys-31 of α-helix 1, Asp-34 which immediately follows this helix and Ser-56 and Lys-57 of the βC-βD turn.

The solvent accessible volume of the ligand binding cavity is estimated to be around 610Å^3. LFABP has the largest lipid cavity of the ten family members that have been measured, exceeding the next largest by 26% in volume and 20% in terms of surface area. Intestinal Fatty Acid Binding Protein (IFABP) for example, has an accessible volume of just 353Å^3. The individual dimensions of the LFABP lipid-binding cavity have

also been calculated using the GRASP program, which found the dimensions of the cavity to be like a flat rectangular box at 13x9x4Å. The portal region is linked to the corner of this cavity 'box' by a channel of about 10Å in length and 3-4Å in width [8].

1.3 Fatty Acid Binding and Targeting to Membranes

The most commonly studied ligands for LFABP are the fatty acids. One bound fatty acid is orientated inwards whilst a second is orientated with the carboxyl group of the ligand facing outwards. These endogenous ligands are most likely to bind if they are sixteen to twenty-two carbon atoms in length, although other ligands and carcinogens bind with lower affinity.

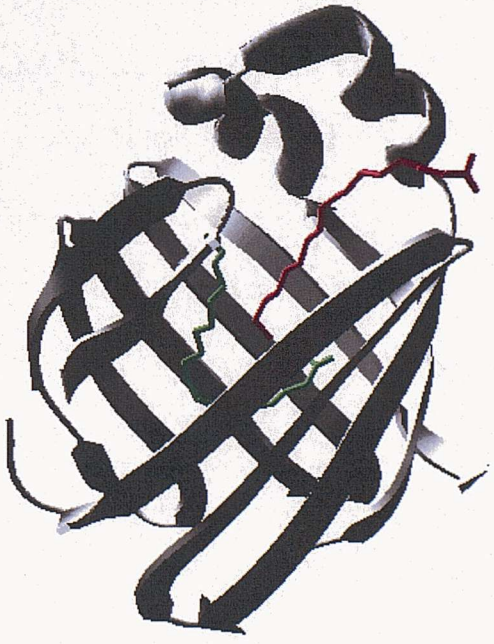

Fig 1.5 Structure of LFABP with two bound oleic acid molecules based on the crystal structure of Thompson *et al.* [11], Rasmol was used to design this image

When two oleic acid molecules bind, as shown in the crystal structure (**Fig 1.5**), they occupy nearly all the cavity space formed by the β-barrel and also appear to stabilise the protein. One fatty acid is positioned in a U-shaped conformation and is at a lower point within the cavity. This is referred to as the primary binding site (or site 1) and the ligand is referred to as oleate 129 in the crystal structure. This U-shaped conformation is common to all members of the FABP family and is facilitated by the C9=C10 double bond, and the C13-C14 single bond. The carboxylate head group of this particular fatty acid is involved in a hydrogen bond network with three of the six bound water molecules. Also a fourth water molecule is within van der Waal's contact distance of the hydrophobic acyl chain. Arg-122 appears to also have a major enthalpic contribution to the binding energy for this site. Indeed mutation of Arg-122 to Ala or Glu reduces the binding affinity of this site by two to four-fold. Mutation to Lys has less of an effect [12]. The reason that the Arg-122 mutants show a reduction and not a loss of binding is probably due to the fact that in the crystal structure Arg-122 is one of several polar residues interacting with the carboxylate head group at the primary binding site. As fatty acid methyl esters and monolein (molecules closely related to fatty acids whose carboxylic acid groups have been converted to uncharged functional groups) are not bound by FABP (Meyjohann and Spener sited in [13]), the interaction of the negatively charged head group of the ligand must be important for the binding process. It is likely that this important ionic interaction takes place at the surface of the protein. This argument is supported by Thumser *et al.* who showed that mutation of Arg-122 and Arg-126 affected the affinity of the protein for ligand [14].

The second molecule (referred to as oleate 128) is both more extended and is also found in an inverted conformation compared to ALBP [8]. This second molecule has its hydrocarbon tail in the space between the limbs of the 'U' formed by the first ligand and binds at the secondary binding site (or site 2). As the atoms of the two oleates interact, their binding energies are linked, achieving co-operativity. The hydrogen bond network for the lower, U-shaped oleate carboxyl head group is more extensive than that for the second bound oleic acid molecule. The cavity residues involved in the primary site bonding network include Arg-122 (discussed above), Ser-39 and Ser-124. The second bound oleate has its carboxylate group positioned away from the cavity and near the residues that form the portal. NMR studies and pKa measurements for the carboxylate suggested that it is solvent exposed [15], this was confirmed in the crystal structure **(REF)**. The hydrogen bond network for this second oleate involves Lys-31, Tyr-54, Ser-56, Asp-88 and a bound water molecule. The affinity for the second oleate is mainly attributable to entropic factors, due largely to displacement of water. The second site has a slower k_{on} rate [16]. The more internalised primary site needing to bind fatty acid first possibly explains this.

The two oleic acid molecules do not completely fill the cavity; they leave room for six bound water molecules. Aside from their role in the hydrogen bonds outlined above, they also form hydrogen bonds with the interior hydrophilic residues. The water molecules are also likely to affect ligand affinity and play a structural role. NMR and fluorescence evidence indicates that in LFABP the fatty acid carboxylate is more

accessible to bulk solvent than in other FABP family members [17]. This suggests that the role of water in ligand binding to LFABP may be different than for other iLBPs.

The second ligand is more solvent exposed. The oleate exposed to the surface of the protein is in contact with the deeply bound oleate and residues Leu-28, Gly-32, Ile-35, Ile-52, Tyr-54, Gly-55, Lys-57, Met-113 and Arg-122. Chemical modification or a mutation in this area affects the protein's binding affinity and kinetics. As the outermost binding site interacts with the innermost it would be logical to conclude that an ordered binding mechanism is involved. In actual fact the crystallographic data may even suggest that the second site does not exist until the first ligand is bound, however this is not consistent with recent NMR data that indicates that a molecule of oleate can exchange between the two sites [18].

The dissociation constants for the two sites have been calculated. The primary site has K_d between 0.009 and 0.2μM, the secondary site has K_d between 0.06 and 4.0μM [13;19]. The affinities for these binding sites have been shown to vary between five and twenty fold at temperatures below 37°C. Above 37°C the affinities converge towards equal values. The temperature at which the affinities of the two sites become equivalent depends on the fatty acid; higher temperatures (45-50°C) are required for the unsaturated fatty acids and myristate than for the longer chain saturated fatty acid (<37°C) [16]. For all fatty acids k_{off} values for dissociation from both sites are similar. This indicates that binding affinity differences at low temperatures reflect low on-rates for binding to the low affinity sites. Large specific heat capacity changes have been observed on fatty acid

binding to the high affinity site [16]. The thermodynamics of this binding indicate that a large negative heat capacity partners ligand binding in LFABP. Such a large negative heat capacity points to conformational changes occurring upon ligand binding. However, CD spectra for the apo and oleate bound LFABP and the small 2-3% reduction in Tyr anisotropy upon fatty acid binding in this same study are both inconsistent with a significant conformational change [16].

A similar heat capacity change has been observed in the interaction of Na^+ with thrombin [20]. As there was no detectable conformational change in the thrombin structure it was suggested that the large specific heat capacity change may be due to increased water binding to the protein upon Na^+ binding, causing a loss of entropy. However, results for other FABPs indicate that the binding cavity of the apo proteins contain large numbers of ordered and disordered water molecules. Upon fatty acid binding to these FABPs several of these waters, including some of the ordered water molecules in the case of IFABP, are displaced from the cavity [4;21]. Therefore either LFABP stands on its own in that the number of highly ordered water molecules increase upon fatty acid binding, or another mechanism is required to explain the specific heat capacity measurements discussed above. Further evidence for such a conformational change was provided by the crystal structure. This showed that the side chain of Met-74 that is positioned just 3.0Å away from the ω terminus of the oleic acid bound at site 1, has a degree of ambiguity as to its position in the latter stages of refinement.

It has been proposed that the rate of dissociation of long chain fatty acids from phospholipid bilayers is sufficiently rapid not to require a protein-mediated event [20;22]. A soluble FABP could then take up such an aqueous phase fatty acid (see **Fig 1.6a**). The transfer of a long chain fatty acid from a complex with a binding protein back to a membrane environment may be less favourable however, due to a high affinity of FABP for the long chain fatty acid. A collissional mechanism involving FABP binding to a membrane could facilitate this process (**Fig 1.6b**). As FABPs have a high affinity for fatty acids it is unlikely that release of ligand by diffusion would be sufficient to allow for targeting of fatty acids to membranes. In a collisional mechanism the fatty acid still binds to the protein with high affinity, however the protein then binds to the membrane bilayer causing a conformational change in the protein that lowers its affinity for the ligand and the ligand is then released. Such a process has been advocated for intestinal, muscle, and adipose FABP where model fluorescence studies have led to the proposal of a collisional mechanism for explaining the FABP-mediated transfer of fatty acids between phospholipid membranes and vesicles (reviewed in [23]). In these studies the rate of transfer of fluorescent Anthroyloxy Fatty Acid (AOFA) analogues from the FABP to vesicles containing a fluorescence quencher was monitored using stopped-flow fluorescence. However, such a process was not observed for LFABP under the same conditions where it is proposed that ligand transfer between the membrane and protein occurs by aqueous diffusion. AOFA transfer rate from phosphatidylcholine containing vesicles to LFABP in TRIS-HCl buffer containing 150 mM NaCl and 0.1mM EDTA, was similar to that observed with intermembrane n-(9-anthroyloxy) fatty acid transfer, a diffusional process [24].

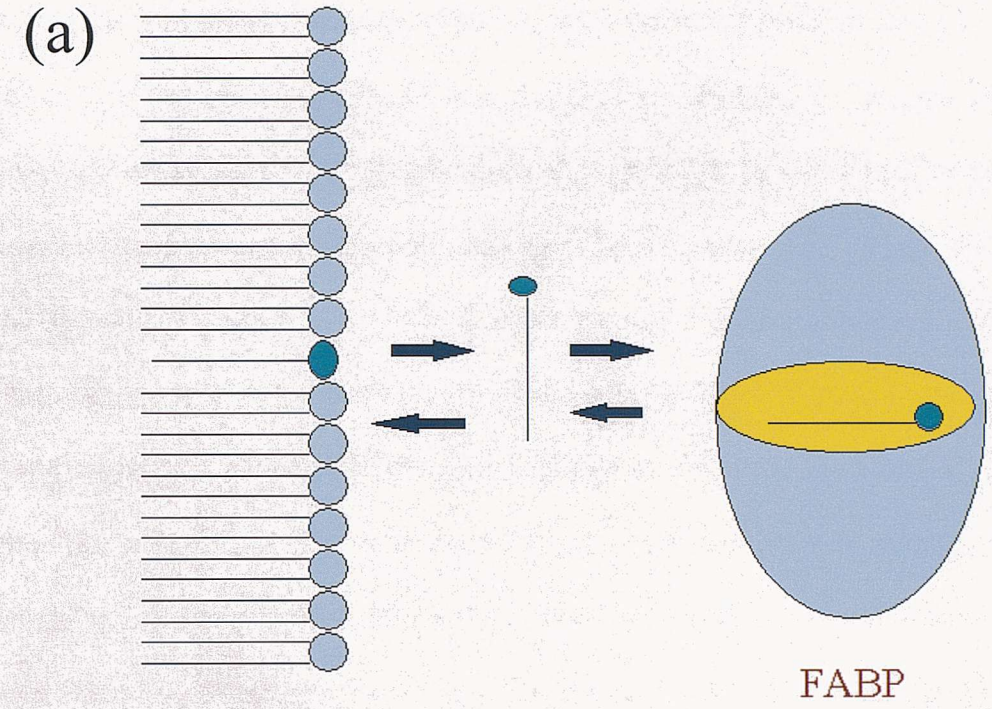

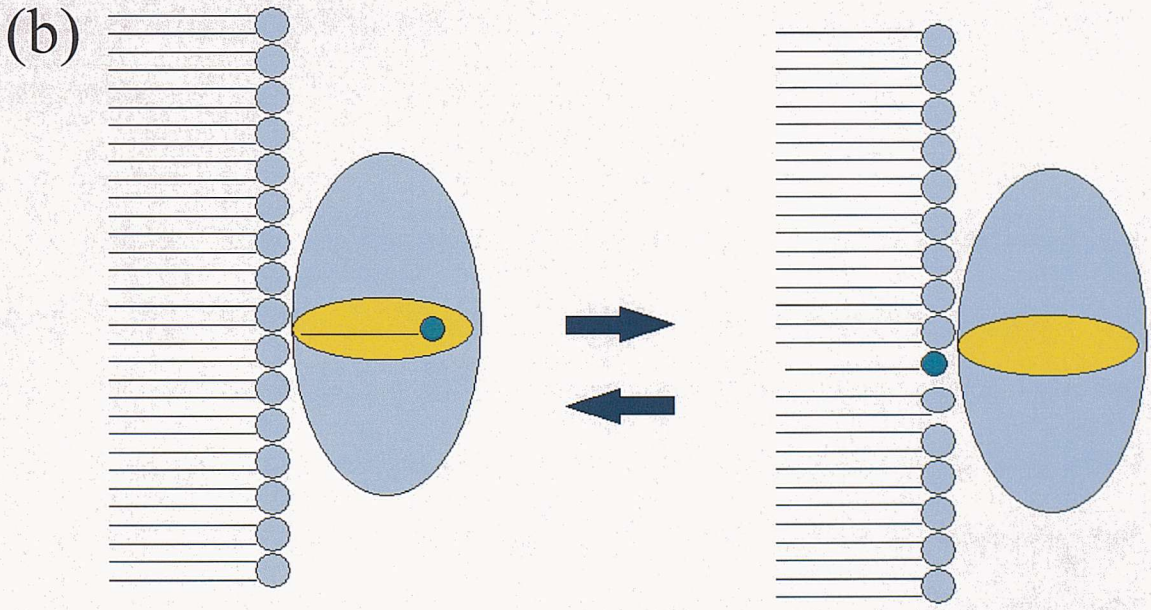

Two hypothesized ligand transfer mechanisms between LFABP and the phospholipid bilayer. Ligand transfer by aqueous diffusion between protein and membrane (a). Ligand transfer by a collisional mechanism (b).

The collisional mechanism for ligand release may occur with LFABP in the presence of phospholipid vesicles that contain a significant proportion of anionic phospholipids at conditions of low ionic strength [25]. In this equilibrium assay, the release of the fluorescent fatty acid analogue DAUDA from recombinant rat liver FABP was found to occur at low ionic strength, in the presence of phospholipid vesicles containing a significant proportion of anionic phospholipids. This is supported by recent Fourier transform infrared (FT-IR) spectroscopy, monolayers at air-water interface, and low angle X-ray diffraction, which also found LFABP to bind to anionic phospholipid vesicles at low ionic strength, but not at 0.1 M NaCl. In the same study X-ray diffraction experiments indicated that the binding of LFABP produces a rearrangement of the membrane structure, increasing the interlamellar spacing and decreasing the compactness of the lipids [26]. Interestingly LFABP overexpression has been shown to increase the targeting of long chain fatty acids and long chain fatty acyl CoAs into the nuclear membrane [27;28].

Although the interfacial mechanism of ligand release has not been determined it is clear that if LFABP does interact with microsomes and anionic phospholipids to release ligand, then the positive electrostatic field surrounding LFABP should play an important physiological role. Such a phenomenon would also involve non-polar interactions because once the LFABP is bound to anionic vesicles it is only partly released by high salt, although high salt prevents the initial interactions [25]. The residues in rat LFABP most responsible for creating a positive potential are Arg-122 within the cavity, and Lys-31, Lys-36, Lys-47, Lys-57 and Arg-126 on the surface. This positive surface region

interestingly, covers a region where an unknown molecule was found in the crystal structure [9]. The interactions involved in binding of this unknown molecule included the mainchain nitrogens of Asn-14, Phe-15 and Glu-16 and the positive helical dipole of α helix I, suggesting the unknown molecule has anionic properties. The authors speculated that this density might suggest an exterior binding site for fatty acids. In addition to positive regions, F3W and F18W mutant studies suggest that the amino terminal region of the protein is involved as there is a large change in the fluorescence of the F3W mutant on binding to anionic vesicles [25].

The reported rate of DAUDA release from LFABP at the phospholipid interface ($23s^{-1}$) would be consistent with partial unfolding of LFABP at the anionic interface [25]. This mechanism may make it possible for ligand to be released at the membrane surface so that membrane bound proteins such as acyl CoA synthetases are also able to further metabolise the fatty acids. The LFABP α helical domain is the obvious region that would be involved in ligand release induced by interactions with phospholipid membranes. This would be in line with previous work by Cistola *et al.* who showed that in the absence of α helices, ligand dissociation from IFABP was affected, their conclusion being that α helices control ligand transfer within the cell [29]. Furthermore it has recently been shown that the α-helical domain is responsible for the decreased rate of fatty acid transfer observed with LFABP relative to that of IFABP [30]. In addition to the portal region, experiments with F3W mutants suggested that there was a conformational change around the amino terminal region, this may be the generation of a second portal for allowing ligand to exit, see **Fig 1.7** [25]. In the discussion about the crystal structure of the first

FABP to be solved, IFABP, the authors highlighted a potential portal in this region but which was occluded by amino acid residues. Hence a significant conformational change was required to open this potential portal in IFABP.

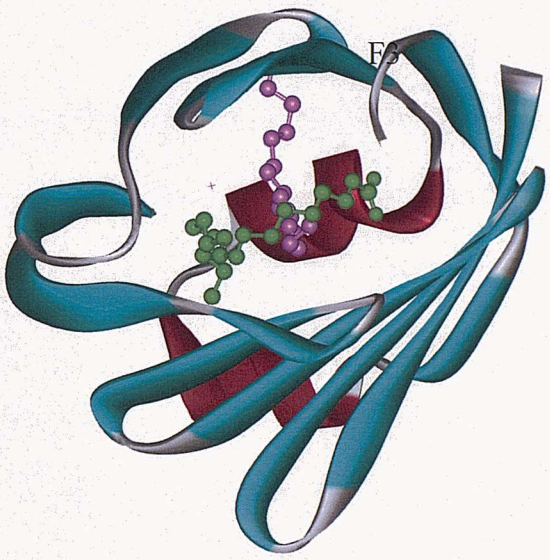

Fig 1.7 The potential second portal region for ligand exit. The protein structure is shown with oleic acid molecules bound at site 1 (green) and site 2 (pink) [11]

1.4 Multiple Ligand Binding and Multiple Roles for LFABP

1.4.1 Ligand Binding

LFABP is able to bind a large variety of ligands aside from fatty acids. LFABP will bind hydrophobic molecules much larger in size than the ligands that will associate with other iLBPs. It is these ligands that are considered in this section. The ligands that

have been documented thus far for LFABP include heme, acyl CoAs, fatty acids, lysophospholipids, warfarin and eicosanoids. The structures of these molecules can be found in **Fig 1.8**. At the same time, the fact that these other ligands bind means that LFABP may have a role involving these other ligands; some physiological possibilities are considered in **Fig 1.8**.

It is likely to be partially the effect of the water molecules and the van der Waal's interactions between the hydrocarbon chains that give rise to the lack of specificity of LFABP for ligands. The large size of the LFABP cavity further explains the ability of LFABP to bind a variety of more bulky non-anionic ligands, be it at lower affinities than long chain fatty acids. The wide range of ligands bound by LFABP has made it difficult to assign roles to the protein. However this multi-ligand binding has been helpful in studying the protein as well. The varied ligand binding properties has also made it possible to bind a number of artificial ligands to study the protein such as Bexafibrat, WY-14,643, tiadenol, warfarin, 11 (dansyl) amino-undecanoic acid (DAUDA) as well as certain carcinogens.

As stated above there are many natural ligands for LFABP these include heme, bilirubin, lysophospholipids, bile salts and prostaglandins as well as a host of other hydrophobic compounds such as acyl-CoA esters, bromosulphothalein, hexachlorophene and cyclopentanone. For the larger ligands it is generally agreed that the protein can only bind one molecule of ligand per molecule of protein. Competition binding assays show

Class	Structure	Potential Function(s)
Fatty acids(oleate)	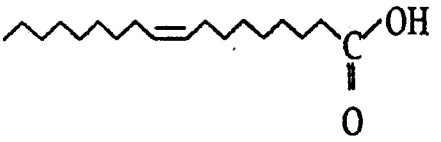	energy storage/ mobilization modulate enzyme function
Acyl-CoAs (palmitoyl CoA)	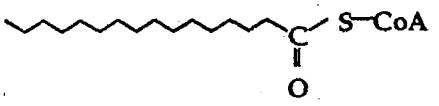	beta-oxidation
Eicosanoids (5-HPETE)	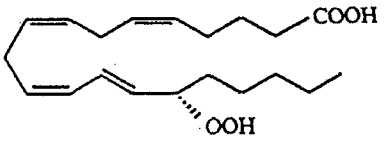	modulate enzyme function (inflammatory response)
Lysophospholipids (lysophosphatidyl- lethanolamine)	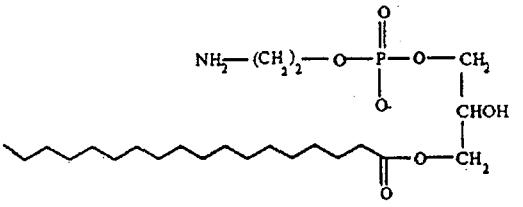	Signaling
Carcinogens (methylsulfone PCB)	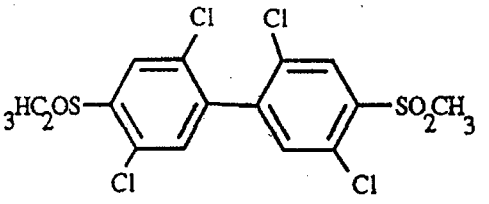	Detoxification
Anti-Coagulants (warfarin)	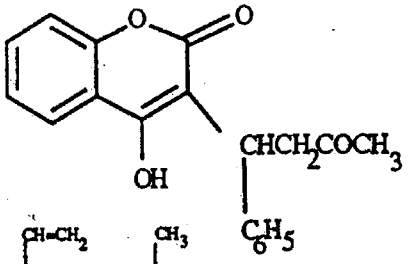	uptake/mobilization of warfarin
Heme	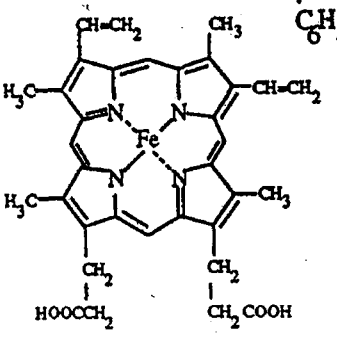	Heme catabolism

Fig 1.8 Ligands and correlative functions of liver fatty acid binding protein (Coe & Bernlohr) [5]

that both fatty acid binding sites are required to bind larger ligands [8]. It is questionable whether LFABP binds cholesterol. Nemecz and Schroeder put forward evidence that it does when they determined a K_d of 1.53μM. They also claim to have determined a stoichiometry of 0.47 mol/mol for rat LFABP in a Lipidex assay and a stoichiometry of 0.83 mol/mol of the same protein in a liposome assay [31]. Rolf *et al.* however, were unable to show any binding of cholesterol despite using a similar method [13]. The only real difference being that Rolf *et al.* carried out their experiments on bovine LFABP. These results could be explained in two ways. Firstly there may be some evolutionary difference between the proteins and although this seems unlikely it cannot be ruled out. Secondly, it may just be the problems that are associated with any cholesterol binding assay, in that cholesterol has a very low solubility. Unfortunately, no positive control for a cholesterol binding assay exists to determine a solution to this problem. There is disagreement about whether cholesterol binds to LFABP, but anionic cholesterol sulphate does bind [9]. One explanation for this could be that cholesterol sulphate binds to the secondary site and cholesterol binds to the secondary site only when the primary site is occupied by fatty acid.

1.4.2 Physiological Role of LFABP

The precise physiological role of LFABP has still to be determined. The most commonly accepted role for LFABP has it transporting through the cytosol and compartmentalising fatty acids, being effective at this by enhancing the aqueous solubility of the lipids. The capacity of FABP to release fatty acids to intracellular

membranes such as mitochondria and peroxisomes, makes this carrier function plausible. More specifically potential roles have been discussed in (a) fatty acid uptake and transport; (b) regulation of various fatty acid metabolic pathways; (c) protection of membranes against the deterioratory effects of high concentrations of fatty acid metabolites and fatty acids themselves. Such conditions may arise in disorders of fatty acid metabolism; (d) trapping, selection/sensing of specific types of fatty acid or of other lipophillic substances; (e) compartmentalisation of fatty acids and generation of high local concentrations of fatty acid; (f) it may be a co-factor for reactions in which fatty acids are substrates or regulators.

McCormack and Brecher have demonstrated that the presence of LFABP had a positive effect on the transport of radiolabelled oleic acid from multilamellar liposomes to rat microsomes separated by a capillary pore membrane in an equilibrium dialysis cell [32]. Noy and Zakim have reported with unilamellar vesicles and microsomes that the transfer of fatty acids was retarded by LFABP [33]. Thus at the present time the role of LFABP in transporting fatty acids between membrane components is not clear.

The localisation of the protein should be considered in assigning the role of LFABP. The protein has been found predominantly in tissues with an active fatty acid metabolism. Cytoplasmic FABP content is related directly to the capacity of tissues to oxidise fatty acids. LFABP is most abundant in the cytosol and is assumed to carry out its role here, however it is clearly of a small enough size to be capable of being located in the nucleus. Free fatty acids within the cell are apparently in equilibrium with a LFABP

binding site. This suggests that LFABP has a metabolic role as either a buffer or shuttle. The cytosolic concentration levels of LFABP are actually high enough for it to be suggested that the protein itself may act as a store of fatty acids [34]. In this respect it is of interest that LFABP binds unsaturated in preference to saturated fatty acids, although the fact that saturated fatty acids are more insoluble than unsaturated fatty acids may have affected some of the measurements. There is some debate as to the relative binding affinities of the protein for fatty acids and fatty acyl CoAs, and whether LFABP binds the two with similar affinities. Recent knockout studies have highlighted the importance of LFABP in fatty acyl CoA binding, reporting a 95% loss of binding in the soluble fraction of mouse livers in LFABP knockout mice [35]. The deletion of the LFABP gene does not lead to gross phenotypical changes in the subjects, most likely due to compensatory increased expression of proteins performing similar roles.

One area of current interest is that LFABP delivers ligands that activate Peroxisome Proliferator Activated Receptor (PPAR) α and γ receptors to the nucleus where an interaction between LFABP and PPARα is proposed [36]. Using a CAT reporter gene linked to PPAR α, enhanced activation of CAT by a wide range of long chain fatty acids that would also be ligands for FABP was observed. Moreover, a direct interaction between murine LFABP and murine PPARα was detected using pull-down assays and two-hybrid assays. Using a number of HepG2 clones expressing varying amounts of LFABP, a positive correlation between LFABP concentration in the cell and PPARα activation was demonstrated.

Recently, immunofluorescence studies have demonstrated that LFABP significantly colocalised with PPARα in the nucleus [28]. In addition, it was observed that the fluorescent nonmetabolizable 4,4-difluoro-5,7-dimethyl-4-bora-3a,4a-diaza-s-indacene (BODIPY) derivatives of long chain fatty acids and BODIPY long chain fatty acyl CoAs were also found in the nucleus. The targeting of these ligands to the nucleus was increased by overexpression of LFABP in these cells. Thus this study provides further evidence for a role for LFABP in delivering ligands to the nucleus and highlights a possible role for fatty acyl CoAs in regulating the PPAR system. However, Erol *et al.* found that LFABP was not required for the action of PPARα in fasting mice [37].

LFABP gene knockout studies should provide data that supports or refutes a direct role for LFABP in delivering ligands to the PPAR system. At this time one report has addressed this problem in fasting mice [37]. In this system they showed that LFABP was required to facilitate the high rates of fatty acid oxidation seen in fasting but lack of LFABP did not effect PPARα activation, indicating that LFABP does not have a role under these physiological conditions.

When considering the potential role for LFABP, note should be taken of physiological conditions where the protein has an altered level of expression. For example fasted rats have been shown to have an increased level of LFABP expression [5]. Secondly, hypolipidemic drugs of the peroxisome proliferator type like fibrates have also been shown to enhance LFABP expression [38].

Pathological conditions such as ischemia [39] alcoholism [40], diabetes [41], Reye's syndrome [42] and cancer [43;44] have all been associated with LFABP level abnormalities.

1.5 Aims

The primary aim is to investigate the relationship between structure and function in LFABP in such a way as to make it possible to propose a potential mechanism by which LFABP can target fatty acids and other ligands to membrane sites.

The experimental approach will use site directed mutagenesis and involve both charge reversal mutagenesis and tryptophan insertion mutagenesis. All mutants will be assessed both in terms of their interaction with anionic phospholipids vesicles and the effect of mutagenesis on ligand binding.

Chapter 2 – Materials and Methods

2. Materials and Methods

2.1 Materials

2.1.1 Chemicals List

All chemicals were purchased from Fisher Scientific (Loughborough, UK), Sigma-Aldrich Chemical Company (Poole, UK) and ICN (Thame, UK), except for the following specialist items.

11-(Dansylamino)-undecanoic acid (DAUDA)
Molecular Probes (Oregon, USA)

Expression plasmid pET 11A
Novagen (Wisconsin, USA)

Sepharose 4 Fast Flow
Amersham Pharmacia Biotech (Amersham, UK)

Wizard Plus SV Miniprep Kit
Promega, (Southampton, UK)

Pfu polymerase
Promega (Southampton, UK)

Dpn I restriction enzyme
Novagen (Wisconsin, USA)

2.1.2 Bacterial Strains

Escherichia coli-BL21(DE3)
Novagen (Wisconsin, USA)

XL-1 Blue Ultracompetent Cells
Stratagene (London, UK)

2.2 DNA Techniques

2.2.1 Site Directed Mutagenesis

Site directed mutagenesis to produce the single charge reversal mutants and the F3W and F18W LFABP mutants, had already been carried out by Joanne Davies in this laboratory using the Kunkel and PCR methods of mutagenesis [45;46]. The triple charge reversal mutant and the remaining tryptophan mutants under investigation in this thesis were produced by the QuickChange method of mutagenesis.

The QuickChange site-directed mutagenesis method uses miniprep plasmid DNA. The basic procedure starts with a supercoiled, a double stranded DNA vector with an insert of interest and two synthetic oligonuleotide primers containing the desired mutation.

2.2.2 Oligonucleotide Primers

Oligonucleotide primers used for construction of the single mutants were:

*F3W Primer: 5'-AAAAGAATTCCATATGAACTGGTCTGGTTAAATAC-3'

Y7W Forward Primer: 5'- CTTCTCTGGTAAATGGCAGGTGCAGTCTC-3'

Y7W Reverse Primer: 5'-GAGACTGCACCTGCCATTTACCAGAGAAG-3'

*F18W Forward Primer: 5'-GAAAATTCGAACCGTGGATGAAAGCCATGGGT-3'

*F18W Reverse Primer: 5'-ACCCATGGCTTTCATCCACGGTTCGAAGTTTTC-3'

*K20E Primer: 5'-TTCGAACCGTTCATGGAAGCCATGGGTCTGCCG-3'

L28W Forward Primer: 5'-GGGTCTGCCGGAAGACTGGATCCAGAAAGGTAAAG-3'

L28W Reverse Primer: 5'-CTTTACCTTTCTGGATCCAGTCTTCCGGCAGACCC-5'

*K31E Primer: 5'-GAAGACCTGATCCAGGAAGGTAAAGATATCAAA-3'

*K33E Primer: 5'-CTGATCCAGAAAGGTGAAGATATCAAAGGTGTT-3'

*K36E Primer: 5'-AAAGGTAAAGATATCGAAGGTGTTTCTGAAATC-3'

*K47E Primer: 5'-GTTCACGAAGGTAAAGAAGTTAAACTGACCATC-3'

Y54W Forward Primer: 5'-CTGACCATCACCTGGGGATCCAAAGTTATCC-3'

Y54W Reverse Primer: 5'-GGATAACTTTGGATCCCCAGGTGATGGTCAG-3'

*K57E Primer: 5'-ATCACCTACGGATCCGAAGTTATCCACAACGAG-3'

M74W Forward Primer: 5'-TGCGAACTCGAGACCTGGACCGGTGAAAAAG-3'

M74W Reverse Primer: 5'-CTTTTTCACCGGTCCAGGTCTCGAGTTCGCA-3'

*Indicates primer designed and used by Joanne Davies to produce mutant LFABP.

The triple charge reversal mutant was produced using the K57E mutant DNA created previously and using two new pairs of forward and reverse primers to produce the other two mutations:

K31E Forward Primer: 5'-CGGAAGACCTGATCCAGGAGGGTAAAGATATCAAAGG-3'

K31E Reverse Primer: 5'-CCTTTGATATCTTTACCCTCCTGGATCAGGTCTTCCG-3'

K36E Forward Primer: 5'-CCAGGAGGGTAAAGATATCGAGGGTGTTTCTGAAATCGTTCACG-3'

K36E Reverse Primer: 5'-CGTGAACGATTTCAGAAACACCCTCGATATCTTTACCCTCCTGG-3'

The underlined bases indicate the location of the mutations in the primers. All oligonucleotides were purchased from MWG Biotech already purified by fast polynucleotide liquid chromatography (FPLC).

2.2.3 The QuickChange Site Directed Mutagenesis Method

As stated, this method uses a supercoiled double-stranded DNA (dsDNA) vector with an insert of interest and two synthetic oligonucleotide primers containing the desired mutation (see **Fig 2.2.1**). The oligonucleotide primers, each complimentary to opposite strands of the vector, are extended during temperature cycling by Pfu DNA polymerase. Incorporation of the oligonucleotide primers generates a mutated plasmid containing staggered nicks. Following temperature cycling, the product is treated with *Dpn* I. The *Dpn* I endonuclease (target sequence; 5'-Gm^{6}ATC-3') is specific for methylated DNA and is used to digest the parental DNA template and to select for mutation-containing synthesized DNA [47]. DNA isolated from *E.coli* the BL21 DE3 strain is dam methylated and therefore susceptible to *Dpn* I digestion. The nicked vector DNA containing the desired mutations is then transformed into XL1-Blue ultracompetent cells.

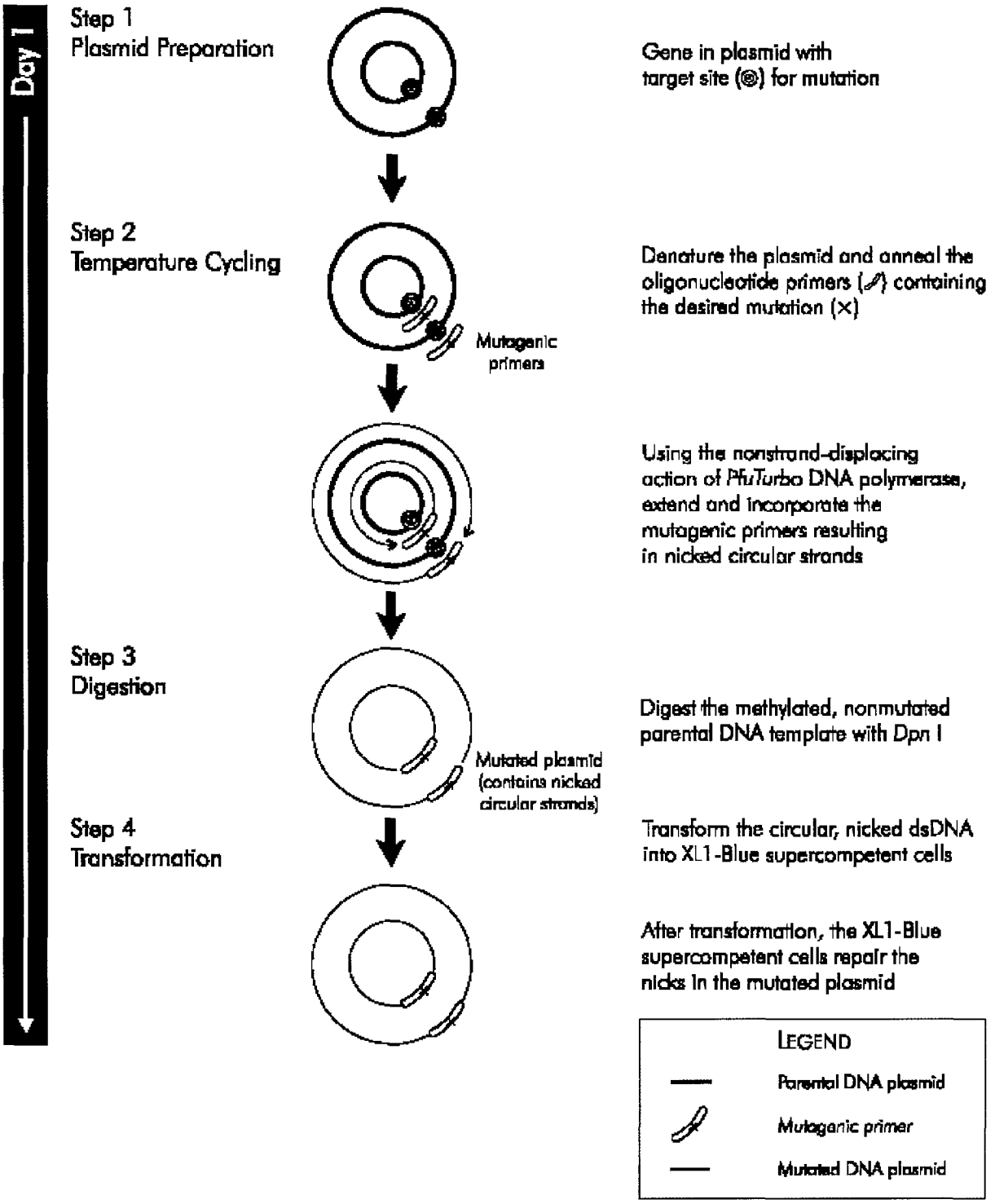

Fig 2.2.1 Overview of the QuickChange site directed mutagenesis method [48]

The sample reaction was prepared using 5 µl reaction buffer (20 mM Tris-HCl (pH 8.8 at 25 °C), 10 mM KCl, 10 mM $(NH_4)_2SO_4$, 2 mM $MgSO_4$, 0.1% Triton X-100 and 0.1 mg/ml nuclease free BSA). To the buffer was added 50 ng of dsDNA template (miniprepped pET11A-FABP expression plasmid), 125 ng of forward oligonucleotide primer, 125 ng of reverse oligonucleotide primer and 2 mM dNTP mix. Distilled water was then added to the reaction mixture to give a final volume of 50 µl. After heating the reaction mixture as outlined below for the hot start, 2.5 units of Pfu DNA polymerase was added to catalyse the reaction.

The reactions were carried out using a Techne Progene PCR machine and utilized the following programme;

1.	94 °C	1 min	Hot Start
2.	Added Pfu DNA polymerase		
---	---	---	---
3.	94 °C	1 min	Melting
4.	55 °C	1 min	Annealing
5.	68 °C	13 mins	Extension
---	---	---	---
		16 cycles	
6.	68 °C	10 mins	Amplification
7.	4 °C		Stop

PCR products were checked for size and purity by loading 5 µl on a 1.5% Agarose gel.

2.2.4 Restriction Digest

The parental (nonmutated) supercoiled dsDNA was then digested by adding 10 units of the *Dpn* I restriction enzyme directly to the amplification reaction in a sterile eppendorf using a glass pipette with a pointed tip. The reaction mixture was then spun down in a microcentrifuge for 1 minute and then immediately incubated at 37 °C in a water bath for 1 hour.

2.2.5 Transformation of XL1-Blue Ultracompetent Cells

XL1-Blue cells were prepared from a glycerol stock by streaking on an LB agar plate, incubating the plate overnight and then selecting a colony for growing in an LB overnight culture. 10 ml of the overnight culture was added to 250 ml SOB (2% Bacto Tryptone, 0.5% Yeast Extract, 10 mM NaCl, 2.5 mM KCl, 10 mM $MgCl_2$ and 10 mM $MgSO_4$, pH 6.8) and grown at 37 °C until an optical density ($O.D_{600}$) of 0.6 at 600 nm was reached.

The culture was then spun down at 3000 rpm for 10 minutes at 4 °C in a sterile centrifuge tube. The pellet was re-suspended in 80 ml of ice-cold transformation buffer (10 mM PIPES, 15 mM $CaCl_2$, 250 mM KCl and 55 mM $MnCl_2$, pH 6.07). The solution

was placed on ice for 10 minutes and then respun at 3000 rpm for 10 minutes. The pellet was then re-suspended in 20 ml transformation buffer. Dimethylsulfoxide (DMSO) was then added to a give a final concentration of 7%. The solution was then placed on ice for 10 minutes and then aliquotted in 250 µl volumes and snap frozen in liquid nitrogen.

XL1-Blue ultracompetent cells were thawed on ice. 200 µl of XL1-Blue ultracompetent cells were then mixed with 50 µl of the sample reaction and 2.72 µl of 0.14M β-mercaptoethanol in Falcon 2059 polypropylene tubes. The transformation reactions were placed on ice for 45 minutes and then heat pulsed in a water bath at 42 °C for 45 seconds before being placed on ice for 2 minutes. 200 µl of SOC and carbenicillin (50 µg/ml) at 42 °C were then added to the digested sample that was then placed in an incubated shaker at 37 °C for 1 hour. The sample was then spread on LB-agar plates with carbenicillin (50 µg/ml). A colony from this plate was then grown in LB broth, miniprepped and sequenced by Oswel (Southampton, UK).

2.2.6 Transformation of Mutant DNA Into BL21 DE3 Calcium Competent Cells

4 µl of the mutant DNA miniprep from the XL1-Blue cells was then added to 300 µl of calcium competent cells ($O.D._{600} \approx 0.6$). This mixture was then chilled on ice for 30 minutes. The cells were then heat shocked by placing the solution in a water bath at 42 °C for up to 3 minutes, before immediately returning the sample to ice. 200 µl of LB broth containing carbenicillin (50 µg/ml)was then added to the mutant DNA-calcium competent cells mixture. The solution was then placed in an incubated shaker at 37 °C for

30 minutes. The mixture was then plated on LB-agar plates containing carbenicillin (50 μg/ml) as before and the resulting colonies were used to prepare an overnight culture that was then spun down, miniprepped and sequenced by Oswel (Southampton, UK) after checking the plasmid for size and purity on a 0.8% agarose gel.

900 μl of the overnight culture was placed into sterile cryotubes containing 100 μl of sterile glycerol to make glycerol stocks.

2.3 Preparation of Rat Liver Fatty Acid Binding Protein

The gene for rat liver fatty acid binding protein has been inserted into pET-11a vector, which has carbenicillin resistance using the *Nde* I and *Hind* III restriction sites [49] and is expressed in BL21(DE3) cells. The *E.coli* bacteria were streaked on LB-agar plates containing carbenicillin (50 μg/ml) and grown overnight at 37 °C. Individual colonies were then selected, ensuring a homogeneous population. These colonies were subsequently grown overnight in four sterile universal containers, in a 10 mL solution of LB broth with carbenicillin (50 μg/ml). The universal containers were incubated at 37 °C overnight with agitation.

The cultures were then used to inoculate two 1 litre sterile flasks containing LB and carbenicillin (50 μg/ml) and were grown at 37 °C until $O.D_{600}$ of 0.6-0.8 was achieved (this took 2.5 hours).

IPTG was then added giving 0.4 mM final concentration to induce the cells, followed by a period of incubation at 37°C for five hours. The cells were then harvested on the Beckman centrifuge at 5,000 rpm for twenty minutes at 4 °C.

The LB supernatant was subsequently poured off and the pellet was weighed (≈10 g). The pellet was re-suspended in 2 ml cell lysis buffer per gram of *E. coli* and the solution was frozen and stored at –20 °C.

2.3.1 Isolation of FABP

4 μl of PMSF (100 mM) and 80 μg lysozyme per gram of *E.coli* were added to the pellet solution and the new solution was stirred at 4 °C for twenty minutes.

4 mg deoxycholate was then added per gram of *E.coli* and the solution was incubated at 37 °C for thirty minutes. The solution was sonicated at 10 μ to lyse the cells (five repetitions of twenty seconds on, twenty seconds off). The cell debris was subsequently removed by centrifugation at 10,000 rpm for twenty-five minutes in an 8x50 ml rotor.

Addition of ammonium sulphate precipitated other proteins present in the solution. Ammonium sulphate was added gradually, to give a 30% saturation. The solution was then stirred for one hour at 4 °C. At the end of this period the solution was centrifuged to remove cell debris at 10,000 rpm at 4 °C for thirty minutes. A further

addition of ammonium sulphate gave a 60% saturation, and then the stirring and centrifugation were repeated.

The resulting supernatant was dialysed overnight at 4°C in four litres of 0.1 M phosphate buffer (KH_2PO_4) at pH 7.4 or 0.02 M Tris buffer at pH 9.0, dependent on the purification method (Tris used with DEAE cellulose and KH_2PO_4 used with agarose beads, as outlined in **section 2.3.2**).

2.3.2 Purification of FABP

At this stage there have been two different methods employed to purify the LFABP. A second method was necessary as the manufacturer ceased to supply dodecyl-agarose.

Dodecyl-agarose Purification

Dodecyl-agarose was then used to isolate the FABP. The agarose was washed three times to equilibrate it with 0.1 M KH_2PO_4, pH 7.4, buffer. The amount of FABP in 20 ml of sample was estimated after measuring the fluorescence of 50 µl of sample using DAUDA cocktail. 20 ml of the FABP solution was spun at 10,000 rpm for one minute with dodecyl-agarose. The supernatant was decanted off and checked for FABP using DAUDA cocktail, after each addition of FABP solution. After checking the supernatant

for fluorescence a further 20 ml of FABP solution was added and the process was repeated.

After the entire FABP solution had been attached to the dodecyl agarose, the agarose was washed three times with 20 ml of KH_2PO_4 (0.1 M, pH 7.4). The fluorescence of the supernatant was subsequently checked to make sure that no FABP was being removed from the dodecyl agarose.

Next the FABP was eluted with 20 ml of KH_2PO_4 (0.05 M, pH 7.4) and 40% ethanol, pH 6.0. This was repeated using 10 ml of elution buffer until no fluorescence remained in the supernatant.

The elution fractions were then combined and dialysed overnight to remove ethanol.

DEAE Cellulose Column

This method was used to replace the dodecyl agarose that was no longer available.

LFABP solution was dialysed overnight into 20 mM Tris, pH 9. 35 ml of packed DEAE cellulose in 20 mM Tris, pH 9, was poured into a 120 ml capacity column. The concentration of the LFABP solution was estimated using DAUDA cocktail and up to 20 mg of protein were loaded slowly onto the column and the LFABP bound to the DEAE

cellulose beads under these conditions. The column was then washed with 40 ml of 20 mM Tris, pH 9, and at this point the eluent was checked for LFABP using DAUDA cocktail. If the eluent at this point contained no LFABP the column was then washed with 400 ml of 20 mM Tris pH 9.

A solution of 60 mM NaCl, 20 mM Tris pH 9.0 was then used to elute LFABP from the DEAE cellulose, until the eluent ceased to significantly increase the fluorescence of DAUDA cocktail.

2.3.3 Delipidation on Lipidex

Once the LFABP had been separated from other proteins, the remaining task was to remove bound fatty acids. This was achieved using a Lipidex (hydroxyalkoxypropyldextran) column. The Lipidex was left to hydrate overnight in AnalaR water and then equilibrated with 10 mM KH_2PO_4, pH 7.4 buffer before loading on the protein. The same buffer was used to wash the LFABP through the column and the fatty acids remain bound to the Lipidex.

2.3.4 Sodium Dodecyl Sulphate Polyacrylamide Gel Electrophoresis (SDS-PAGE)

SDS-PAGE was carried out using the method described by Laemmli [50], to analyse the protein content of the collected protein solutions. This required a Biometra vertical gel electrophoresis tank and a Bio-Rad Power Pac 2000. A two layered gel was

set up with the bottom layer being a 15% resolving gel (5 ml resolving gel buffer (0.75 M Tris, 0.2% SDS, pH 8.8), 5 ml Protogel (30% acrylamide), 5 µl N,N,N',N',-tetramethyl-ethylenediamine (TEMED) and a few crystals of ammonium persulphate). The upper layer was a 4% stacking gel (3.75 ml stacking gel buffer (0.25 M Tris, 0.2% SDS, pH 6.8), 1 ml Protogel (30% acrylamide), 2.75 ml distilled water, 3 µl TEMED and a few crystals of ammonium persulphate).

The gel was then vertically suspended in a tank containing reservoir buffer (1% SDS, 0.1 M Tris, 0.77 M glycine, pH 8.3). Samples were in a 2:1 ratio with sample buffer (2.5 ml stacking gel buffer, 4% SDS, 2 ml glycerol, 0.2 ml ß-mercaptoethanol, a spatula of bromothenol blue and 1.3 ml of distilled water). The gel was run at a constant current of 20 mA, for approximately 1.5 hours until the bromothenol blue front was approximately 1cm from the bottom of the gel.

The gel was then stained for 1 hour in coomassie blue stain (0.25% coomassie blue, 50% trichloro-acetic acid). The stain was then removed from the gel by submergence in a destaining solution (45% methanol, 5% acetic acid).

A typical gel of purified LFABP WT is shown in **Fig 2.3.1**.

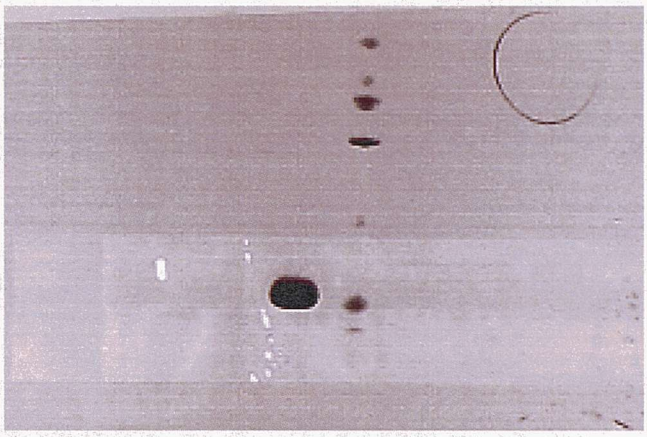

Fig 2.3.1 **SDS-PAGE gel showing pure LFABP WT**
Lane 1 contains LFABP WT, lane 2 contains the low molecular weight markers showing, from the top of the gel, 66 kDa, 45 kDa, 36 kDa, 29 kDa, 24 kDa, 20 kDa and 14.2 kDa markers

2.3.5 Concentration of the Protein

Once the protein had been purified and delipidated it had to be concentrated. The FABP solution was filtered using a 3 kDa membrane under pressure. The system used involved a YM3 membrane in a Centricon protein concentrator (Amicon, Soreham, Gloucestershire, UK). The filtrate was checked for the absence of FABP using a DAUDA fluorescence assay, as described in **section 2.5**.

2.3.6 Calculation of FABP Concentration

BCA Assay

The BCA assay, as described by Smith *et al.* [51] was used. Assays were carried out in triplicate for increased accuracy. The FABP samples were referenced against a standard (1 mg/ml) solution of bovine serum albumin. The bovine serum albumin was diluted giving a range of concentrations between 0.2 and 1.0 mg/ml in 10 µl samples. These standard solutions along with the unknown FABP samples (FABP samples at 50% and 100% concentration) were placed on a 96 well microtitre plate. Following this 200 µl of the BSA reagent was added. The plates were then incubated at 37 °C for thirty minutes and subsequently read on a Dynex Revelation 3.04 plate reader.

Absorbance at 280 nm

A second method used for measuring the protein concentration of LFABP is the absorbance of the solution at 280 nm. This was carried out using the Hitachi U-2000 spectrophotometer and relies upon the Beer-Lambert law ($A=\varepsilon cl$). The absorption coefficient is determined using the Wetlaufer procedure [52] based on the number of tyrosine, tryptophan and cysteine residues in the protein where

$$\varepsilon = 5550\ \Sigma Trp + 1340\ \Sigma Tyr + 150\ \Sigma Cys$$

For LFABP this calculation gives a value of 6300 $cm^{-1}M^{-1}$.

2.3.7 Circular Dichroism (CD)

The CD spectra of wild type and mutant FABP were measured using the Jasco J-270 Spectropolarimeter. Scans were performed in triplicate between 180 and 250nm after incubation at the appropriate temperature for 20 minutes. LFABP in 10 mM potassium phosphate buffer at pH 7.4 was used. The change in the spectrum at 220nm was converted to a molar ellipticity value.

2.4 Preparation of Phospholipid Vesicles

Phospholipids were purchased as solutions in chloroform. The solutions were dried down under a stream of nitrogen gas and then dessicated to remove any trace of solvent. The phospholipids were then dissolved in methanol to produce stock solutions. Phospholipids were added into the assay by methanol injection that produces the small unilamellar vesicles (SUVs).

For the preparation of mixed phospholipids vesicles the required phospholipids methanol stocks were dried down together in the correct molar ratio under a stream of nitrogen gas and then dessicated as described above. The mixed phospholipids were then dissolved in methanol for preparing SUVs.

2.5 Fluorescence Studies of LFABP

2.5.1 The Fluorescence Displacement Assay

The fatty acid analogue 11-(dansylamino) undecanoic acid (DAUDA) (**Fig 2.5.1**) binds to LFABP and upon moving from a polar environment in solution, to a hydrophobic environment, when bound to the LFABP, this probe experiences a huge increase in fluorescence when excited at 350 nm. Upon being displaced from the protein and being released back into a polar environment, it experiences an equally large decrease in fluorescence. The spectral blue-shift of the fluorescence emission of DAUDA upon binding to LFABP of about 50 nm is consistent with the probe binding in the hydrophobic cavity of the protein. The changes in fluorescence intensity upon binding to the protein make DAUDA a suitable probe in ligand binding studies for LFABP.

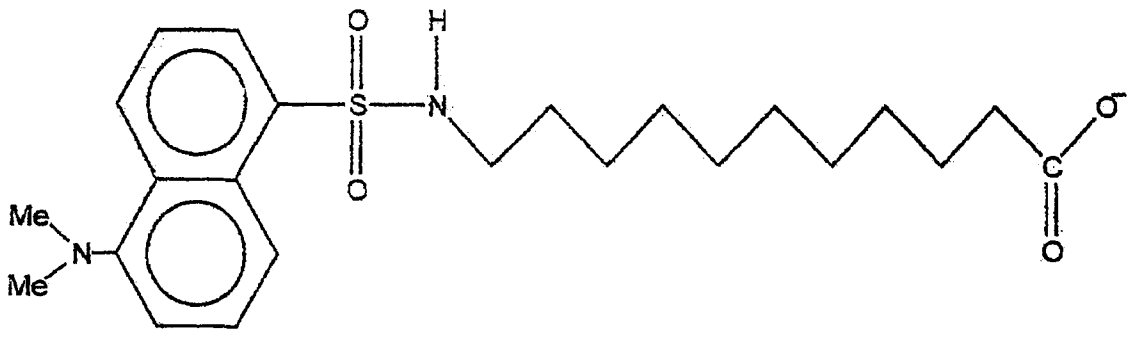

Fig 2.5.1 The fluorescent fatty acid analogue molecule DAUDA

Other ligands for LFABP such as fatty acids and bile acids will displace DAUDA from LFABP when they bind. This can then be used to serve as a direct measure of ligand

binding to LFABP as the loss of fluorescence will be directly proportional, in the absence of excess protein, to ligand binding.

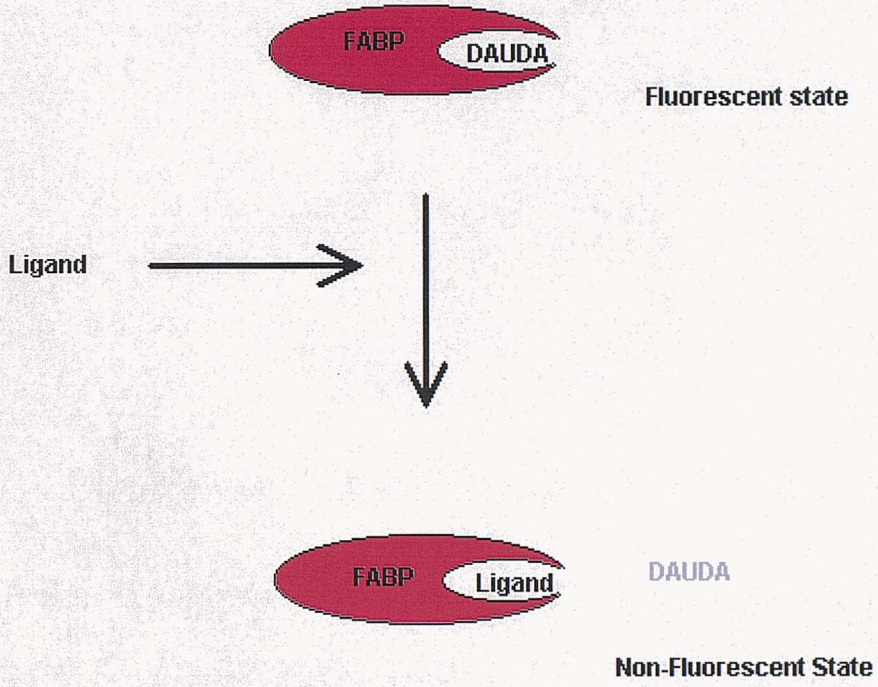

Fig 2.5.2 Cartoon diagram of the fluorescence displacement assay

The DAUDA displacement assay is very sensitive as the DAUDA has a higher K_d for LFABP than the vast majority of ligands known to bind to the protein.

A second fluorescent probe used to study ligand binding in LFABP is 8-anilino-1-naphthalenesulfonic acid (ANS).

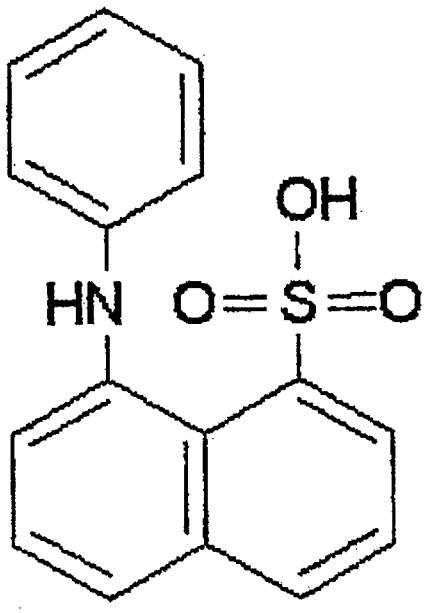

Fig 2.5.3 The structure of 8-anilino-1-naphthalenesulfonic acid (ANS)

ANS is advantageous over DAUDA in that it is cheaper and requires lower concentrations of competing ligand to displace the fluorescent probe as it has a higher K_d for LFABP (0.91-2.72 μM) than DAUDA (0.07-0.19 μM). As a result of its lower K_d, DAUDA appeared to give more consistent results and therefore less error.

The fluorescence displacement assays were carried out in the same way for both probes. The assays were measured using the Hitachi F-2000 fluorescence spectrophotometer. Unless otherwise stated assays were carried out using 1 μM probe, 10 mM HEPES buffer at pH 7.5, and 8 μg of LFABP. Ligands were added in 1 μl volumes using a Hamilton Microliter® syringe attached to a Hamilton repeating dispenser. In the case of DAUDA, the concentrations of the added ligands were $5x10^{-4}$ M, and the spectrophotometer was set to measure at an excitation wavelength of 350 nm and an emission wavelength of 500 nm. In the case of ANS, the concentrations of the added

ligands were $2.5x10^{-4}$ M, and the spectrophotometer was set to measure at an excitation wavelength of 376 nm and an emission wavelength of 460 nm. The excitation and emission values for ANS were obtained by running wavelength scans using fixed values for excitation whilst running a wavelength scan and vice versa, as described by Kane and Bernlohr [53].

For the ligands used DAUDA was always displaced and a loss of fluorescence was observed. Whilst using ANS there have been occasions where due to the small size of the probe the ligand has been able to bind without displacing ANS, in such cases the binding of ligand increased the hydrophobicity of the ANS environment, and in turn caused a fluorescence increase.

2.5.2 Assay of LFABP Binding to Phospholipid Vesicles Monitored by Loss of DAUDA Fluorescence

Assays involving the addition of phospholipid vesicles via methanol injection into the LFABP-DAUDA complex were corrected for changes in fluorescence due to the DAUDA partitioning into vesicles. Blank titrations were carried out of phospholipids into 1 μM DAUDA in 10 mM HEPES, pH 7.5 buffer.

2.5.3 Calculation of K_d and K_i Values

Apparent K_d values were measured by titrating a known concentration of the fluorescent probe into a solution of 10 mM HEPES (pH 7.5) and 0.56 μM FABP. The fluorescence values are corrected for free fluorescent probe. By plotting corrected fluorescence against the concentration of fluorescent probe and fitting a hyperbola to this line, Sigma Plot software can calculate a K_d value as described in chapter 3. With this value an inhibition constant can be calculated using the following formula:

$$K_i = [I_{50}]/(1+[L]/K_d) \text{ [54]}$$

Where K_i = apparent inhibitor constant, $[I_{50}]$ = the ligand concentration at the midpoint of competition, [L] = free concentration of fluorescent probe and K_d = apparent dissociation constant of LFABP for the fluorescent probe.

This method requires 50% displacement of DAUDA by ligands and so is not normally applicable to low affinity ligands such as lysophospholipids that also have limited solubility.

2.5.4 Tryptophan Fluorescence Assays

Tryptophan fluorescence studies were carried out using the Hitachi F-2000 fluorescence spectrophotometer set at an excitation wavelength of 280 nm and measuring

at an emission wavelength between 300 and 550 nm. Assays were carried out in 10 mM HEPES, pH 7.5 buffer using 0.8 μM LFABP. Ligands and phospholipids were titrated into LFABP as described for the fluorescence displacement assay. Fluorescence values were corrected for background fluorescence of the ligands and phospholipids.

2.5.4.1 Fluorescence Resonance Energy Transfer (FRET) Studies

SUVs containing 5 mol% dansyl DHPE in DOPG were titrated by methanol injection into 10 mM HEPES (pH 7.5) and 0.8 μM LFABP as described above. The tryptophan fluorescence was measured at an excitation wavelength of 280 nm and enhanced fluorescence emission was measured at 500 nm.

2.5.4.2 Fluorescence Quenching Using Succinimide

Succinimide was titrated as an aqueous solution into 0.8 μM LFABP in 10 mM HEPES buffer (pH 7.5) up to a concentration of 0.5 M, in the presence and absence of DOPG vesicles. The tryptophan fluorescence was measured at an emission wavelength of 330 nm after excitation at 280 nm. Fluorescence values were corrected for the effect of succinimide on background fluorescence.

Chapter 3 – Ligand Binding Studies With α-Helix Charge Reversal Mutants

3. Ligand Binding Studies With α-Helix Charge Reversal Mutants

3.1 Introduction

Three lysine residues that had been identified as part of the α-helical region of the protein [11], were investigated to determine their role in the binding of ligands to LFABP. These residues were investigated by using charge reversal mutants where lysine residues were replaced with glutamate. Each mutation then replaces a basic amino acid with an acidic residue, a net loss of two positive charges.

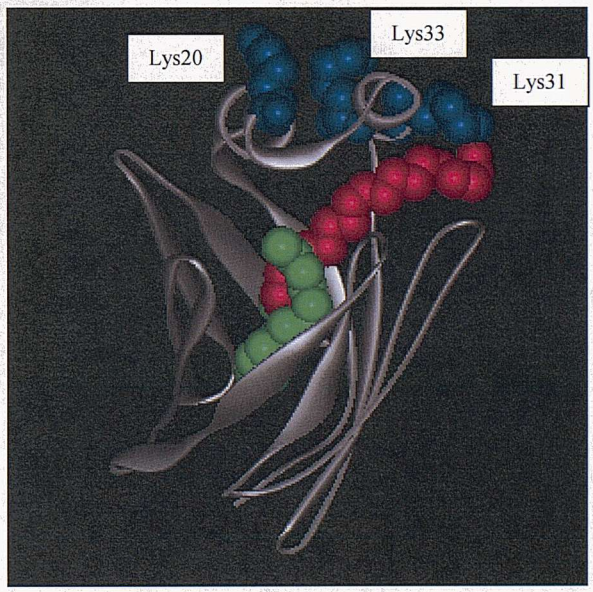

Fig 3.1.1 LFABP showing the locations of the three lysine residues in the α-helical region that are to be replaced by glutamate. The lysine residues that are to be replaced are shown in blue. Also shown are the two oleic acid molecules that bind to LFABP, at site 1 (green) and site 2 (red)

The three single charge reversal mutants were used to determine whether it was specific residues of the protein or overall areas of charge that were responsible for

binding ligands. Also a double mutant was expressed that would aid in assignment of importance to the three lysine residues at positions 20, 31 and 33 on the protein. **Fig 3.1.1** shows the positions of these three residues.

3.2 Expression of Charge Reversal Mutants

Joanne Davies in this laboratory employed the Kunkel method of mutagenesis [45,46] to produce the LFABP single mutants K20E, K31E, K33E as well as the double mutant K31E,K33E. They were expressed and purified using the same method as for wild-type LFABP as described in chapter 2 of this work. The yield of all three mutants was comparable to the wild-type protein at 15-20 mg per litre of culture. Sample purity was checked on SDS-PAGE with coomassie blue staining (see **Fig 3.2.1**) and indicated that protein purity was greater than 99% for all mutants.

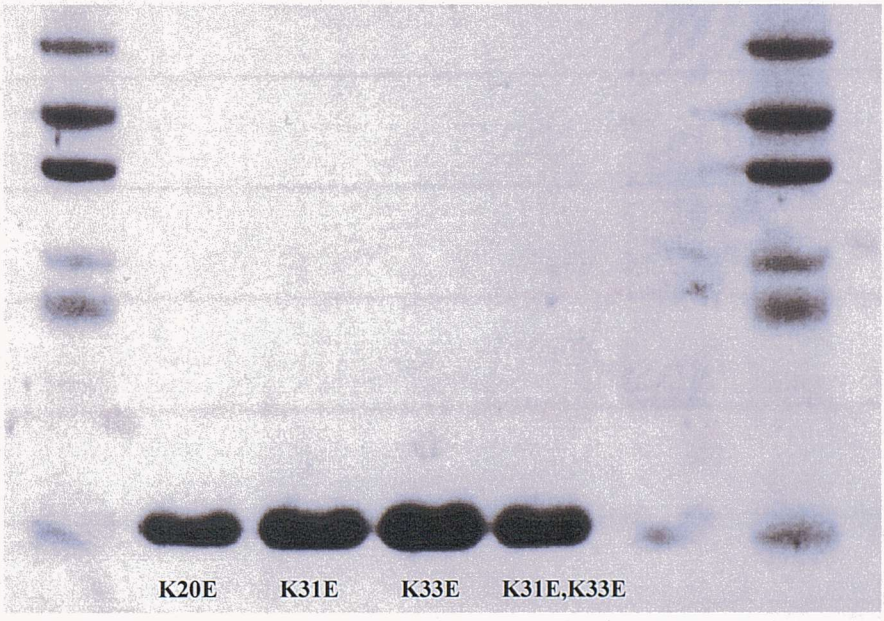

Fig 3.2.1 **SDS-PAGE Gel of α-helical charge reversal mutants**
Lanes 1 and 6 contain low molecular weight markers, showing from the top of the gel, 66 kDa, 45 kDa, 36 kDa, 29 kDa, 24 kDa, 20 kDa and 14.2 kDa. Lanes 2-5 contain the LFABP α-helical charge reversal mutants as labeled

3.3 Circular Dichroism

Circular Dichroism (CD) was used to confirm that the mutants were all correctly folded. The spectra for each of the charge reversal mutants are shown in **Fig 3.3.1**. The spectra for each of the mutants are essentially identical to the wild type spectrum, showing that these mutants are correctly folded.

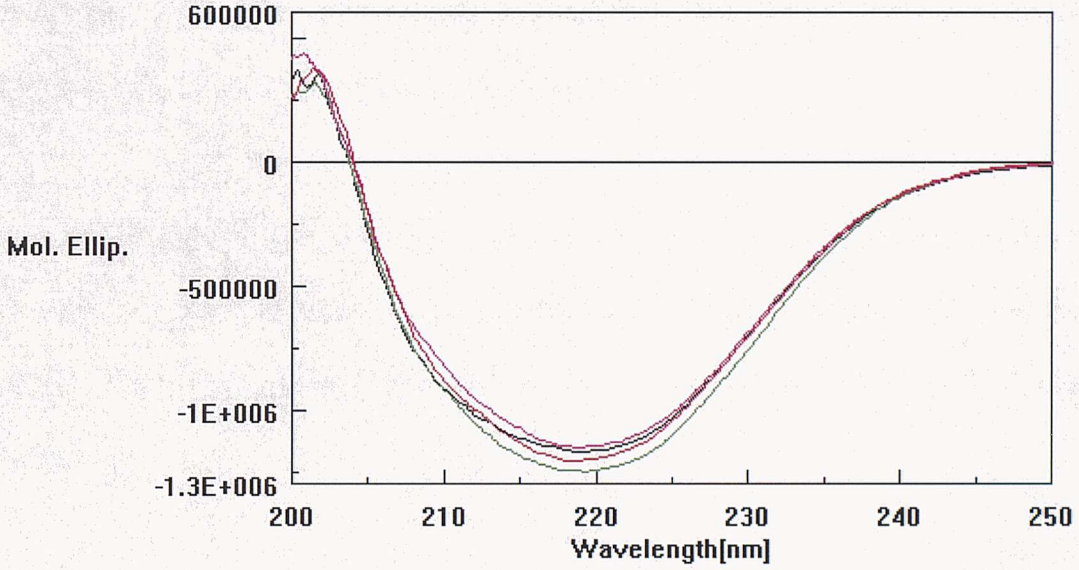

Fig 3.3.1 Molar Ellipticity scan for FABPWT and charge reversal mutants between 200 and 250nm. Each line represents a different protein. FABP WT (black); FABP K20E (red); FABP K31E (pink) and FABP K31E,K33E (green)

3.4 DAUDA and ANS Binding to LFABP Charge Reversal Mutants

DAUDA was titrated into each of the mutants, as a solution in methanol, to achieve a final concentration of 1 μM. The final methanol concentration did not exceed 1% of the total volume and a methanol blank titration was used to correct for this. The increase in fluorescence when DAUDA binds to LFABP was corrected for DAUDA

fluorescence in buffer and the K_d values were calculated from the resultant saturation curves using SigmaPlot software.

A similar technique was used for calculating ANS K_d values. ANS was titrated into each of the mutants, as a solution in water, to achieve a final concentration of 2 μM. The total volume of ANS solution did not exceed 2% of the total volume and a blank titration was used to correct for this. The increase in fluorescence when ANS binds to LFABP was corrected for ANS fluorescence in buffer and the K_d values were calculated from the resultant saturation curves using SigmaPlot software.

A maximum fluorescence and a K_d value can be calculated by plotting a graph of fluorescence against fluorescent probe concentration. The saturation curve for DAUDA is shown in **Fig 3.4.1**. SigmaPlot can then fit a curve to this line that obeys the standard hyperbola equation:

$$y = ax/(b + x)$$

Where a = the maximum fluorescence value

and b = the value of x when y is at 50% of its maximum

The values for a and b are then calculated by SigmaPlot for the hyperbolic curve that fits closest to the curve produced from experimental data.

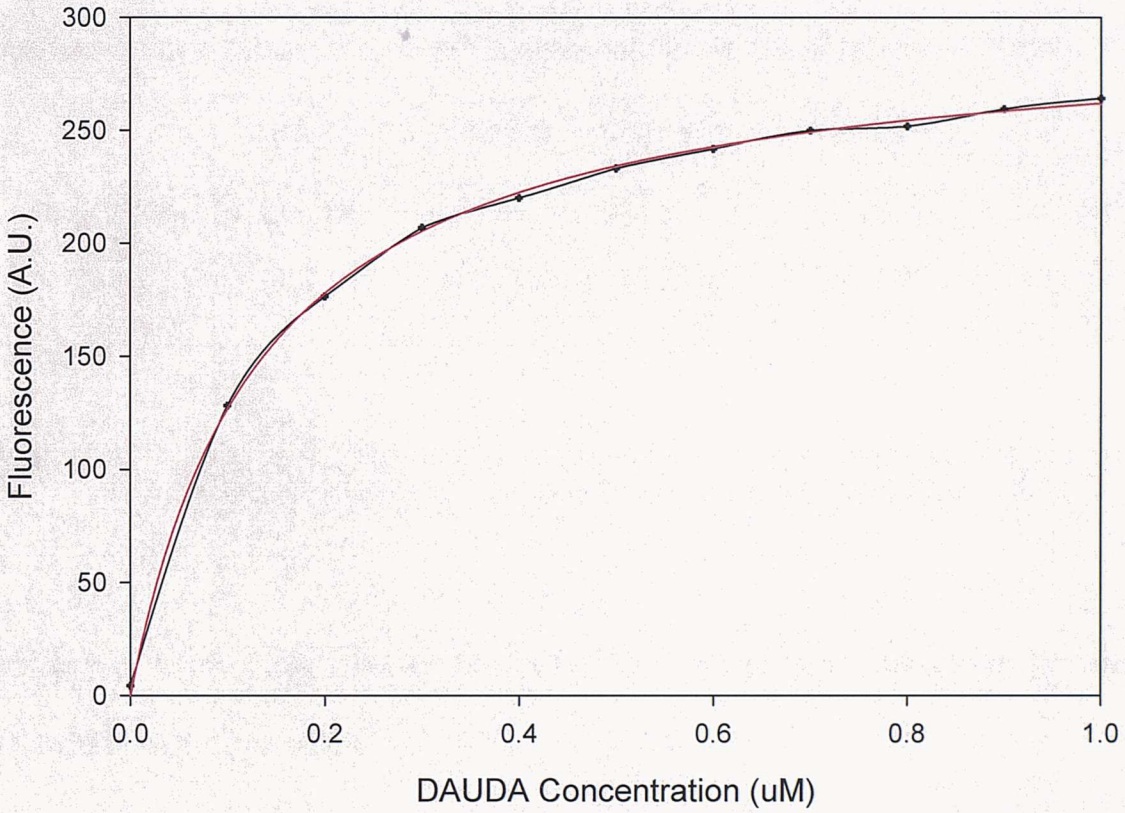

Fig 3.4.1 **Example LFABP-DAUDA Binding Curve for Calculation of Kd Values**
To a sample of LFABP (0.56 μM) in 10 mM HEPES DAUDA was added up to a maximum concentration of 1 μM. Excitation was at 350 nm and emission measured at 500 nm. The experimental data (black) had a hyperbolic curve fitted to it (red) to allow for calculation of a maximum fluorescence value and an apparent Kd value, using SigmaPlot software.

The K_d values of the proteins for DAUDA and ANS are shown in **Table 3.4.1**. The results show no difference in the DAUDA and ANS binding properties of any of the mutant LFABP proteins compared to the wild type LFABP. Therefore there were no apparent adverse affects of charge reversal mutagenesis on DAUDA or ANS binding. However it should be noted that ANS data was subject to a large experimental error.

	FABP WT	FABP K20E	FABP K31E	FABP K33E	FABP K31E,K33E
DAUDA K_d (μM)	0.12 ± 0.03	0.13 ± 0.01	0.15 ± 0.004	0.07 ± 0.02	0.14 ± 0.04
ANS K_d (μM)	1.2 ± 0.93	0.91 ± 0.40	2.5 ± 1.2	1.8 ± 0.39	2.7 ± 1.2

Table 3.4.1 Apparent DAUDA and ANS K_d values for FABP wild type and charge reversal mutants. All values are the mean of titrations performed in triplicate ± S.D.

3.5 Displacement of the Fluorescent Probes DAUDA and ANS from Wild Type and Mutant LFABPs by Ligands

The effectiveness of a ligand to displace a fluorescent probe is a measure of its affinity. If the displacement exceeds 50% then it is possible to calculate the K_i value for the ligand. The method of Kane and Bernlohr was used, as described in chapter 2. Where appropriate values will be mentioned, which are summarised in **Table 3.6.1** and **Table 3.6.2** at the end of this chapter.

The ligands that were investigated included oleic acid, as this was the ligand seen in the only crystal structure for liver FABP [11], oleoyl CoA which may compete with

oleic acid for LFABP in the cell and lithocholic acid derivatives, as these showed the highest affinity of the bile acids that have been evaluated as ligands [57]. Other ligands included the lysophospholipids lysophosphatidic acid and lysophosphatidylcholine.

3.5.1 Oleic Acid

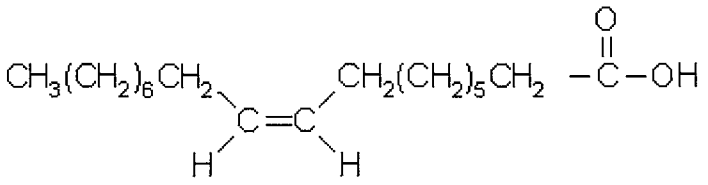

Using DAUDA as the fluorescent probe there was no major difference between the wild type and any of the mutants in terms of fluorescence displacement, as seen in **Fig 3.5.1**. This is consistent with both DAUDA and oleic acid competing for the primary binding site for oleic acid (site 1) as seen in **Fig 3.1.1**, which is remote from and therefore not expected to be affected by mutations within the α-helical region. Hence although it would have been anticipated that K31 would affect the binding of oleic acid at site 2 this may not show up in the DAUDA fluorescence displacement assay. However, when K_i values were calculated for oleic acid binding to wild type and mutant LFABPs, there was noted to be a small difference between the wild type protein and the single and double charge reversal mutants containing the K31E mutation. The K31E mutation doubles the K_i value for oleic acid from 0.03-0.04 μM (wild type, K20E and K33E LFABP) to 0.07-0.08 μM (K31E and K31E,K33E LFABP).

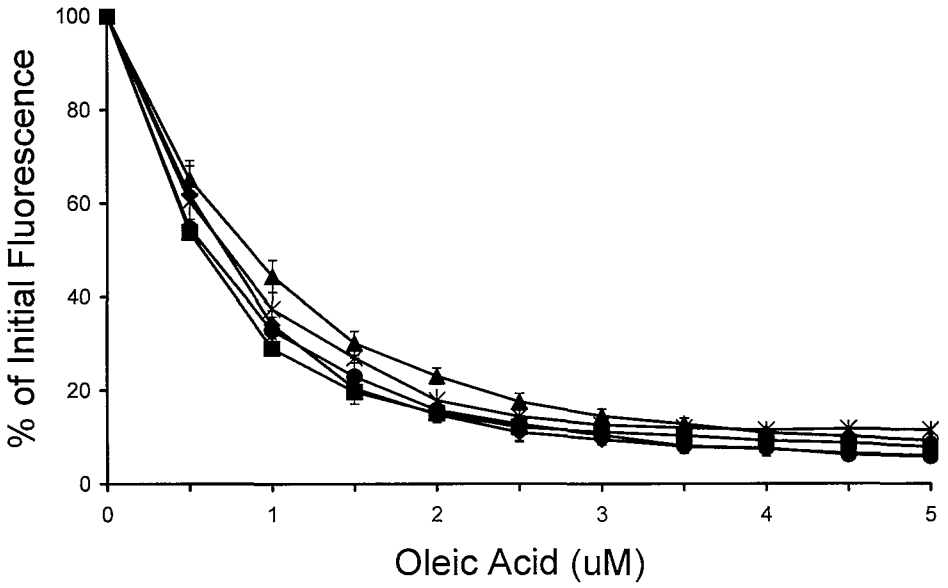

Fig 3.5.1 **The Effects of the Charge Reversal Mutagenesis on the Ability of Oleic Acid to displace DAUDA from Liver FABP**
Oleic Acid was titrated as a methanol solution into 10 mM HEPES containing 1μM DAUDA and 0.56 μM of either wild type (♦), K20E (■), K31E (▲), K33E (●) or K31E,K33E (∗) LFABP. The loss of fluorescence of the LFABP-DAUDA complex was measured at 500 nm following excitation at 350 nm. All data points shown are the mean of three titrations ± S.D.

The DAUDA displacement assay failed to display a major difference between the wild type and mutant LFABPS (**Fig 3.5.1**). However, when the displacement assay used ANS (**Fig 3.5.2**) there was a decreased affinity for the K31E single mutant (K_i 0.31 μM) and equally so for the K31E,K33E double mutant (K_i 0.33 μM), compared to the wild type protein (K_i 0.13 μM). These results would suggest that under these assay conditions the lysine residue at position 31 is important for binding oleic acid whereas the lysines at positions 20 and 33 are less significant (K_i 0.13 μM and 0.14 μM respectively). These results are consistent with the conclusion that ANS may bind at the second fatty acid binding site in contrast to DAUDA, which is binding at site 1 (see later). Therefore ANS is reporting on site 2 and the oleic acid binding at this site.

3.5.2 Displacement of Fluorescent Probe from Wild Type and Mutant LFABPs by Other Ligands

Unlike the binding of fatty acids such as oleic acid, the binding of other non-polar anions has only been seen with a 1:1 stoichiometry. Moreover, although there is no crystal structure available for these ligands bound to LFABP, it would be expected that binding might involve structural elements from both sites 1 and 2. This would certainly be expected for more bulky ligands, where the portal region would also allow the accommodation of larger anionic groups rather than having to bind these anionic groups within the cavity at site 1. As a result, displacement studies using DAUDA and ANS will reflect this complexity.

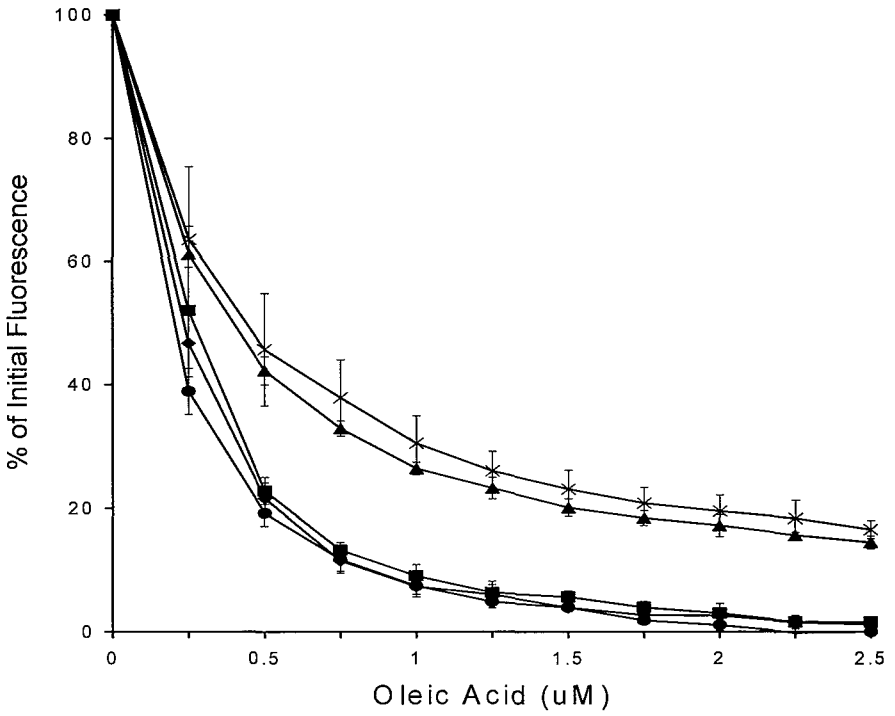

Fig 3.5.2 **The Effects of the Charge Reversal Mutagenesis on the Ability of Oleic Acid to displace ANS from Liver FABP**
Lithocholic Acid was titrated as a methanol solution into 10 mM HEPES containing 1μM ANS and 0.56 μM of either wild type (♦), K20E (■), K31E (▲), K33E (●) or K31E,K33E (∗) LFABP. The loss of fluorescence of the LFABP-ANS complex was measured at 460 nm following excitation at 376 nm. All data points shown are the mean of three titrations ± S.D.

In this section the binding of bile acids, lysophospholipids and oleoyl CoA has been investigated. The bile acids provide a chemically diverse and structurally informative group of ligands while lithocholic acid and its derivatives have previously been shown to bind with high affinity [11, 83] and are the major focus of this binding study.

3.5.2.1 Lithocholic Acid

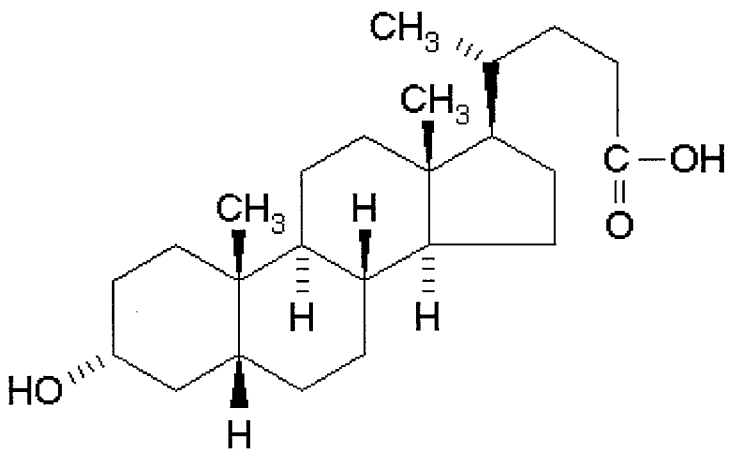

Using DAUDA as the fluorescent probe there was significantly weaker binding of lithocholic acid measured with the K31E (K_i 0.8 μM) and the K31E,K33E double mutant (K_i 0.78 μM) compared to the wild type (K_i 0.31 μM) and the other single mutants of LFABP (K_i 0.45 μM) (**Fig 3.5.3**). There is no significant difference between the single mutant K31E and the double mutant K31E,K33E. Hence the lysine residue at position 31 is the only lysine residue in the α-helical region of the protein that plays a role in the binding of lithocholic acid to the protein.

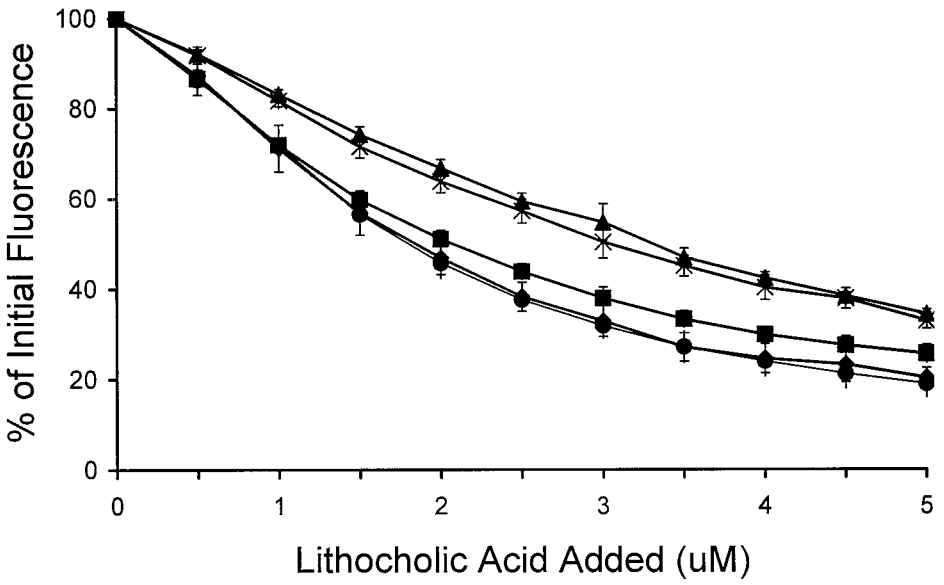

Fig 3.5.3 **The Effects of the Charge Reversal Mutagenesis on the Ability of Lithocholic Acid to displace DAUDA from Liver FABP**
Lithocholic Acid was titrated as a methanol solution into 10 mM HEPES containing 1μM DAUDA and 0.56 μM of either wild type (♦), K20E (■), K31E (▲), K33E (●) or K31E,K33E (✳) LFABP. The loss of fluorescence of the LFABP-DAUDA complex was measured at 500 nm following excitation at 350 nm. All data points shown are the mean of three titrations ± S.D.

The results from the DAUDA binding studies are replicated when ANS is used as the fluorescent probe (**Fig 3.5.4**). The K31E single mutant and the K31E,K33E double mutant both showed a significantly reduced binding (K_i 1.32 μM and 1.49 μM respectively) compared with the wild type enzyme (K_i 0.30 μM) and the other mutants (K_i 0.32-0.44 μM). The difference between the K31E mutant and the wild type and other single mutants is greater than with DAUDA. However, the conclusion remains the same and I would propose that lithocholic acid is binding in such a way as to involve the portal region of the protein.

3.5.2.2 Taurolithocholic Acid 3-Sulphate

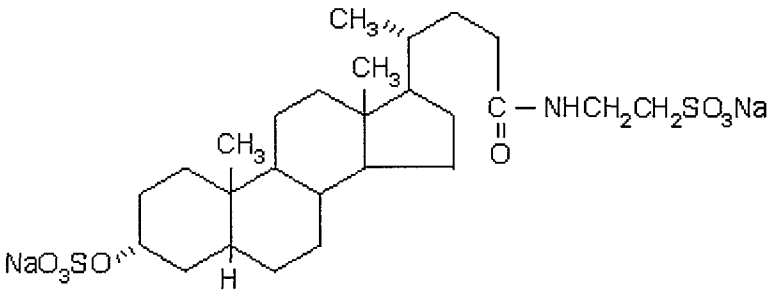

The displacement results for taurolithocholic acid 3-sulphate lead to similar conclusions to those with lithocholic acid using either the DAUDA or the ANS probe. With DAUDA the K33E mutant experiences a decreased affinity for ligand (K_i 1.3 μM) compared with the wild type (K_i 0.29 μM) and K20E mutant (K_i 0.42 μM). The K31E mutant (K_i > 1.1 μM) shows a significantly lower binding affinity than the K33E mutant. The double mutant has a lower binding affinity than either of these two single mutants

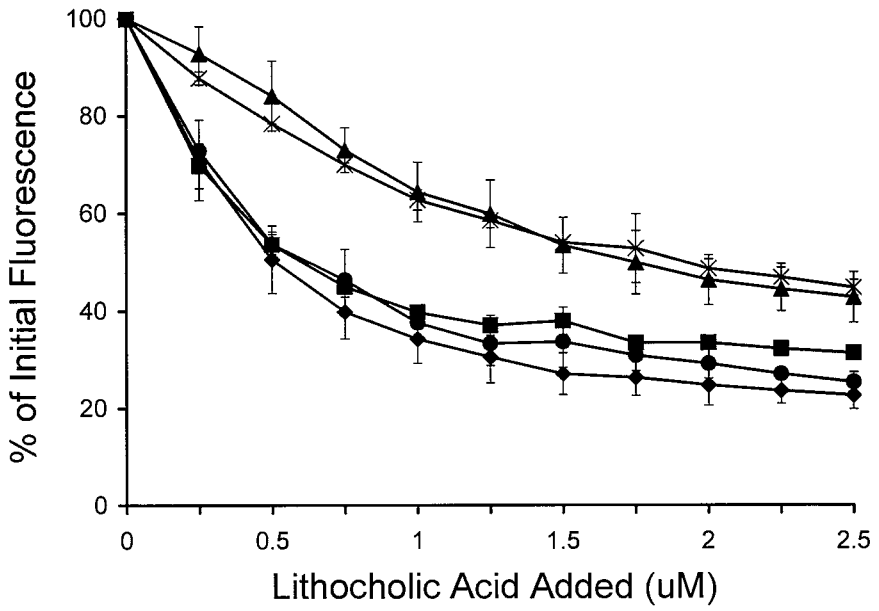

Fig 3.5.4 **The Effects of the Charge Reversal Mutagenesis on the Ability of Lithocholic Acid to displace ANS from Liver FABP**
Lithocholic Acid was titrated as a methanol solution into 10 mM HEPES containing 1μM ANS and 0.56 μM of either wild type (♦), K20E (■), K31E (▲), K33E (●) or K31E,K33E (✳) LFABP. The loss of fluorescence of the LFABP-ANS complex was measured at 460 nm following excitation at 376 nm. All data points shown are the mean of three titrations ± S.D.

(K_i > 1.3 μM), this is representative of the cumulative effect of the two single mutations (**Fig 3.5.5** and **Fig 3.5.6**). The K_i values could not be calculated because of the limited displacement (<50%) seen with K31E and K33E single mutants, as well as with the K31E,K33E double mutant. In these cases a minimal K_d value is shown corresponding to a theoretical 50% displacement at the highest concentration of ligand used which is 5 μM with DAUDA. However, it is clear that the α-helical mutations, particularly K31E, have a more dramatic effect on taurolithocholic acid 3-sulphate binding than lithocholic acid binding. This would suggest that either the anionic sulphate or the anionic taurine group is located within the portal region and thus is affected by the mutation.

Repeating the titrations using ANS as the fluorescent probe produces similar results (**Fig 3.5.6**). Taurolithocholic acid 3-sulphate again binds with lower affinity to the K33E single mutant (K_i 0.27 μM), than to the wild type and K20E mutant LFABP (K_i 0.11 μM and 0.098 μM respectively). There is weaker binding to the K31E single mutant (K_i 1.4 μM) than to the K33E single mutant. The K31E,K33E double mutant showed a cumulative effect of the K31E and K33E single mutants, with much weaker binding (K_i >1.9μM) than either of these single mutants.

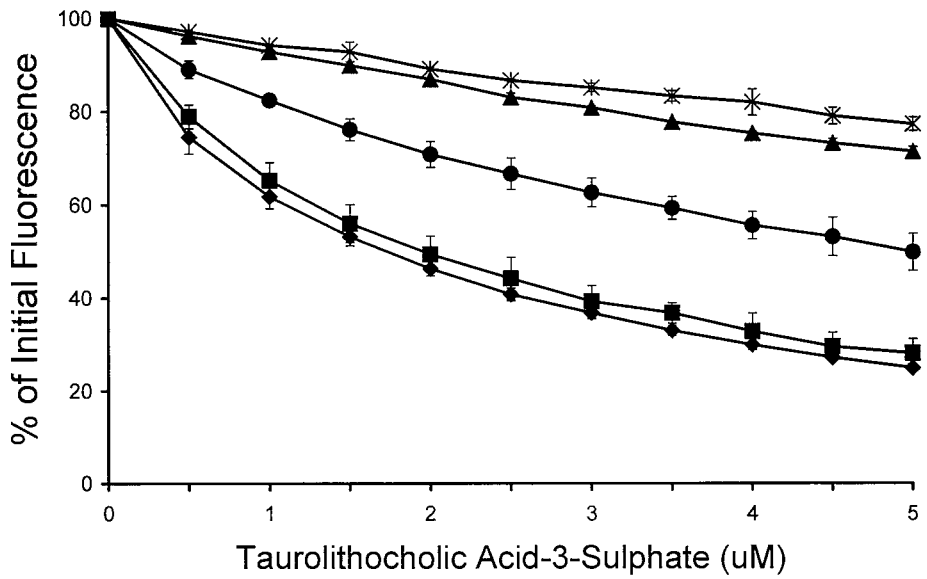

Fig 3.5.5 **The Effects of the Charge Reversal Mutagenesis on the Ability of Taurolithocholic Acid 3-Sulphate to displace DAUDA from Liver FABP**
Taurolithocholic Acid 3-Sulphate was titrated as a methanol solution into 10 mM HEPES containing 1μM DAUDA and 0.56 μM of either wild type (♦), K20E (■), K31E (▲), K33E (●) or K31E,K33E (∗) LFABP. The loss of fluorescence of the LFABP-DAUDA complex was measured at 500 nm following excitation at 350 nm. All data points shown are the mean of three titrations ± S.D

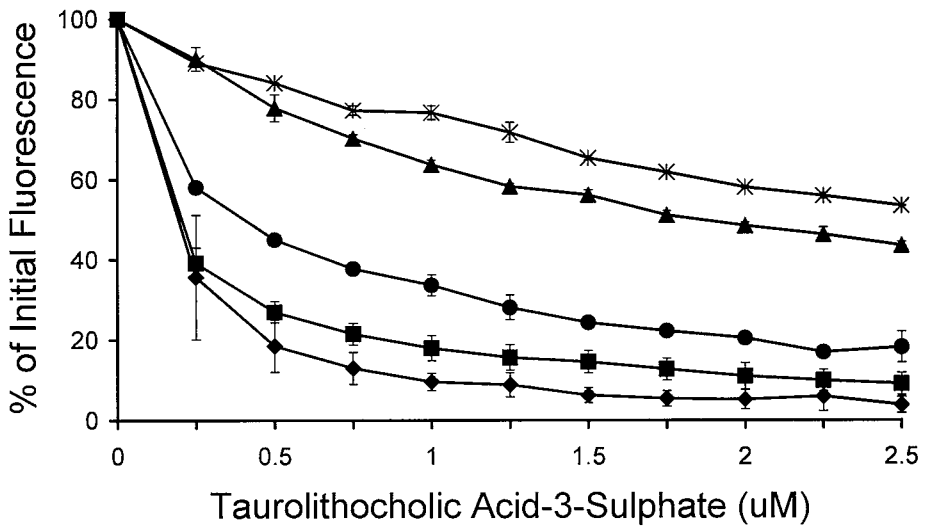

Fig 3.5.6 **The Effects of the Charge Reversal Mutagenesis on the Ability of Taurolithocholic Acid 3-Sulphate to displace ANS from Liver FABP**
Taurolithocholic Acid 3-Sulphate was titrated as a methanol solution into 10 mM HEPES containing 1μM ANS and 0.56 μM of either wild type (♦), K20E (■), K31E (▲), K33E (●) or K31E,K33E (✳) LFABP. The loss of fluorescence of the LFABP-ANS complex was measured at 460 nm following excitation at 376 nm. All data points shown are the mean of three titrations ± S.D.

3.5.2.3 Deoxycholic acid

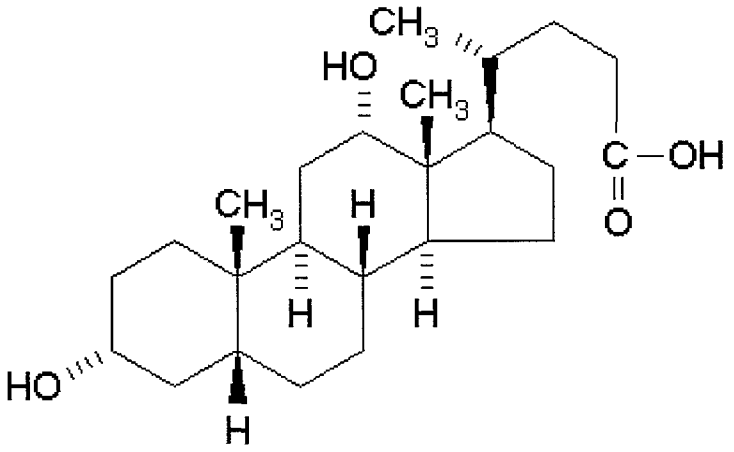

Deoxycholic acid is known to be a poor ligand for LFABP [11] and provided a useful control. When deoxycholic acid was titrated into LFABP solutions, both mutant and wild type, caused very little change in the fluorescence of the solutions. There was no major difference between any of the proteins (**Fig 3.5.7**). This result is consistent with minimal binding of deoxycholic acid to LFABP and confirms previous work with this ligand [11] that indicated that LFABP has a very low affinity for this bile acid.

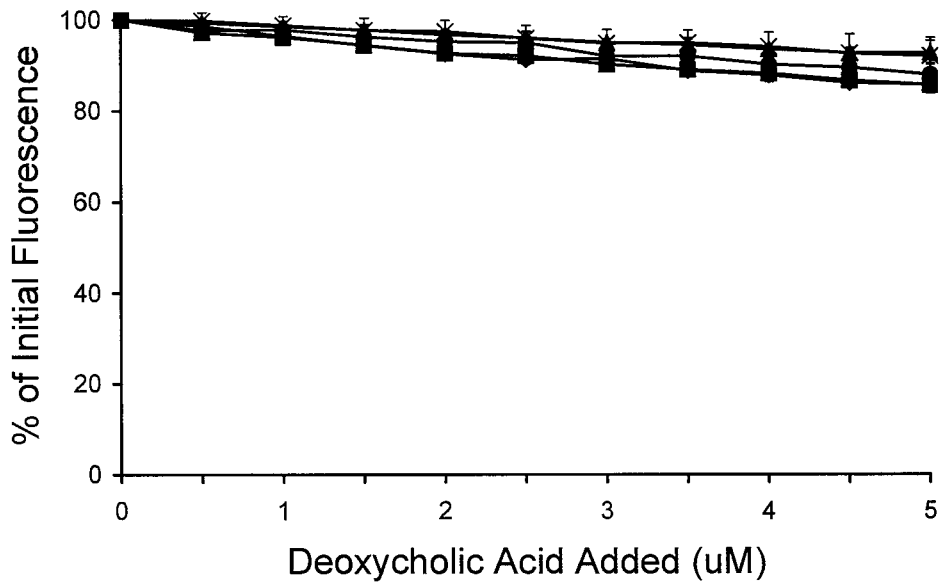

Fig 3.5.7 **The Effects of the Charge Reversal Mutagenesis on the Ability of Deoxycholic Acid to displace DAUDA from Liver FABP**
Deoxycholic Acid was titrated as a methanol solution into 10 mM HEPES containing 1μM DAUDA and 0.56 μM of either wild type (♦), K20E (■), K31E (▲), K33E (●) or K31E,K33E (✳) LFABP. The loss of fluorescence of the LFABP-DAUDA complex was measured at 500 nm following excitation at 350 nm. All data points shown are the mean of three titrations ± S.D.

3.5.2.4 Displacement of Fluorescent Probe from Wild Type and Mutant LFABPs by Lysophosphatidic Acid

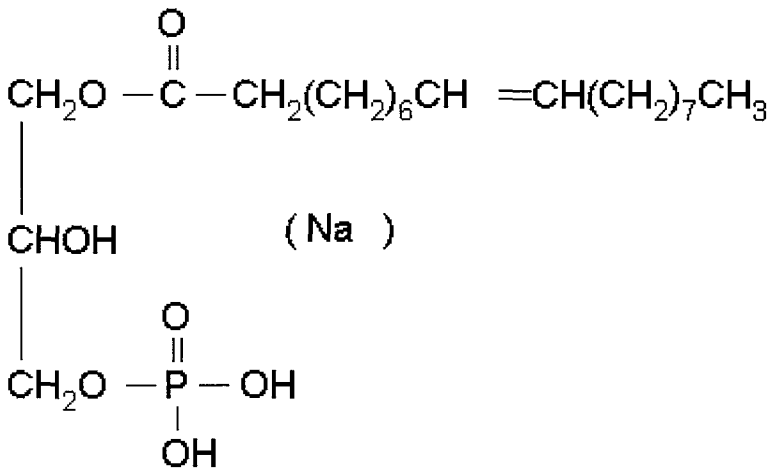

It has previously been shown that lysophospholipids are ligands for LFABP and that the lysophospholipid with the highest apparent affinity was lysophosphatidic acid [83].

The displacement of DAUDA by lysophosphatidic acid was determined and the results followed a similar overall pattern to that seen with the bile acids (see **Fig 3.5.8**). The K31E and K33E mutants show reduced binding compared with the wild type and K20E mutants. The K31E,K33E double mutant shows weaker binding than either of the K31E or K33E single mutants. Again the double mutant represents a cumulative effect of the two single mutations and no binding could be detected. There is no difference between the wild type and the K20E mutant.

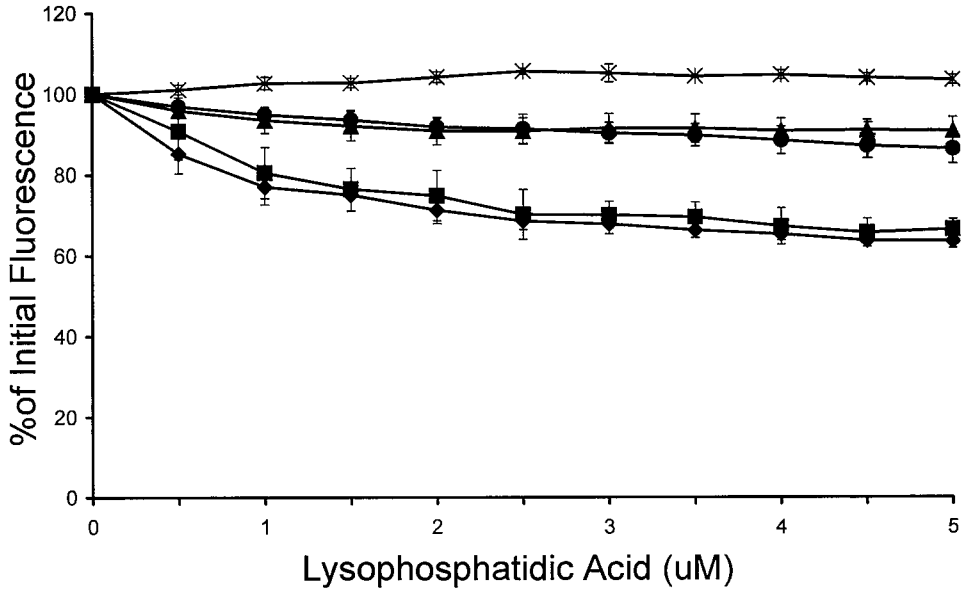

Fig 3.5.8 **The Effects of the Charge Reversal Mutagenesis on the Ability of Lysophosphatidic Acid to displace DAUDA from Liver FABP**
Lysophosphatidic Acid was titrated as a methanol solution into 10 mM HEPES containing 1μM DAUDA and 0.56 μM of either wild type (♦), K20E (■), K31E (▲), K33E (●) or K31E,K33E (✳) LFABP. The loss of fluorescence of the LFABP-DAUDA complex was measured at 500 nm following excitation at 350 nm. All data points shown are the mean of three titrations ± S.D.

When using ANS as the probe (**Fig 3.5.9**), the results are different to the displacement studies using bile acids. The addition of lysophosphatidic acid to wild type LFABP results in a large increase in fluorescence also seen with the K20E mutant. However, the increase is reduced with the other mutants and has been eliminated when using the double mutant. One possible explanation is that lysophosphatidic acid binds to LFABP without displacing ANS. This is possible because lysophosphatidic acid has only a single flexible acyl chain that should insert into the binding cavity at site 2 allowing solvent exposure of the bulky glycerolphosphate head group. Thus, this ligand should have a minimal effect on site 1. In doing so the ligand increases the hydrophobicity of the environment in which the ANS is placed, presumably now at site 1, and hence causes an increase in fluorescence. Thus a lack of fluorescence increase indicates a lack of binding.

Working on that principle, lysophosphatidic acid appears at low concentrations to bind most strongly to the K20E mutant. At concentrations of ligand up to 1 μM binding is greater to the K20E mutant than to the wild type. At concentrations of ligand higher than 1 μM, the difference in binding strength between wild type and K20E is no longer clear. A similar story is true for the K31E and K33E single mutants compared with the double mutant. At concentrations of ligand up to 0.5 μM, there appears to be little difference between the K33E mutant and the wild type. At concentrations greater than this a clear difference is observed. K31E and the double mutant have a clearly weaker binding capability than the wild type at all concentrations. At concentrations above 1.75 μM the difference between the double mutant's, K31E's and K33E's binding capabilities disappears. At this time it is not clear why there is a fall in fluorescence at higher

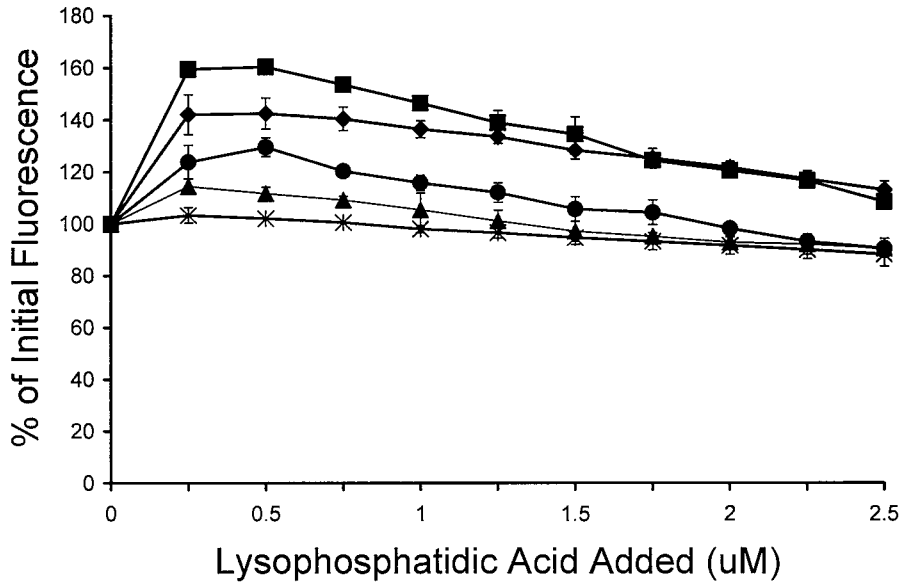

Fig 3.5.9 **The Effects of the Charge Reversal Mutagenesis on the Ability of Lysophosphatidic Acid to displace ANS from Liver FABP**
Lysophosphatidic Acid was titrated as a methanol solution into 10 mM HEPES containing 1μM ANS and 0.56 μM of either wild type (♦), K20E (■), K31E (▲), K33E (●) or K31E,K33E (✳) LFABP. The loss of fluorescence of the LFABP-ANS complex was measured at 500 nm following excitation at 350 nm. All data points shown are the mean of three titrations ± S.D.

concentrations of lysophosphatidic acid. However, it is possible that at higher concentrations, lysophosphatidic acid is forming anionic micelles and the LFABP binds to these resulting in probe displacement as seen with DOPG vesicles [25].

In conclusion the overall pattern again reflects those results already discussed in that the K31 residue is more clear than the K33 residue in binding ligand, both of which are more clear than the K20 residue which shows no difference compared with the wild type.

3.5.2.5 Displacement of Fluorescent Probe from Wild Type and Mutant LFABPs by Lysophosphatidylcholine

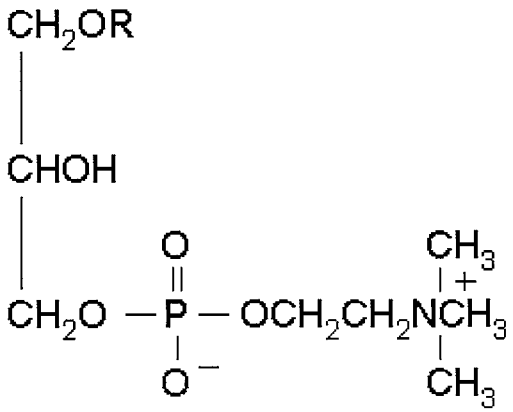

Using DAUDA with lysophosphatidylcholine, it can be seen that the ligand binds clearly less strongly to the double mutant and to the K31E mutant than to any of the other single mutants or to the wild type (**Fig 3.5.10**). The difference in binding strengths

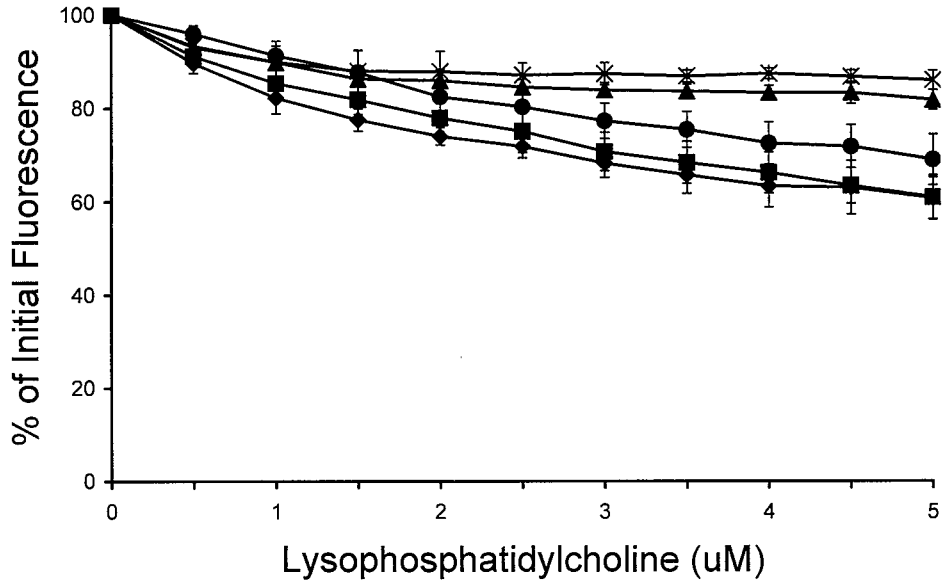

Fig 3.5.10 **The Effects of the Charge Reversal Mutagenesis on the Ability of Lysophosphatidylcholine to displace DAUDA from Liver FABP**
Lysophosphatidylcholine was titrated as a methanol solution into 10 mM HEPES containing 1μM DAUDA and 0.56 μM of either wild type (♦), K20E (■), K31E (▲), K33E (●) or K31E,K33E (✳) LFABP. The loss of fluorescence of the LFABP-DAUDA complex was measured at 500 nm following excitation at 350 nm. All data points shown are the mean of three titrations ± S.D.

between the K33E single mutant and the wild type is not large enough to be considered significant. Some studies were also performed involving ANS displacement by lysophosphatidylcholine but the results were variable and are not included. However, like with lysophosphphatidic acid, an increase in ANS fluorescence was noted with the addition of lysophosphatidylcholine.

From the results with DAUDA displacement it can be concluded that although lysophosphatidylcholine is a low affinity ligand for LFABP, the Lys31 residue plays a role in lysophosphatidylcholine binding.

3.5.2.6 Displacement of Fluorescent Probe from Wild Type and Mutant LFABPs by Oleoyl Coenzyme A

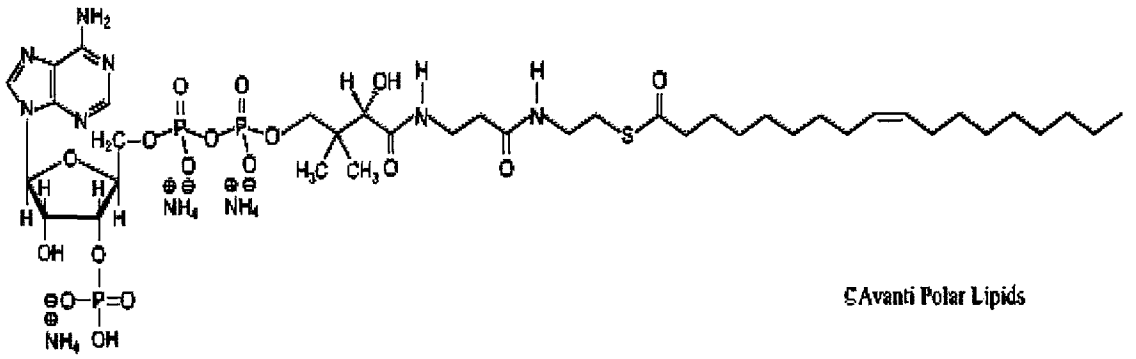

The results for the displacement of DAUDA by oleoyl coenzyme A are shown in **Fig 3.5.11**. The K31E and K33E single mutants and the K31E,K33E double mutant bind the ligand more weakly than the K20E mutant and the wild type enzyme. The K20E

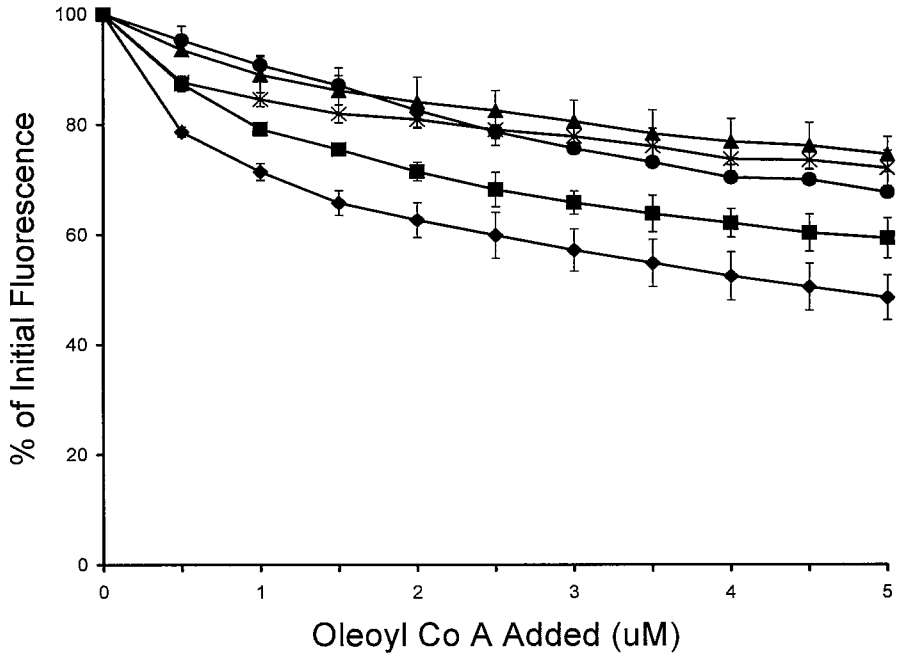

Fig 3.5.11 **The Effects of the Charge Reversal Mutagenesis on the Ability of Oleoyl CoA to displace DAUDA from Liver FABP**
Oleoyl CoA was titrated as a solution in 10 mM HEPES into 10 mM HEPES containing 1μM DAUDA and 0.56 μM of either wild type (♦), K20E (■), K31E (▲), K33E (●) or K31E,K33E (✳) LFABP. The loss of fluorescence of the LFABP-DAUDA complex was measured at 500 nm following excitation at 350 nm. All data points shown are the mean of three titrations ± S.D.

mutant and the wild type enzyme show no difference in their ability to bind oleoyl coenzyme A.

It had been observed that oleoyl CoA binding is sensitive to the salt concentration of the medium. When the assay is carried out in the presence of 100mM NaCl, there is no observed difference between the wild type and any of the mutants (**Fig 3.5.12**). The presence of the high salt concentration promotes hydrophobic interactions between the ligand and the protein. The increased preferance for the ligand to be in a hydrophobic environment is enough to overcome the charge reversal mutations and hence wild type enzyme and the mutants have very similar binding properties in a solution with a high salt concentration. However, small differences in the calculated K_i values for oleoyl CoA binding can be seen in the presence of NaCl. The K_i value for wild type LFABP (0.21 μM) is lower than the K_i values for the single mutants K31E and K33E LFABP (both 0.49 μM).

3.6 K_i Values

The apparent K_d values listed in **section 3.4** were used to determine K_i values for ligand binding to FABP using the methods described in **section 2.5.3**.

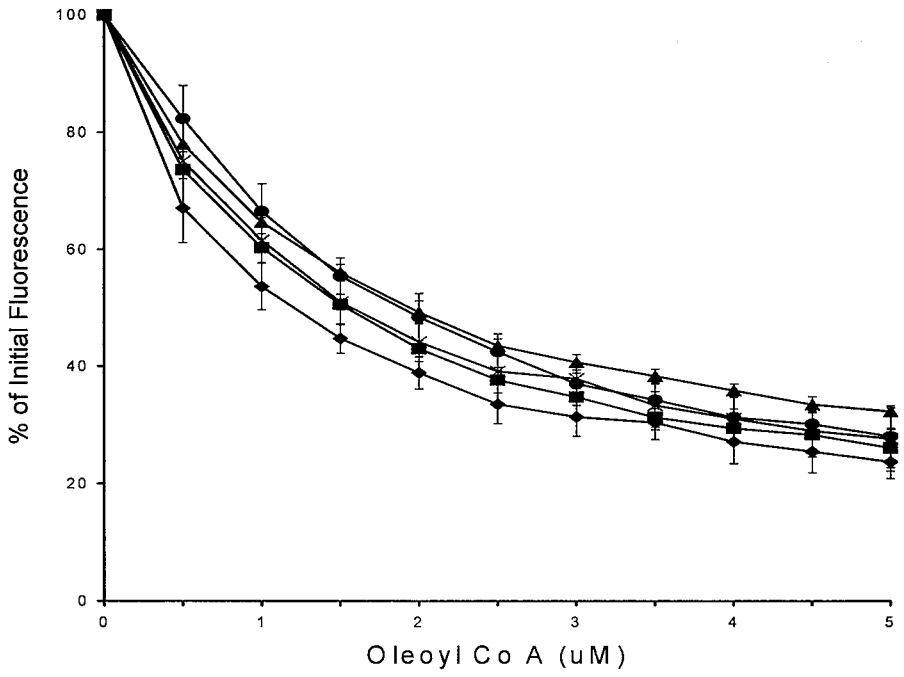

Fig 3.5.12 **The Effects of the Charge Reversal Mutagenesis on the Ability of Oleoyl CoA to displace DAUDA from Liver FABP in the presence of NaCl**
Oleoyl CoA was titrated as a solution in 10 mM HEPES into 10 mM HEPES containing 100 mM NaCl, 1μM DAUDA and 0.56 μM of either wild type (♦), K20E (■), K31E (▲), K33E (●) or K31E,K33E (∗) LFABP. The loss of fluorescence of the LFABP-DAUDA complex was measured at 500 nm following excitation at 350 nm. All data points shown are the mean of three titrations ± S.D.

	FABP WT (μM)	FABP K20E (μM)	FABP K31E (μM)	FABP K33E (μM)	FABP K31E,K33E (μM)
Oleic Acid	**0.04±0.004**	**0.04±0.005**	**0.08±0.009**	**0.03±0.002**	**0.07±0.008**
Lithocholic Acid	**0.31±0.004**	**0.45±0.02**	**0.80±0.04**	**0.45±0.04**	**0.78±0.07**
Taurolithocholic Acid 3-Sulphate	**0.29±0.03**	**0.42±0.08**	**>1.1**	**1.25±0.07**	**>1.1**
Oleoyl CoA	**0.81**	**>1.1**	**>1.1**	**>1.1**	**>1.1**
Oleoyl CoA (+0.1M NaCl)	**0.21±0.04**	**0.34±0.02**	**0.49±0.03**	**0.49**	**0.42±0.06**

Table 3.6.1 K_i values for ligand binding to FABP, displacing DAUDA. These values were determined using the method of Kane and Bernlohr (section 2.5.3). These values will represent a composite value for the two binding sites for ligand where applicable. All values are the mean of titrations performed in triplicate ± S.D.

	FABP WT (μM)	FABP K20E (μM)	FABP K31E (μM)	FABP K33E (μM)	FABP K31E,K33E (μM)
Oleic Acid	**0.13±0.02**	**0.13±0.04**	**0.31±0.02**	**0.14±0.008**	**0.33±0.09**
Lithocholic Acid	**0.30±0.09**	**0.32±0.04**	**1.32±0.24**	**0.44±0.06**	**1.49±0.27**
Taurolithocholic Acid 3-Sulphate	**0.11±0.03**	**0.098±0.009**	**1.39±0.06**	**0.27±0.12**	**>1.90**

Table 3.6.2 K_i values for ligand binding to FABP, displacing ANS. These values were determined using the method of Kane and Bernlohr (section 2.5.3). These values will represent a composite value for the two binding sites for ligand where applicable. All values are the mean of titrations performed in triplicate ± S.D.

3.7 Discussion

The α-helical region of FABPs has been reported as playing a major role in binding to phospholipid vesicles [84, 85, 30]. In this laboratory, this region in LFABP has also been shown to play a role in the protein binding to anionic vesicles [25]. In addition,

LFABP binds a series of ligands with anionic side chains that are thought to enter the protein through a region adjacent to the α-helical portion of LFABP. It was therefore of interest to determine whether cationic residues in the two α-helices are also of importance to ligand binding. To test this theory charge reversal mutants of LFABP where Lys-20, Lys-31 and Lys-33 were converted to glutamate have been produced and their ligand-binding properties compared to the wild type protein.

LFABP is unique amongst the FABP family in that it binds fatty acids in a 2 : 1 stoichiometry. The two oleic acid binding sites are shown in **Fig 3.1.1**. The oleic acid at site 1 is positioned deep within the binding cavity of LFABP, whereas the oleic acid at site 2 extends through a hypothesized portal region of LFABP with the carboxyl group exposed to the solvent. It is site 2 that is in close proximity to the three cationic lysine residues investigated in this chapter. Whilst fatty acids bind in a 2 : 1 stoichiometry, other more bulky ligands bind in a 1 : 1 stoichiometry. These mutations should therefore provide information as to where the more bulky ligands, such as the bile acids investigated in this chapter, are positioned in LFABP. The results in this chapter have shown that the lysine residue at position 31 that is part of the α-helical region of the protein and also contributes to the surface charge of the protein, plays a significant role in ligand binding to LFABP.

As a general summary mutation of Lys-33 and to a greater extent Lys-31, to glutamate, significantly reduces the affinity of the protein for its ligands. Lys-33 appears to have a role in the binding of some ligands to the protein, but not others. Lys-31 on the

other hand plays a significant role in the binding of every physiological ligand of LFABP investigated in this chapter. The importance of Lys-31 is apparent in every displacement study from the figures in this chapter with the exception of oleic acid. In **Fig 3.5.1** a significant difference between the wild type and charge reversal mutants, in terms of ability of oleic acid to displace DAUDA is not apparent. However, K_i values for this ligand showed that LFABP WT (K_i 0.04μM) bound oleic acid with significantly higher affinity than LFABP K31E (K_i 0.08 μM). The explanation for oleic acid binding reporting a small but significant difference between the wild type and K31E mutant LFABP is related to the position of the mutation. Lys-31 is positioned in the portal region of LFABP at oleic acid binding site 2. DAUDA however, binds at oleic acid binding site 1 which is not directly affected by the mutation. Lowering the affinity of site 2 for oleic acid will still indirectly affect site 1 as the two sites are structurally linked with site 2 only being fully formed after oleic acid binds at site 1 [11]. Thus, binding of an oleic acid at site 2 stabilises ligand bound at site 1.

ANS was able to graphically display greater differences in affinity of oleic acid for LFABP WT and K31E than seen for DAUDA displacement. Such a result makes it tempting to speculate that ANS binds at site 2. However, lysophosphatidic acid binding provides evidence to the contrary. From **Fig 3.5.8** and **Fig 3.5.9** it appears that lysophosphatidic acid binds to LFABP and is affected by the mutation in the portal region. As lysophosphatidic acid binds in a 1:1 stoichiometry it would appear that it binds, at least in part, at oleic acid binding site 2. The results of the binding study using this ligand in the presence of ANS **Fig 3.5.9** suggest that the ligand does not displace

ANS. The suggestion is that ANS must therefore be binding at oleic acid binding site 1. A further possibility is that ANS can bind at either site 1 or site 2, it may be that this molecule binds preferentially binds at site 2, but is displaced to site 1 by lysophosphatidic acid. NMR work has suggested that flipping between the two sites occurs with fatty acids [18].

ANS is advantageous over DAUDA in that it binds with lower affinity and is more sensitive to ligand binding. DAUDA on the other hand is preferable because of its lower K_d value, hence it is more strongly bound to the protein than ANS and in turn therefore produces less error in binding studies.

Comparing the results from lithocholic acid and taurolithocholic acid 3-sulphate binding studies in this chapter shows that the latter is more greatly affected by the charge reversal mutagenesis than the former. This result suggests that either the taurine group or the 3-sulphate group of taurolithocholic acid 3-sulphate protrudes through the portal region of LFABP where Lys-31 is positioned. If either one of these anionic side chains does protrude through the portal region it would account for this large difference in the effect of charge reversal mutagenesis between these two ligands. The orientation of taurolithocholic acid 3-sulphate is further investigated in chapter 5 of this work.

The results of DAUDA displacement by oleoyl CoA are consistent with the portal region and specifically K31 and K33, making a contribution to binding. It is not known how oleoyl CoA binds to LFABP but this ligand has been modeled into the crystal

structure of LFABP. It is apparent that the binding of this complex molecule involves a large number of interactions with LFABP with a major contribution coming from hydrophobic binding within the cavity. The results described in this chapter are consistent with electrostatic interactions within the portal region playing a minor role in the binding of this ligand.

Chapter 4 – Charge Reversal Mutagenesis of Surface Cationic Residues Outside the α-Helical Region

4. Charge Reversal Mutagenesis of Surface Cationic Residues Outside the α-helical Region

4.1 Introduction

In chapter 3 the effect on ligand binding of three charge reversal mutants, K20E, K31E and K33E, in the α-helical region of LFABP were investigated using fluorescent ligand binding and displacement studies. The effect of these mutations on the binding of LFABP to anionic phospholipids vesicles had been described previously by Davies *et al* [25]. A number of other cationic residues make a significant contribution to the surface positive charge of LFABP. These residues are Lys-36, Lys-47 and Lys-57 [9]. In this chapter these residues have been individually changed to glutamate by charge reversal mutagenesis resulting in a net loss of two positive charges. The resultant mutants have been studied in terms of ligand binding and binding to anionic phospholipids vesicles.

Three single charge reversed mutants were produced; K36E, K47E and K57E, the positions of these three residues are shown in **Fig 4.1.1**.

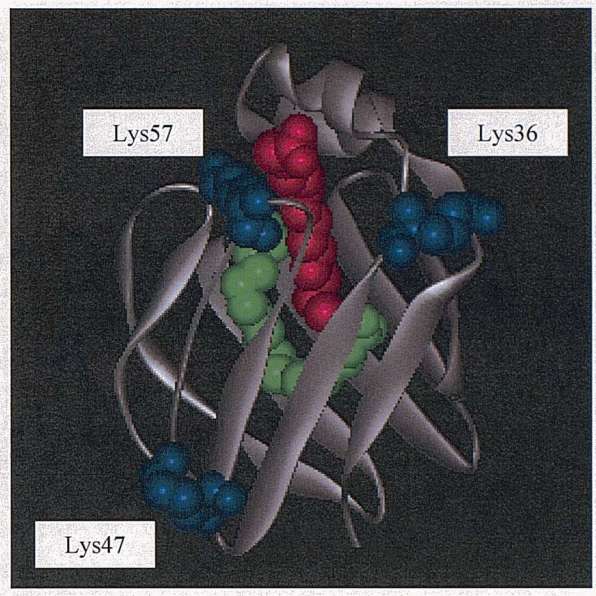

Fig 4.1.1 LFABP showing the locations of the three lysine residues contributing to the surface charge of the protein that are to be replaced by glutamate. The lysine residues that are to be replaced are shown in blue. Also shown are the two oleic acid molecules that bind to LFABP, at site 1 (green) and site 2 (red)

4.2 Expression of Charge Reversal Mutants

Joanne Davies in this laboratory employed the PCR method of mutagenesis [55] to produce the LFABP single mutants K36E, K47E, K57E and these transfected *E. coli* were available at the start of this thesis work. They were expressed and purified using the same method as for wild-type LFABP as described in chapter 2 of this work. The yield of all three mutants was comparable to the wild-type protein at 15-20 mg per litre of culture. Sample purity was checked on SDS-PAGE with coomassie blue staining (see **Fig 4.2.1**) and indicated that protein purity was greater than 99% for all mutants.

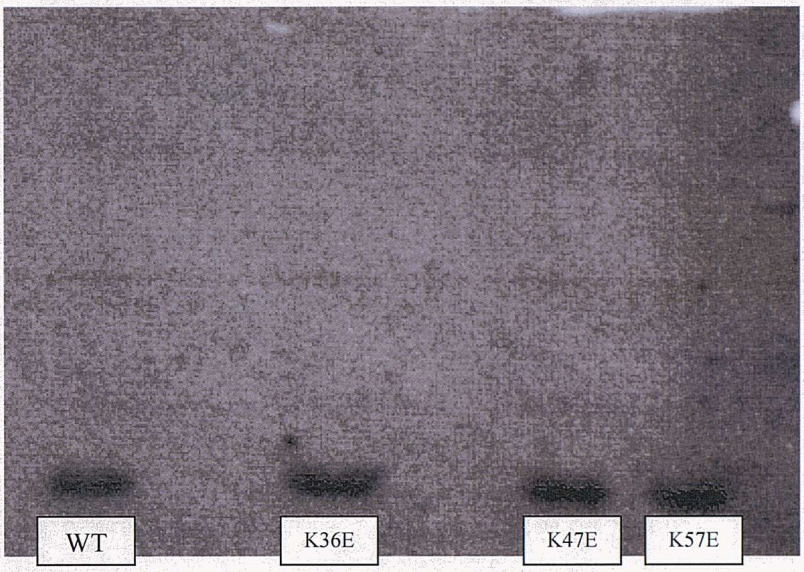

Fig 4.2.1 SDS-PAGE of LFABP WT, K36E, K47E and K57E

4.3 Circular Dichroism

Circular Dichroism (CD) was used to confirm that the mutants were all correctly folded. The spectra for each of the charge reversal mutants are shown in **Fig 4.3.1**. The spectra for each of the mutants are essentially identical to the wild type spectrum, showing that these mutants are correctly folded. The spectra of the α-helical charge reversal mutants are included for comparison.

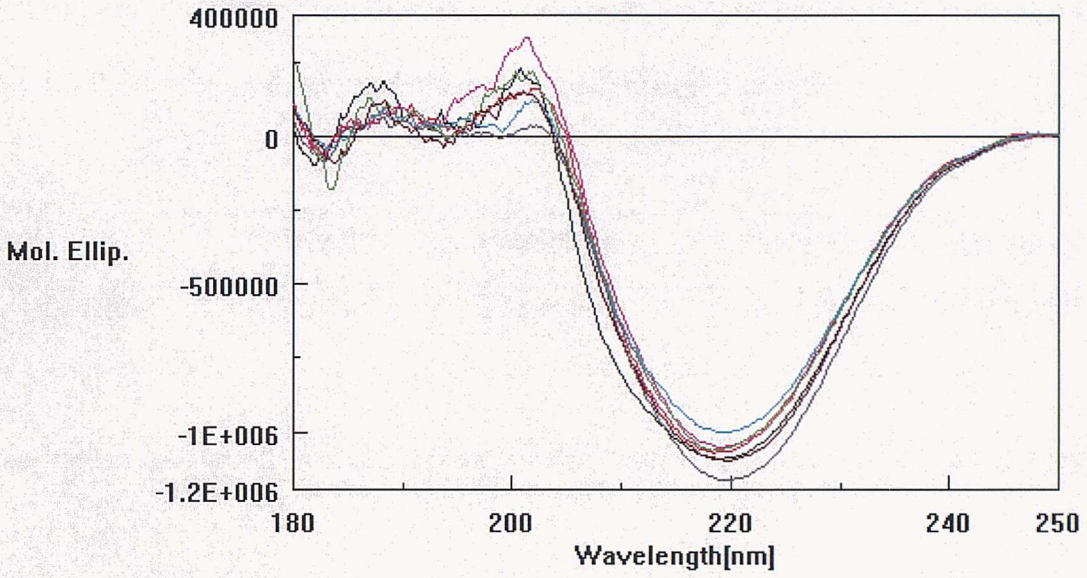

Fig 4.3.1 Molar Ellipticity scan for FABPWT and charge reversal mutants between 180 and 250nm. Each line represents a different protein. FABP WT (black); FABP K20E (red); FABP K31E (pink); FABP K31E,K33E (green); FABP K36E (blue); FABP K47E (brown); FABP K57E (grey)

4.4 DAUDA Binding to LFABP Charge Reversal Mutants

DAUDA was titrated into each of the mutants, as a solution in methanol, to achieve a final concentration of 1 μM. The final methanol concentration did not exceed 1% of the total volume and a methanol blank was used to correct for this. The increase in fluorescence when DAUDA binds to LFABP was corrected for DAUDA fluorescence in buffer and the K_d values were calculated from the resultant saturation curves using SigmaPlot software, as described in chapter 3.

The K_d values of the proteins for DAUDA are shown in **Table 4.4.1**. The results show no significant difference in the DAUDA binding properties of any of the mutant

LFABP proteins compared to the wild type LFABP. Therefore there were no apparent adverse affects of charge reversal mutagenesis on DAUDA binding.

	FABP WT	FABP K36E	FABP K47E	FABP K57E
K_d (μM)	0.14 ± 0.03	0.16 ± 0.03	0.19 ± 0.05	0.14 ± 0.01

Table 4.4.1 Apparent DAUDA K_d values for FABP wild type and charge reversal mutants. All values are the mean of titrations performed in triplicate + S.D.

4.5 Displacement of the Fluorescent Probe DAUDA from Wild Type and Mutant LFABPs by Ligands

The K_i values for displacing ligands were calculated using the method of Kane and Bernlohr as described in chapter 2. This calculation is only possible where displacement is 50% or greater by the ligand that is investigated. Where this is not possible, the minimal K_i value for 50% displacement at 5 μM ligand is indicated. The values are recorded in **Table 4.7.1** at the end of this chapter. Values will be mentioned, where appropriate, throughout this chapter.

4.5.1 Oleic Acid

No major difference was seen between the wild type and the surface residue charge reversal mutants (See **Fig 4.5.1.1**). There may be differences in binding occurring with the K36E and K57E mutants that are not apparent in this assay due to DAUDA

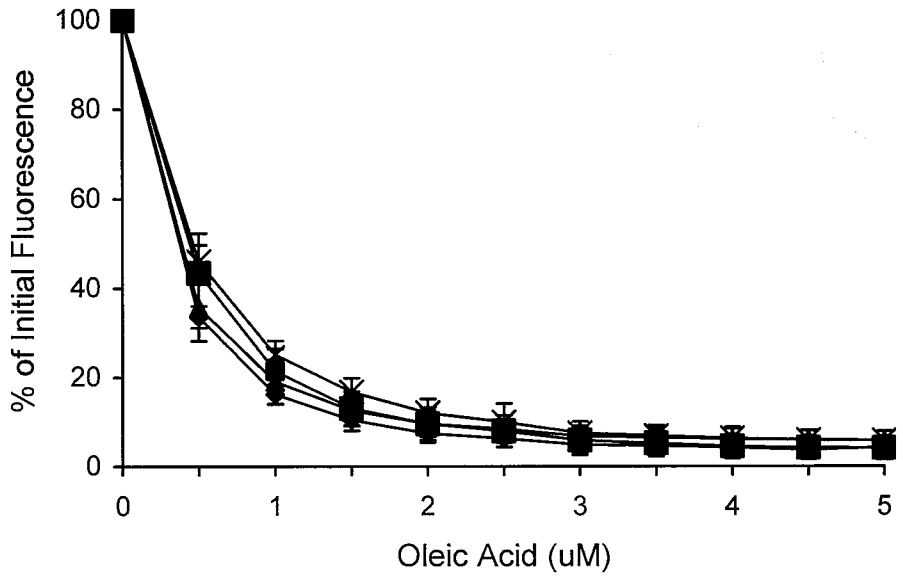

Fig 4.5.1.1 **The Effects of the Charge Reversal Mutagenesis on the Ability of Oleic Acid to displace DAUDA from Liver FABP**

Oleic Acid was titrated as a methanol solution into 10 mM HEPES containing 1μM DAUDA and 0.56 μM of either wild type (♦), K36E (■), K47E (▲) or K57E (X) LFABP. The loss of fluorescence of the LFABP-DAUDA complex was measured at 500 nm following excitation at 350 nm. All data points shown are the mean of three titrations ± S.D.

binding at the first fatty acid binding site, whereas these residues are remote from this site. It is noted that the K_i values suggest that there may be weakened binding of oleic acid to the three mutants (K_i values 0.06-0.07 μM) compared to the wild type protein (0.04 μM). Such small differences are not obvious from DAUDA displacement curves. The small difference in K_i values may represent the weakened binding of oleic acid at site 2 which will in turn affect the binding at site 1, where DAUDA is positioned. The two sites are structurally linked and binding of ligand at site 2 should stabilise bound ligand at site 1. This has been discussed in more detail in chapter 5.

4.5.2 Bile Acids

Many bile acids are physiological ligands [56]. The lithocholic acid derivatives have been selected for investigation in this section as these showed the highest affinity of the bile acids that have been evaluated as ligands [57]. The importance of these ligands is discussed in more detail in **section 3.5.2**.

4.5.2.1 Lithocholic Acid

Titration of the lithocholic acid into DAUDA-FABP complex shows a significantly stronger binding of lithocholic acid to the wild type protein (K_i 0.17 μM) compared with LFABP K57E (K_i 0.32 μM) **Fig 4.5.2.1**. No significant difference is seen between binding of wild type, K36E (K_i 0.2 μM) or K47E (K_i 0.18 μM) LFABP, to lithocholic acid. K57 is therefore proposed to play a role in lithocholic acid binding.

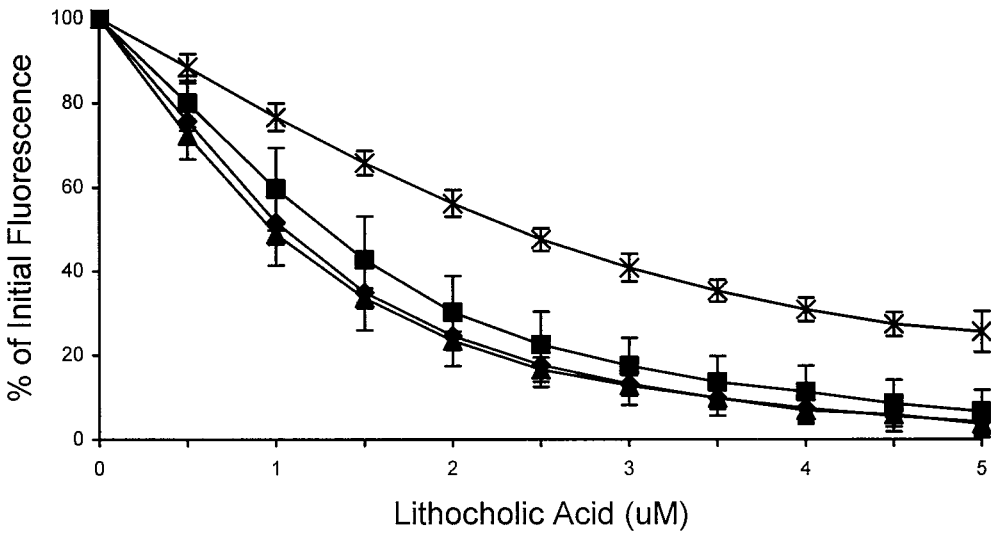

Fig 4.5.2.1 **The Effects of the Charge Reversal Mutagenesis on the Ability of Lithocholic Acid to displace DAUDA from Liver FABP**
Lithocholic Acid was titrated as a methanol solution into 10 mM HEPES containing 1μM DAUDA and 0.56 μM of either wild type (♦), K36E (■), K47E (▲) or K57E (X) LFABP. The loss of fluorescence of the LFABP-DAUDA complex was measured at 500 nm following excitation at 350 nm. All data points shown are the mean of three titrations ± S.D.

4.5.2.2 Taurolithocholic Acid 3-Sulphate

Titrating in the ligand taurolithocholic acid 3-sulphate suggests for the first time that a second surface lysine residue of LFABP under investigation in this section, is involved in ligand binding. Taurolithocholic acid 3-sulphate has a significantly reduced ability to displace DAUDA in both the K57E (K_i > 0.70 μM) and the K36E (K_i 0.77 μM) LFABP mutants compared with the wild type protein (K_i 0.24 μM), **Fig 4.5.2.2**. Again there is no difference seen in the affinity of the K47E mutant (K_i 0.35 μM) and the wild type LFABP.

The degree of reduction of binding strength is greater with taurolithocholic acid 3-sulphate where K_i values increase from 0.24 μM to >0.77 μM, than with lithocholic acid where K_i values increase from 0.17 μM to 0.32 μM as a result of the charge reversal mutagenesis at K57. These differences reflect either the taurine group or the sulphate group of taurolithocholic acid 3-sulphate protruding through the portal region of LFABP where both K36 and K57 are located. Either one of these anionic groups would be expected to be involved in electrostatic interactions with cationic amino acid residues within the portal region. This finding supports the similar conclusion drawn in chapter 3. It is not possible using these results to determine which of the two anionic side chains on taurolithocholic acid 3-sulphate is involved in these electrostatic interactions at the portal region. However, this situation is clarified by protein fluorescence studies described in chapter 5 where the orientation of bile acid binding is investigated in more detail.

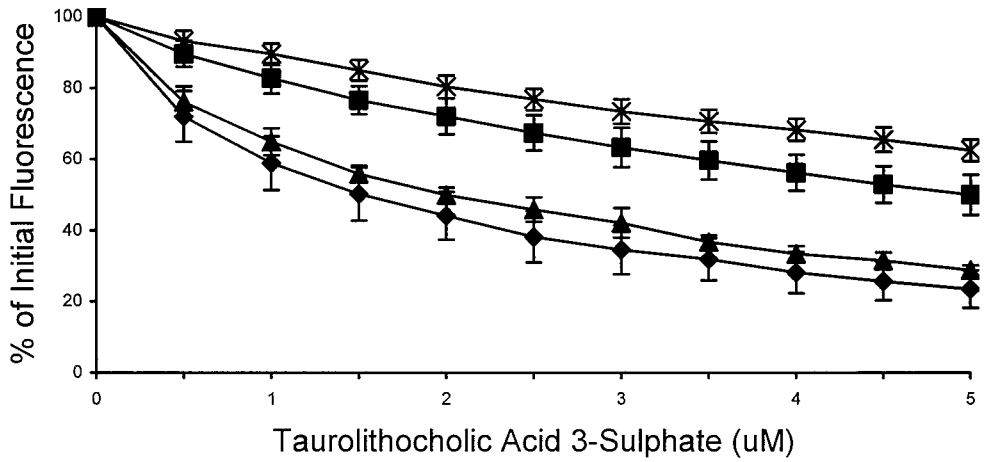

Fig 4.5.2.2 **The Effects of the Charge Reversal Mutagenesis on the Ability of Taurolithocholic Acid 3-Sulphate to displace DAUDA from Liver FABP**
Taurolithocholic Acid 3-Sulphate was titrated as a methanol solution into 10 mM HEPES containing 1μM DAUDA and 0.56 μM of either wild type (♦), K36E (■), K47E (▲) or K57E (X) LFABP. The loss of fluorescence of the LFABP-DAUDA complex was measured at 500 nm following excitation at 350 nm. All data points shown are the mean of three titrations ± S.D.

4.5.3 Oleoyl Coenzyme A

The ligand binding of oleoyl CoA to LFABP has been discussed in chapter 3. Modelling studies require that the oleoyl group together with the pantothenate part of coenzyme A are located in the binding cavity whereas the ADP moiety protrudes through the portal region [9].

DAUDA displacement studies indicate that there is a lowered affinity of the K36E and K57E LFABP mutants for oleoyl coenzyme A (K_i values >0.75 and >0.7 μM respectively) as seen in **Fig 4.5.3.1**, compared with the wild type protein (K_i 0.39 μM). In contrast there was found to be no significant difference between the K47E mutant (K_i 0.49 μM) and the wild type protein. This would suggest that oleoyl coenzyme A undergoes electrostatic interactions with K36 and K57 when binding to LFABP, a result consistent with the modeled structure of oleoyl CoA bound to LFABP [9].

The binding of oleoyl CoA to LFABP is expected to rely to a large extent on hydrophobic interactions. Increasing the salt concentration of the medium in which the ligand and protein are binding should promote these interactions and in turn, promote binding. For this reason titration were repeated in conditions of higher ionic strength.

In the presence of 100mM NaCl the binding affinities of the wild type compared to the mutants are noticeably more similar (**Fig 4.5.3.2**). Only the K57E mutant (K_i 0.53 μM) shows a significant difference from the wild type protein (K_i 0.29 μM) in terms of

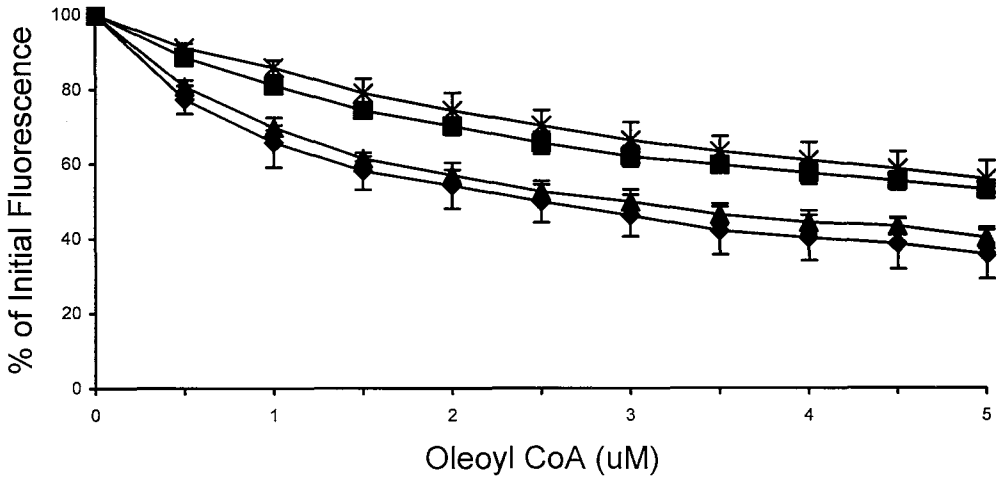

Fig 4.5.3.1 **The Effects of the Charge Reversal Mutagenesis on the Ability of Oleoyl CoA to displace DAUDA from Liver FABP**
Oleoyl CoA was titrated as a methanol solution into 10 mM HEPES containing 1μM DAUDA and 0.56 μM of either wild type (♦), K36E (■), K47E (▲) or K57E (X) LFABP. The loss of fluorescence of the LFABP-DAUDA complex was measured at 500 nm following excitation at 350 nm. All data points shown are the mean of three titrations ± S.D.

binding. The difference in binding affinity of the K57E mutant and the wild type protein is less than that observed in the absence of NaCl. The effect of charge reversal mutagenesis was expected to be reduced in the presence of 100 mM NaCl as the salt will interfere with electrostatic interactions. As it is electrostatic interactions that are under scrutiny with the charge reversal mutants, the presence of a high salt concentration will negate their effect.

4.6 Displacement of the Fluorescent Probes DAUDA from Wild Type and Mutant LFABPs by Anionic Phospholipids

The binding of LFABP to anionic phospholipids at low ionic strength results in a conformational change in LFABP that causes release of DAUDA from the protein. The titration of DOPG vesicles into a highly fluorescent FABP-DAUDA complex results in a dramatic loss of fluorescence consistent with the LFABP coating the surface of the vesicles. A similar coating phenomenon is seen when 14 kDa $sPLA_2$ is added to anionic vesicles [58].

The interaction between LFABP and anionic phospholipids involves electrostatic interactions affected by ionic strength, followed by hydrophobic interactions between the protein and phospholipids [25]. As electrostatic interactions are involved in binding of anionic phospholipids such as DOPG to the protein, it was thought that positively charged residues on the surface of LFABP may be involved. Indeed this has already been

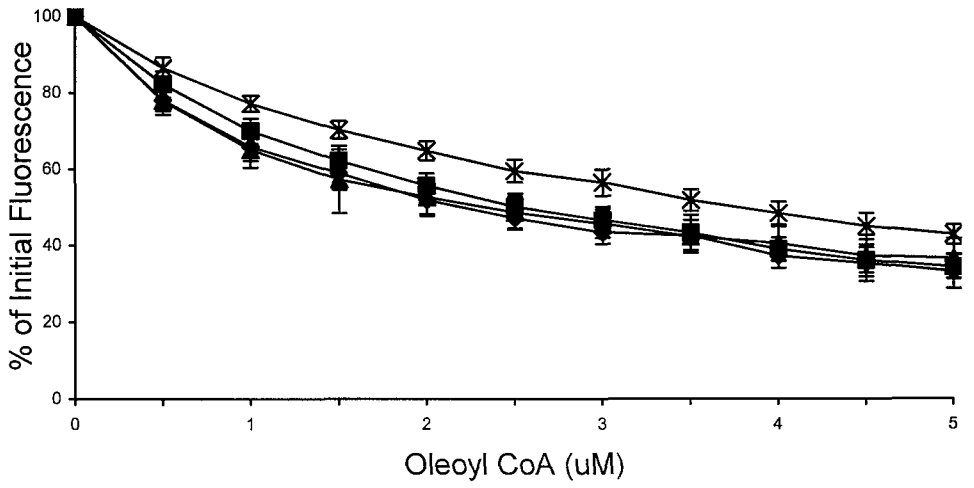

Fig 4.5.3.2 **The Effects of the Charge Reversal Mutagenesis on the Ability of Oleoyl CoA to displace DAUDA from Liver FABP in the presence of NaCl**
Oleoyl CoA was titrated as a methanol solution into 10 mM HEPES containing 1μM DAUDA, 100 mM NaCl and 0.56 μM of either wild type (♦), K36E (■), K47E (▲) or K57E (X) LFABP. The loss of fluorescence of the LFABP-DAUDA complex was measured at 500 nm following excitation at 350 nm. All data points shown are the mean of three titrations ± S.D.

shown to be true for Lys31 [25] by Joanne Davies working in this laboratory. Charge reversal mutagenesis of Lys31 inhibited, but did not prevent, binding of DOPG to LFABP. Therefore it was expected that other residues were involved in the initial electrostatic interaction with anionic phospholipid vesicles and hence the investigation of these three residues which contribute to the surface charge of the protein.

4.6.1 Dioleoyl-phosphatidylglycerol

The binding of wild-type LFABP and the three mutants K36E, K47E and K57E to dioleoyl-phosphatidylglycerol (DOPG) vesicles (**Fig 4.6.1**) highlighted the K36E and K57E mutants as having a reduced binding affinity for these vesicles. The K47E mutant showed showed a very similar affinity for DOPG to that shown by the wild type protein and binds DOPG with a comparable stoichiometry.

The importance of K36 and K57 in anionic phospholipid binding to LFABP, along with the K31 residue previously highlighted as significant by Joanne Davies, is noteworthy. All three of these residues are positioned at the portal region of LFABP. This region of LFABP must play a key role in phospholipid binding to the protein.

The results obtained with DOPG to this point have used 100% DOPG vesicles. In the mammalian cell only 20% of phospholipids in membranes are anionic and so it was

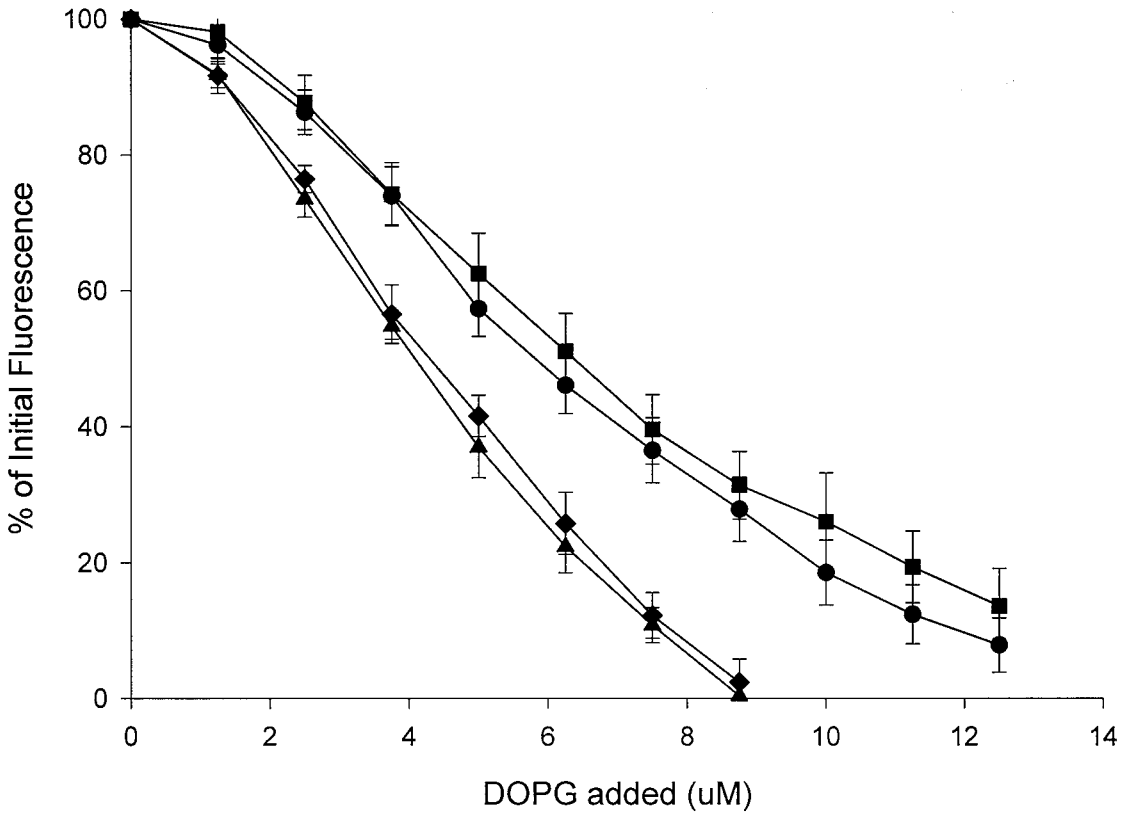

Figure 4.6.1 **The Effects of Charge Reversal Mutations on the Ability of Anionic Phospholipid Vesicles to Displace DAUDA from LFABP**
DOPG was titrated as a methanol solution into 10 mM HEPES containing 1 μM DAUDA and 0.56 μM of either wild type (♦), K31E (■), K47E (▲) or K57E (●) LFABP. The loss of fluorescence of the L-FABP/DAUDA complex was measured at 500 nm following excitation at 350 nm. All data points shown are the mean of three titrations ± S.D.important to confirm that these results were repeatable in equivalent vesicles. DOPG readily mixes with dioleoyl-phosphatidylcholine (DOPC) and so 20mol% DOPG in DOPC vesicles were prepared and the phospholipid titrations repeated.

important to confirm that these results were repeatable in vesicles of an equivalent charge ratio. DOPG readily mixes with dioleoyl-phosphatidylcholine (DOPC) and so 20 mol% DOPG in DOPC vesicles were prepared and the phospholipid titrations repeated.

The results with 20mol% DOPG in DOPC vesicles produced the same result as the 100% DOPG vesicles, confirming the importance of K36 and K57 in binding of LFABP to phospholipid vesicles (**Fig 4.6.2**). Under these conditions binding of K47E appeared to be enhanced compared to wild type, as judged by DAUDA displacement. The titration curve may simply be representative of the higher K_d value of the K47E mutant for DAUDA (0.19 μM) compared to the wild type protein (0.14 μM).

4.7 K_i Values

The apparent K_d values listed in **section 4.4** were used to determine K_i values for ligand binding to FABP using the methods described in **section 2.5.3**.

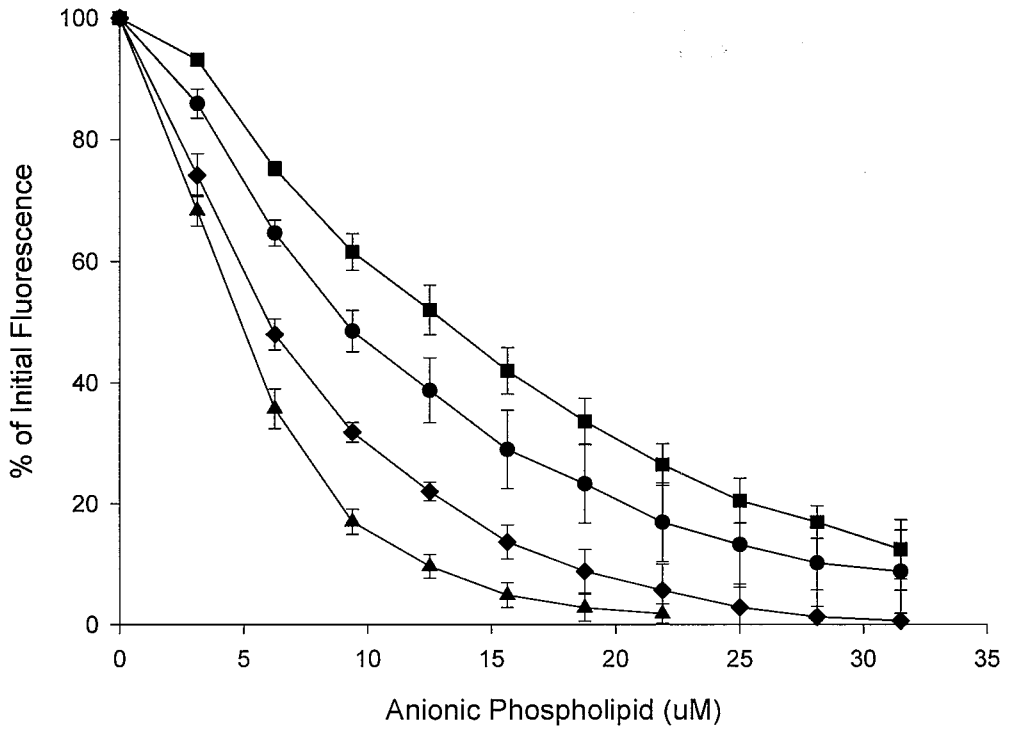

Figure 4.6.2 **The Effects of Charge Reversal Mutations on the Ability of 20 mol% Anionic Phospholipid Vesicles to Displace DAUDA from LFABP**
20 mol% DOPG was titrated as a methanol solution into 10 mM HEPES containing 1 μM DAUDA and 0.56 μM of either wild type (♦), K31E (■), K47E (▲) or K57E (●) LFABP. The loss of fluorescence of the L-FABP/DAUDA complex was measured at 500 nm following excitation at 350 nm. All data points shown are the mean of three titrations ± S.D.

	FABP WT (μM)	FABP K36E (μM)	FABP K47E (μM)	FABP K57E (μM)
Oleic Acid	**0.04 ± 0.004**	**0.07 ± 0.015**	**0.06 ± 0.01**	**0.07 ± 0.003**
Lithocholic Acid	**0.17 ± 0.04**	**0.20 ± 0.04**	**0.18 ± 0.01**	**0.32 ± 0.02**
Taurolithocholic Acid 3-Sulphate	**0.24 ± 0.08**	**0.75**	**0.35 ± 0.04**	**> 0.75**
Oleoyl CoA	**0.39 ± 0.12**	**> 0.75**	**0.49 ± 0.04**	**> 0.75**
Oleoyl CoA (+0.1M NaCl)	**0.29 ± 0.04**	**0.38 ± 0.06**	**0.44 ± 0.09**	**0.53 ± 0.06**

Table 4.7.1 K_i values for ligand binding to FABP. These values were determined using the method of Kane and Bernlohr (**see 2.5.3**). These values will represent a composite value for the two binding sites for ligand where applicable. All values are the mean of titrations performed in triplicate ± S.D. Where addition of ligand fails to decrease fluorescence by 50% a K_i value cannot be calculated and a K_i value is given as greater than the maximum value attainable at 5μM ligand.

4.8 Stability of Mutants

It needed to be established that any differences in the binding of the wild type and mutant FABP to DOPG vesicles, were due to the altered charges of the protein rather than simply a change in stability of the protein at an anionic phospholipid interface. The residues contributing to surface charge under investigation in this chapter were tested and the α-helical charge reverse mutants discussed in chapter 3 are also included for comparison.

To confirm that the differences in DOPG binding and DAUDA release are not due to stability alone Circular Dichroism (CD) of the wild type and mutant proteins were carried out over a range of temperatures. Molar Ellipticity was measured three times at 220nm for each protein at each temperature, after a 15 minute incubation period. The

values have been normalized as a percentage of the value at 25 °C and are shown in **Fig 4.8.1**.

The wild type FABP was the most stable of the proteins tested. The CD results then suggest that the wild type is most resistant to unfolding in high temperatures and hence is the most stable. The remaining proteins show a similar structural stability over this temperature range. These results support the proposal that the observed DAUDA release when the proteins bind to an anionic interface is due to specific electrostatic interactions and is not due to a change in intrinsic protein stability at such interfaces that would require the mutant to be more stable. Therefore, DAUDA release cannot be simply explained by factors affecting intrinsic protein stability at such anionic interfaces, and the release phenomena are most likely the result of initial specific electrostatic interactions at the interface.

4.9 Discussion

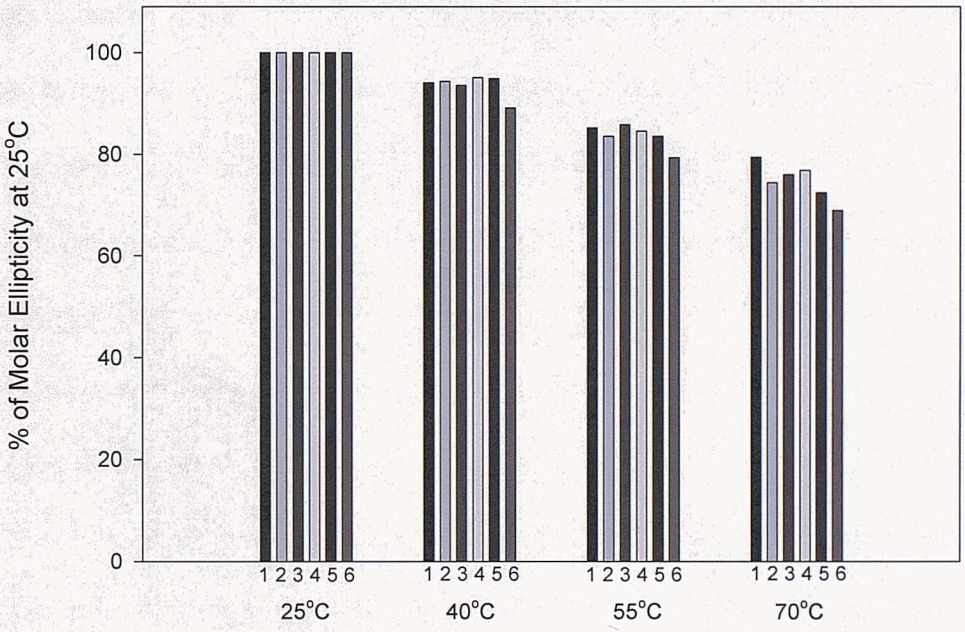

Fig 4.8.1 Measurement of the temperature stability of wild type and charge reversal mutants of liver FABP using CD. Spectra of all proteins (0.5mg/ml) in 10mM potassium phosphate buffer, pH 7.4, were taken after equilibration at 25, 40, 55 and 70°C. After three repetitive scans between 180 and 250nm, the change in molar ellipticity at 220nm at elevated temperature was determined relative to the value at 25°C normalized to 100%. *1* FABP WT; *2* K20E; *3* K31E; *4* K36E; *5* K47E; *6* K57E.

LFABP contains several cationic residues that contribute to the surface positive charge of the protein. In chapter 3 the effect of charge reversal mutagenesis on the ligand binding properties of cationic residues within the α-helical region has been investigated. In this chapter other lysine residues outside the α-helical region that make a significant contribution to surface positive charge have been studied. These residues are Lys-36, Lys-47 and Lys-57 (see **Fig 4.1.1**) and have also been mutated to glutamate (K36E, K47E

and K57E). The effects of these mutations on ligand binding and also binding to DOPG phospholipid vesicles have been investigated.

The results for the surface charge contributing residues show a similar trend through a broad range of ligands and conditions. The K57E mutation significantly reduces the affinity of ligands for the protein, as shown by every ligand that has been investigated in this chapter. The K36E mutant also differed in its binding significantly from the wild type, to many of the ligands on which it was tested. It should be noted that these ligands that are predicted to have a more bulky anionic group located within the portal region are affected by the K36E mutation. Though as with the K33E mutation investigated in chapter 3, there are some ligands that do not show any change in their affinity for K36E mutant compared with wild type FABP, these being lithocholic acid and oleic acid. The K47E mutation did not show any significant difference in its binding compared with the wild type protein.

The K57E mutation has previously been shown to have physiological implications. A mutation in the equivalent position of intestinal FABP in Pima Indians was found to correlate to increased lipid oxidation rates post-absorption [59;60], as well as insulin resistance and obesity in other human populations [61-64]. Such a mutation emphasises the link between FABP structure and lipid metabolism in human beings.

The significance of these results becomes clear when the lysine residues that were deemed to have a significant effect on binding to anionic vesicles both in this chapter and

the last, and the most significant effect on overall ligand binding, are highlighted on the structure of LFABP (See **Fig 4.9.1**).

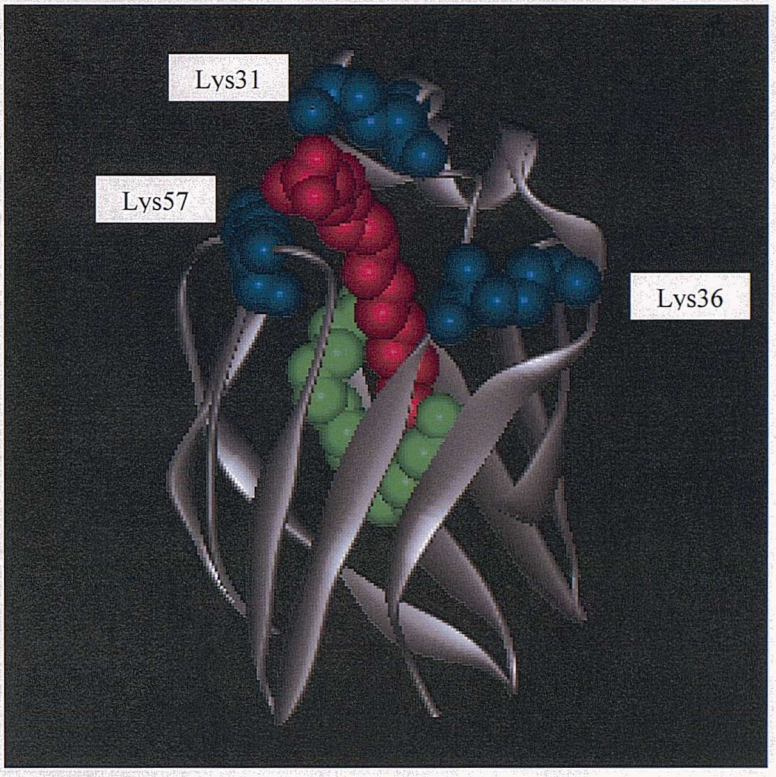

Fig 4.9.1 3-D ribbon diagram of LFABP WT to show positions of K31, K36 and K37 (blue CPK representation). Also shown are the oleic acid binding sites *1* (green CPK representation); and *2* (red CPK representation). Graphic produced using WebLab Viewer Pro

Lys-31, Lys-36 and Lys-57 are all positioned around the hypothesised portal region of LFABP and contribute to the surface charge of the protein. This strongly supports the argument that this region plays a major role in ligand binding to the protein. The positions of Lys-31, Lys-36 and Lys-57 are equivalent to those regions of IFABP that were found to have a degree of disorder as measured by the Cistola laboratory using NMR techniques [65;66]. Further to this, the crystal structure of LFABP has also shown there to be a high degree of disorder at the C-terminal end of α-helix II and within Lys-57 suggesting conformational mobility in this area [9;11]. The conformational mobility

combined with the importance of electrostatic interactions involving the three cationic lysine residues investigated in this chapter, strongly support the theory that ligands enter the binding cavity through this region of the protein.

Chapter 5 – The Portal Region Triple Charge Reversal Mutant K31E,K36E,K57E

5. The Portal Region Triple Charge Reversal Mutant K31E,K36E,K57E

5.1 Introduction

A triple charge reversed mutant was produced that incorporates the three positions of mutation that had had the most significant effect on both ligand binding and interaction with anionic phospholipid vesicles, namely positions 31, 36 and 57 (see **Fig 5.1.1**). The Quickchange method of mutagenesis was used to produce this mutant. The hypothesis was that this triple mutant would show the cumulative effect of the three single mutations in terms of reduced ability to bind site 2 ligands and to anionic phospholipids vesicles. The mutant produced was K31E, K36E, K57E, herein referred to as the triple mutant.

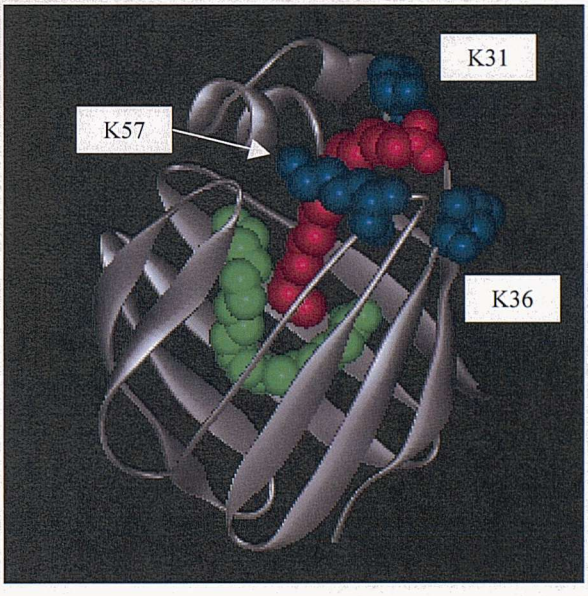

Fig 5.1.1 **Crystal structure of LFABP showing the positions of the three mutations in the triple charge reversal mutant**
The three mutated residues are shown in blue in CPK representation. Also shown are the two bound oleic acid molecules at site 1 (green) and site 2 (red)

5.2 Expression and Purification of the Triple Mutant

The triple mutant was expressed and purified using the same method as used for wild type LFABP, described in chapter 2 of this work. The protein purity after the ion exchange chromatography was approximately 50% and must reflect the change in the overall charge on the mutant. Therefore a gel filtration chromatography stage was added to the purification process, as described in chapter 2. The resulting overall yield for the triple mutant was much lower than that for the wild type protein, producing just 0.5 mg per litre of culture. This is 40-fold lower than a normal yield for the wild type protein. This lower yield is attributed to the additional gel filtration chromatography stage, but also in a large part to the expression of the protein that was also reduced compared to the wild type protein.

Sample purity was checked on SDS-PAGE with coomassie blue staining (Figure 5.2.1) and confirmed that the ligand was greater than 99% pure.

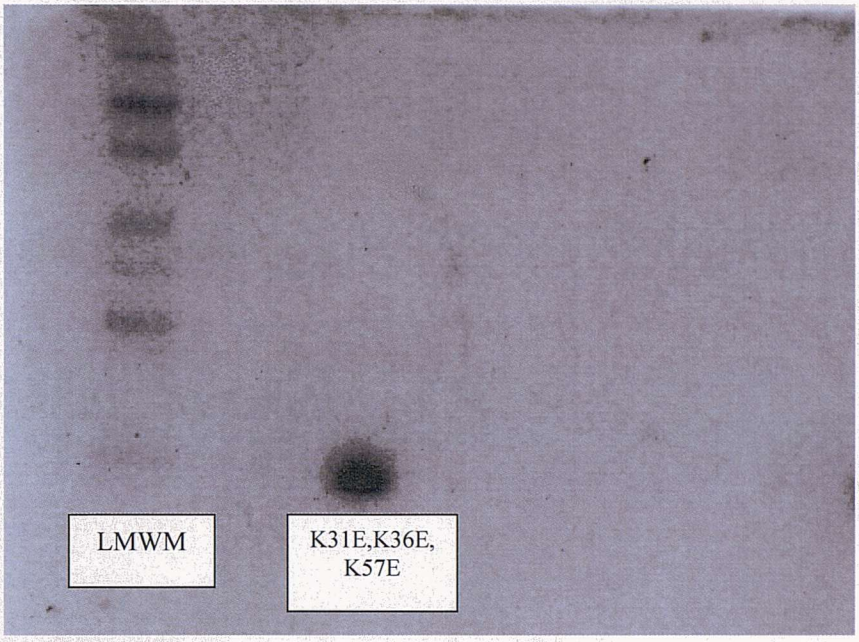

Figure 5.2.1 SDS-PAGE of LFABP K31E, K36E, K57E
Lanes 1 and 3 contain low molecular weight markers showing, from the top of the gel, 66 kDa, 45 kDa, 36 kDa, 29 kDa, 24 kDa, 20 kDa and 14.2 kDa. Lane 2 contains a sample of LFABP K31E, K36E, K57E

5.3 DAUDA Binding to the Triple Mutant

DAUDA was titrated into each of the tryptophan mutants following methods used with the single charge reversed mutants (chapters 3 and 4). The increase in fluorescence when DAUDA binds to LFABP was corrected for DAUDA fluorescence in buffer and the K_d values were calculated from the resulting saturation curves. The triple mutant had a DAUDA K_d value of 0.15 ± 0.02 μM, which was no different to the wild type protein K_d value for DAUDA (0.14 ± 0.03 μM).

5.4 Displacement of DAUDA from Wild Type and Mutant LFABPs by Oleic Acid

Displacement of DAUDA by added oleic acid was most reduced in the case of the triple mutant compared with individual single mutants (**Fig 5.4.1**). However in all cases the effects were modest, consistent with DAUDA binding at the primary site which is unaffected by the mutations. The oleic acid effects must reflect the reduced binding of the oleic acid at the secondary site having a small effect on the binding of oleate to the primary site. This is to be expected as the two sites are not separate. They are structurally linked with site 2 only being fully-formed after an oleic acid binds at site 1 [9]. Furthermore as the oleic acid molecules at site 1 and site 2 must both be in dynamic equilibrium, Le Chatellier's principle dictates that weakened binding at site 2 must affect binding at site 1. Binding of a second oleic acid at site 2 must stabilise ligand bound at site 1.These conclusions are in line with those of Wang *et al*, from their NMR work with oleic acid binding to FABP where NMR resonance suggested exchange of fatty acids between the two sites [18].

5.5 Bile Acids

The effect of the triple charge reversal mutagenesis on lithocholic acid and taurolithocholic acid 3-sulphate binding to LFABP were investigated as these bile acid derivatives show the highest affinity for LFABP [57] and may be physiological ligands [56].

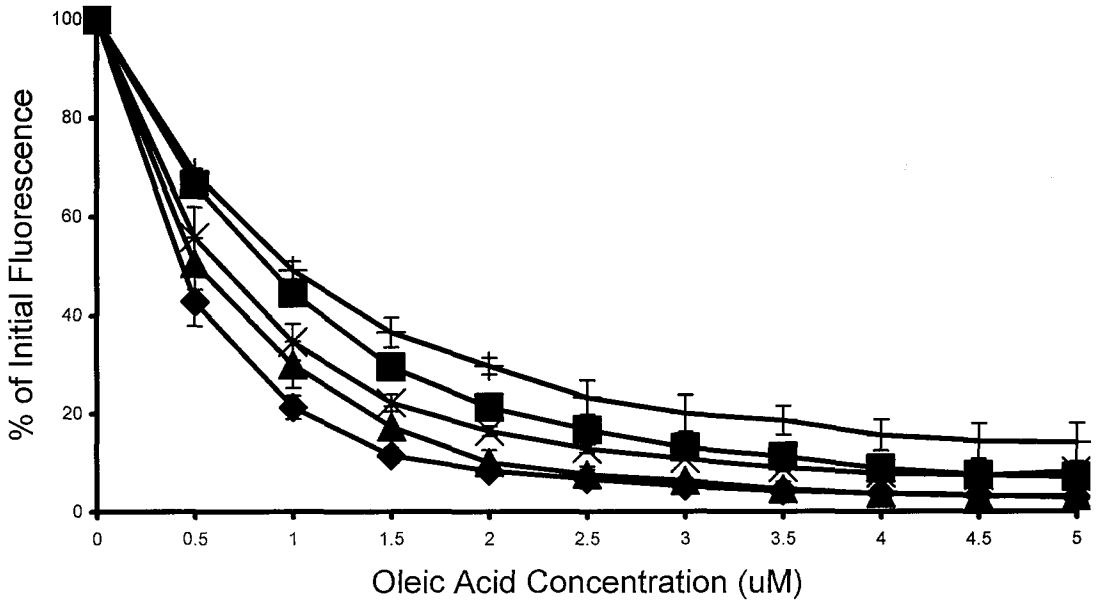

Figure 5.4.1 **The Effects of the Triple and Single Charge Reversed Mutations on the Ability of Oleic Acid to Displace DAUDA from LFABP**
Oleic Acid was titrated as a methanol solution into 10 mM HEPES containing 1 μM DAUDA and 0.56 μM of either wild type (♦), K31E (■), K36E (▲), K57E (×) or Triple Mutant (+) LFABP. The loss of fluorescence of the LFABP/DAUDA complex was measured at 500 nm following excitation at 350 nm. All data points shown are the mean of three titrations ± S.D.

5.5.1 Lithocholic Acid

Titration of lithocholic acid into the LFABP-DAUDA complex results in loss of fluorescence with the triple mutant that is very similar to the K31E single mutant (**Fig 5.5.1**). This similarity is attributed to the small overall effect of the other mutations, K36E and K57E, on lithocholic acid binding.

The overall modest effect of the triple mutation on ligand binding is consistent with the hypothesis that the carboxyl group of the ligand is buried within the binding cavity and not located within the portal region. Thus there is no requirement for electrostatic interactions between LFABP and ligand within the portal region.

5.5.2 Taurolithocholic Acid 3-Sulphate

It has previously been established that taurolithocholic acid 3-sulphate has a high affinity for LFABP(chapters 3 and 4). The binding of taurolithocholic acid 3-sulphate to LFABP was therefore of particular interest because it contains two anionic residues, one of which must reside in the portal region of the protein. It was anticipated that binding of this ligand would be dramatically affected in the triple mutant, showing the cumulative effects of the single mutations. This was indeed the case as shown in **Fig 5.5.2** and negligible binding was detected as measured by DAUDA displacement.

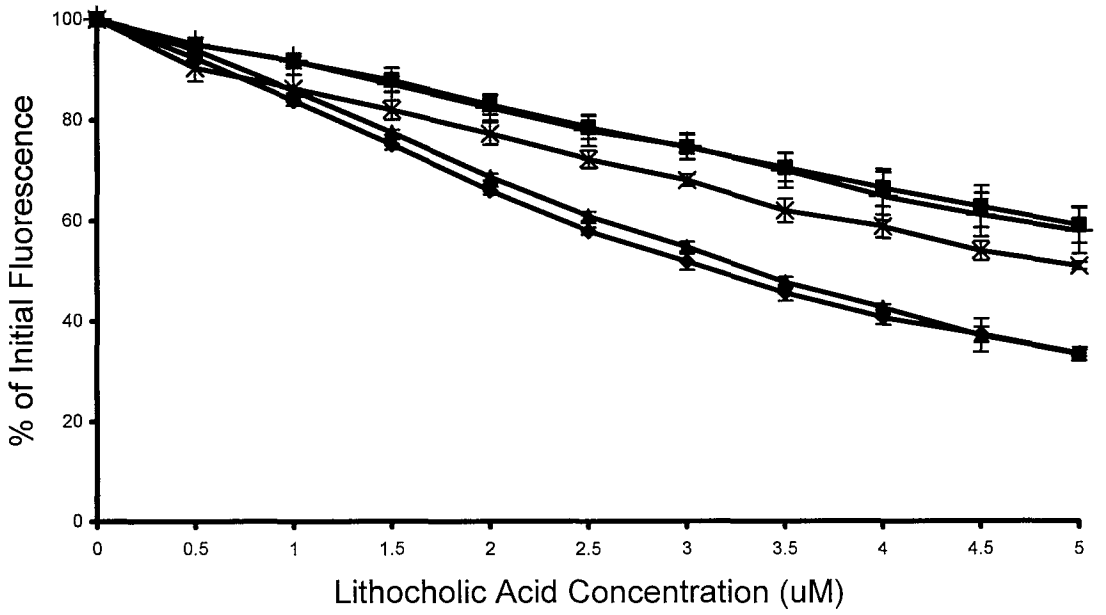

Figure 5.5.1 **Investigation of the Effects of the Triple and Single Charge Reversed Mutants on the Ability of LFABP to Bind Lithocholic Acid with Comparison to Wild Type LFABP**

Lithocholic Acid was titrated as a methanol solution into 10 mM HEPES containing 1 μM DAUDA and 0.56 μM of either wild type (♦), K31E (■), K36E (▲), K57E (×) or Triple Mutant (+) LFABP. The loss of fluorescence of the LFABP/DAUDA complex was measured at 500 nm following excitation at 350 nm. All data points shown are the mean of three titrations ± S.D.

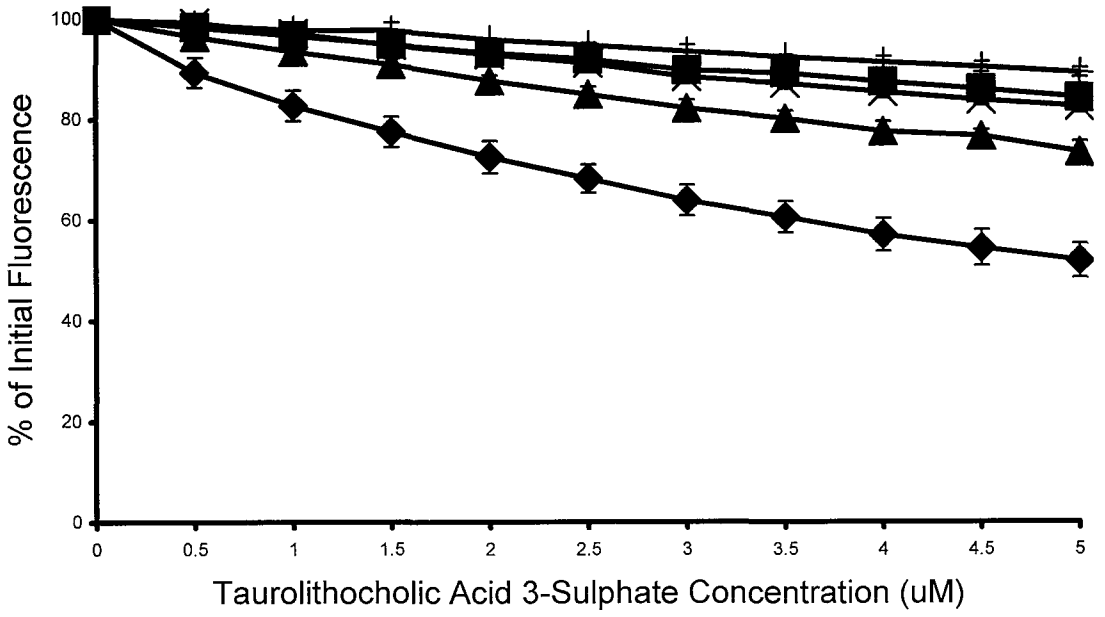

Figure 5.5.2 **The Effects of the Triple and Single Charge Reversal Mutations on the Ability of Taurolithocholic Acid 3-Sulphate to Displace DAUDA from LFABP**
Taurolithocholic Acid 3-Sulphate was titrated as a methanol solution into 10 mM HEPES containing 1 μM DAUDA and 0.56 μM of either wild type (♦), K31E (■), K36E (▲), K57E (×) or Triple Mutant (+) LFABP. The loss of fluorescence of the LFABP/DAUDA complex was measured at 500 nm following excitation at 350 nm. All data points shown are the mean of three titrations ± S.D.

The results of the binding of this ligand to the triple mutant are an excellent example of the effect that non-specific electrostatic interactions can have on ligand binding to the protein. The interactions between these lysine residues and the ligand individually have only a limited effect on binding. However, the cumulative effect of all three charge reversal mutations results in negligible binding of taurolithocholic acid 3-sulphate to this LFABP in comparison to wild type protein.

The dramatic effect of the triple mutation on the binding of taurolithocholic acid 3-sulphate provides an important basis for determining the orientation of this ligand in the binding cavity of LFABP. Clearly one of the anionic groups of this ligand is bound within the portal region, but the orientation is undetermined.

5.6 Lithocholic Acid 3-Sulphate and Taurolithocholic Acid

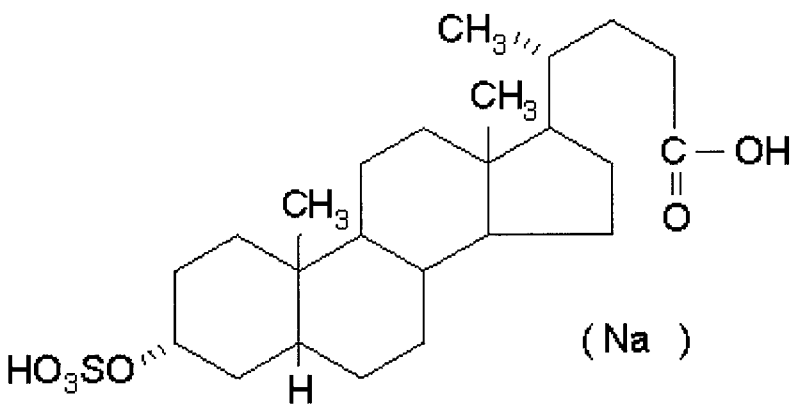

Fig 5.6.1 The structure of lithocholic acid 3-sulphate

The evaluation of these lithocholic acid derivatives as ligand for LFABP should allow the orientation of lithocholic acid derivatives within the binding cavity to be confirmed.

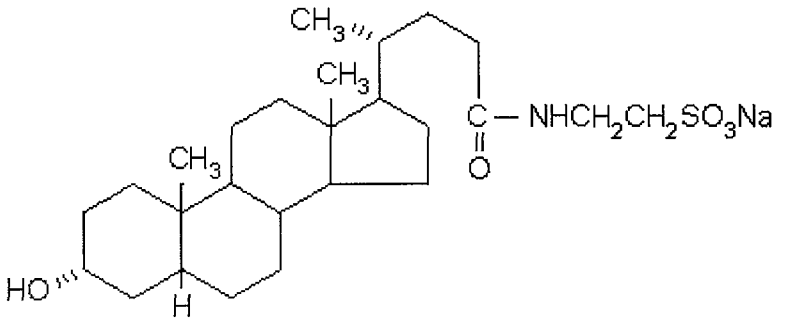

Fig 5.6.2 The structure of taurolithocholic acid

If the sulphate group of lithocholic acid 3-sulphate (see **Fig 5.6.1**) is preferably accommodated in the portal region, then the binding of this ligand should be dramatically affected by the triple mutation. In contrast, the binding of taurolithocholic acid (See **Fig 5.6.2**) should be much less affected as it is anticipated that the side chain will be buried. The results of the displacement studies shown in **Fig 5.6.3** suggest that this is indeed the orientation of the ligand.

The data in **Fig 5.6.3** at a ligand concentration of 5.0 μM is represented as a bar chart in **Fig 5.6.4**. Comparing the bars representing lithocholic acid and taurolithocholic acid, the triple mutation appears to have essentially the same effect on ligand binding. The triple mutation in both cases halves the loss of fluorescence. In contrast, the triple mutation has a much larger effect on the binding of lithocholic acid 3-sulphate, in this

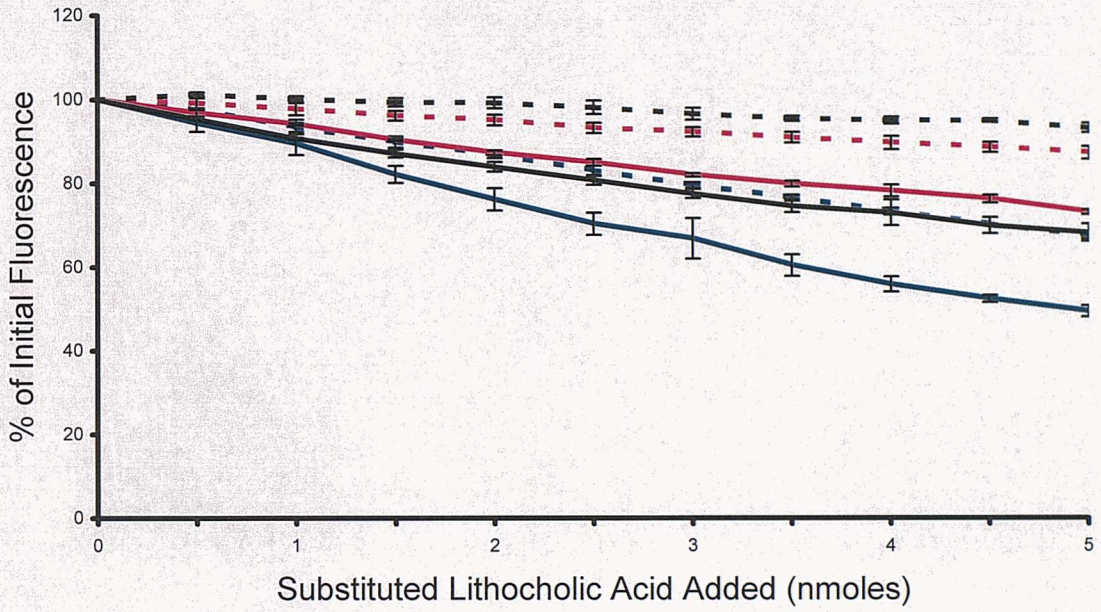

Figure 5.6.3 **The Effects of the Sulphate and Tauro groups of Lithocholic Acid Derivatives on the Ability of Lithocholic Acid Derivatives to Bind to LFABP**
Ligand was titrated as a methanol solution into 10 mM HEPES containing 1 μM DAUDA and 0.56 μM of either wild type (----) or triple mutant (—) LFABP; ligands used were Lithocholic Acid (blue), Taurolithocholic Acid (red) and Lithocholic Acid 3-Sulphate (black). The loss of fluorescence of the LFABP/DAUDA complex was measured at 500 nm following excitation at 350 nm. All data points shown are the mean of three titrations ± S.D.

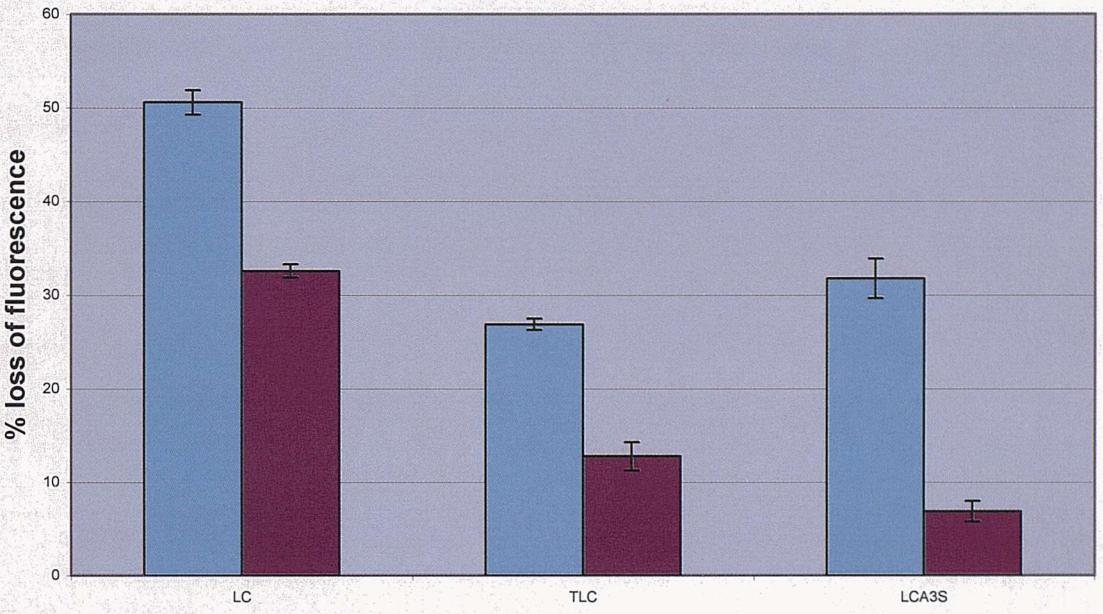

Fig 5.6.4 **The percentage loss of fluorescence from the LFABP-DAUDA complex in the presence of 5.0 μM ligand**

Lithocholic acid (LC), taurolithocholic acid (TLC) or lithocholic acid 3-sulphate (LCA3S), to give a 5.0 μM concentration, was added to a solution of 0.56 μM LFABP WT (blue) or triple mutant (purple) in 10 mM HEPES and 1 μM DAUDA. The loss of fluorescence was recorded at an emission wavelength of 500 nm after excitation at 350 nm

case the triple mutation reduces the loss of fluorescence by 80%. Hence the 3-sulphate group is effected significantly more than the taurine group by charge reversal mutagenesis in the portal region.

The conclusion that can be drawn from these results is that the sulphate group of taurolithocholic acid 3-sulphate must protrude through the portal region of L-FABP and be solvent exposed. The corollary is that the tauro group must be located within the binding cavity and interact with oleate binding site 1. This interpretation of the results is supported by the effect of the triple mutation on the taurolithocholic acid binding being similar to the effect of the triple mutation on lithocholic acid binding.

A cartoon illustrating the proposed orientation of bound lithocholic acid 3-sulphate is shown in **Fig 5.6.5** in which the ligand has been docked into the crystal structure. The carboxyl side chain is adjacent to the cationic site (Arg122) within the binding cavity. It is Arg-122 and the associated hydrogen bonding network that provides the cations for the oleic acid, which is bound at site 1. In the absence of a crystal structure any attempt to produce a spatially accurate model of the ligand bound to the protein would be premature because of the large size of the binding cavity.

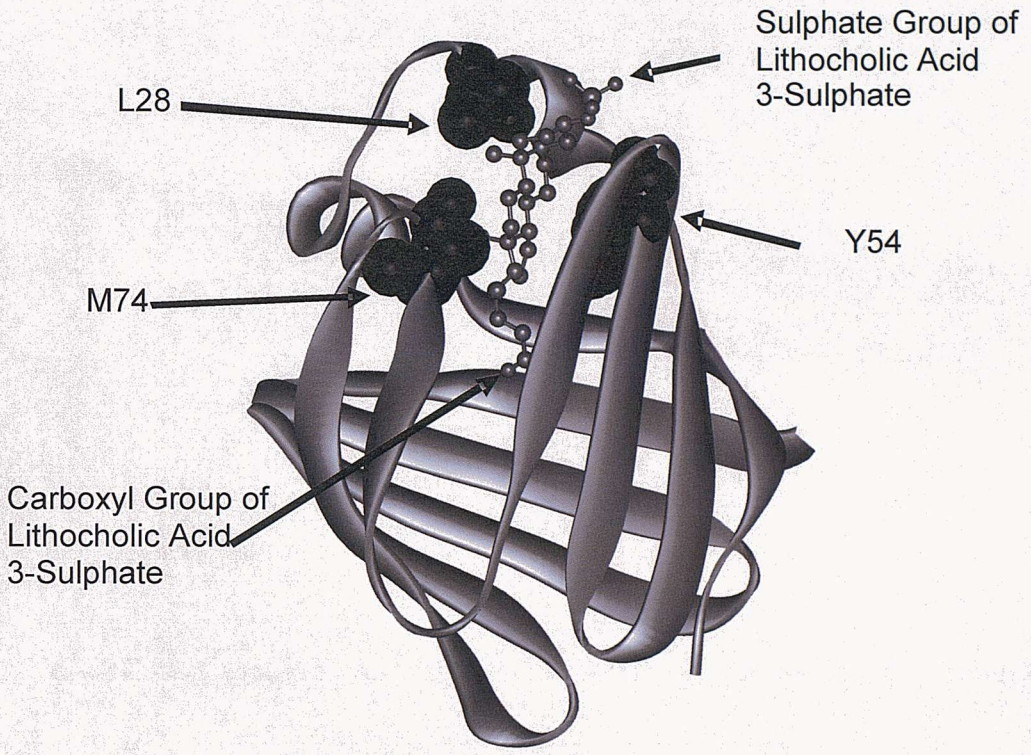

Figure 5.6.5 **The proposed orientation of bound lithocholic acid 3-sulphate**
A molecule of lithocholic acid 3-sulphate has been superimposed onto a ribbon diagram of rat liver FABP in order to position the sulphate group within the portal region of Site 2

5.7 Oleoyl Coenzyme A

The displacement of DAUDA by oleoyl CoA was as expected. The least displacement was seen with the triple mutant indicating a lower affinity of this mutant for the ligand (**Fig 5.7.1**). Overall, as seen previously the K31E mutation had the greatest effect of the single mutants while binding to the triple mutant was slightly weaker than to K31E.

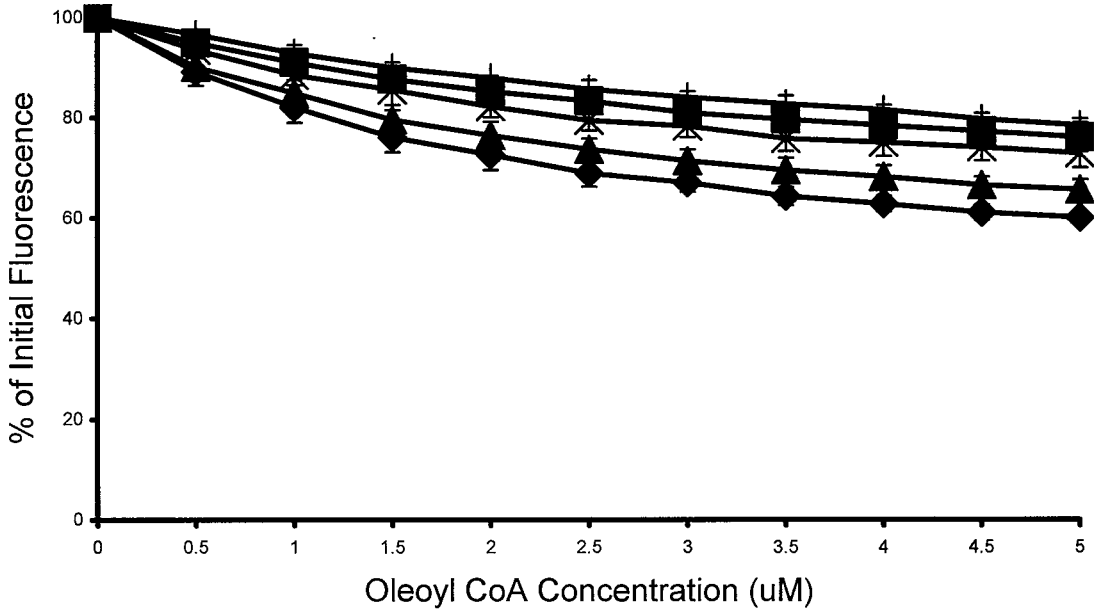

Figure 5.7.1 **The Effects of the Triple and Single Charge Reversal Mutations on the Ability of Oleoyl Coenzyme A to Displace DAUDA from LFABP**
Oleoyl Coenzyme A was titrated as a methanol solution into 10 mM HEPES containing 1 μM DAUDA and 0.56 μM of either wild type (♦), K31E (■), K36E (▲), K57E (×) or Triple Mutant (+) LFABP. The loss of fluorescence of the LFABP/DAUDA complex was measured at 500 nm following excitation at 350 nm. All data points shown are the mean of three titrations ± S.D.

5.8 Dioleoyl-phosphatidylglycerol

In chapter 4 the binding of LFABP WT and mutants to DOPG was described and how specific charge reversal mutants affect such binding.

The titration studies involving DOPG produced unexpected results. It was found that, as anticipated, there was significantly weaker binding of the triple mutant than of the wild type protein to DOPG vesicles. However, it was also found that each of the single charge reversal mutations had a greater effect on lowering the affinity of the protein and the vesicles, than was apparent in the triple mutant (**Fig 5.8.1**).

This result in terms of binding to DOPG vesicles using the triple mutant was surprising. It had been anticipated that this binding to these vesicles would be reduced compared with the binding of single mutations as a result of the cumulative effect of the charge reversal mutagenesis. Because electrostatic interactions are sensitive to the ionic strength of the medium, it was of interest to repeat these binding studies in the presence of NaCl.

5.9 Dioleoyl-phosphatidylglycerol With 0.15 M NaCl

The binding of LFABP to DOPG vesicles, assessed by DAUDA displacement, was repeated in the presence of 0.15 M NaCl. However, it was observed that it took some time for the fluorescence value to become stable after the addition of DOPG. As a result a

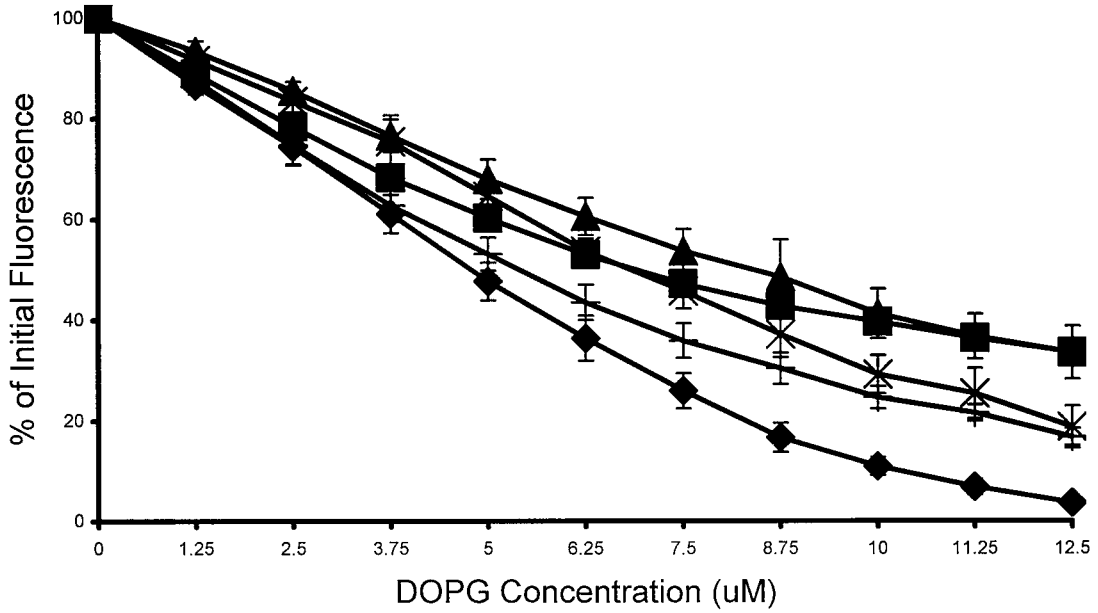

Figure 5.8.1 **The Effects of the Triple and Single Charge Reversal Mutations on the Ability of Anionic Vesicles to Displace DAUDA from LFABP**
DOPG was titrated as a methanol solution into 10 mM HEPES containing 1 μM DAUDA and 0.56 μM of either wild type (♦), K31E (■), K36E (▲), K57E (×) or Triple Mutant (+) LFABP. The loss of fluorescence of the LFABP/DAUDA complex was measured at 500 nm following excitation at 350 nm. All data points shown are the mean of three titrations ± S.D.

period of 15 minutes was allowed between each addition of phospholipid so that the fluorescence reading became constant. The results are shown in **Fig 5.9.1** and it is apparent all mutants behaved similarly and showed minimal binding to DOPG vesicles as compared with wild type FABP. Thus using a higher salt concentration highlighted the importance of electrostatic interactions when LFABP binds to DOPG vesicles but failed to further discriminate between the various charge reversal mutants.

5.10 Discussion

The major role of the cationic residues Lys-31, Lys-36 and Lys-57 in both ligand binding to the protein and the protein interacting with anionic phospholipid vesicles, has been demonstrated and discussed in chapters 3 and 4. Individually, it is clear that mutating these residues to anionic glutamate significantly inhibits interaction of the protein with anionic phospholipids and ligand binding to the protein. A triple mutant was produced in order to investigate the cumulative effect of these three charge reversal mutations.

The results for the triple charge reversal mutant on ligand binding were very much as had been predicted prior to experimentation. With the exception of the lithocholic acid, the ligand binding studies revealed that the triple mutant had a weakened binding to ligands equivalent to the cumulative effect of each of the single mutations.

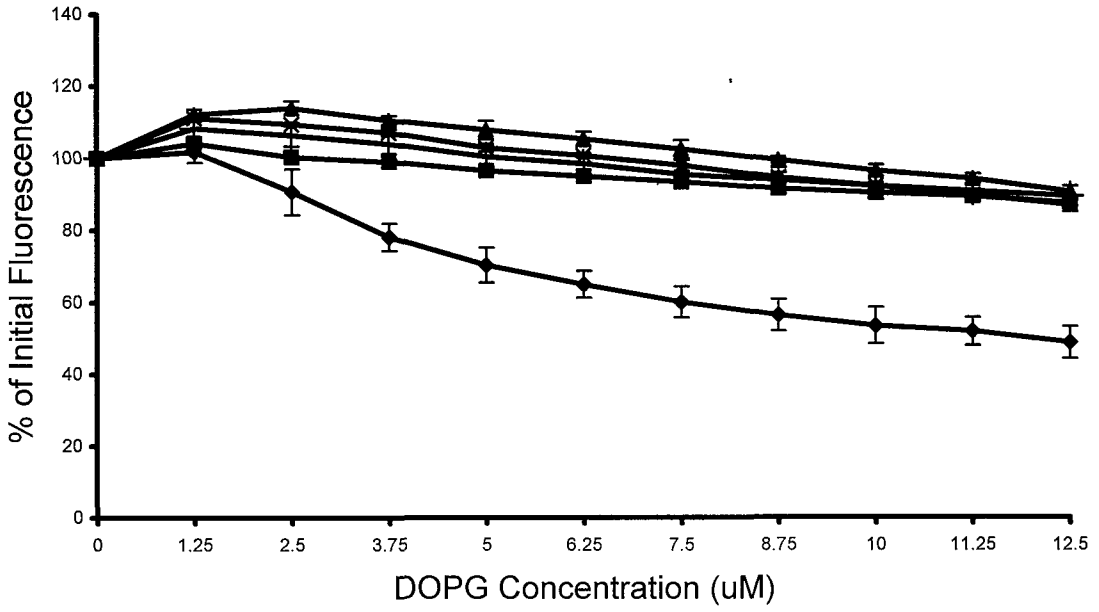

Figure 5.9.1 **The Effects of the Triple and Single Charge Reversal Mutations on the Ability of Anionic Vesicles to Displace DAUDA from LFABP in the Presence of 0.15 M NaCl**

DOPG was titrated, at 15 minute intervals, as a methanol solution into 10 mM HEPES containing 1 μM DAUDA, 0.15 M NaCl and 0.56 μM of either wild type (♦), K31E (■), K36E (▲), K57E (×) or Triple Mutant (+) LFABP. The loss of fluorescence of the LFABP/DAUDA complex was measured at 500 nm following excitation at 350 nm. All data points shown are the mean of three titrations ± S.D.

The overall effect of the triple mutation is most dramatically seen when taurolithocholic acid 3-sulphate was titrated in to displace DAUDA. The combined effect of the three single mutations, as represented by the triple mutant, results in almost total loss of binding of taurolithocholic acid 3-sulphate to the protein.

The bile acid that was least affected by the triple mutation was lithocholic acid. The binding of this ligand is consistent with the hypothesis that the carboxyl group of the ligand is buried within the binding cavity and not located within the portal region. This ligand does not contain a sulphate group.

By comparing lithocholic acid derivatives it has been possible to determine the orientation of bile acids such as taurolithocholic acid 3-sulphate. It was found in **section 5.6** that lithocholic acid 3-sulphate binding was far more affected by the triple charge reversal in the portal region than taurolithocholic acid. Taurolithocholic acid was affected to the same extent as lithocholic acid by this triple mutation and both lack a sulphate group. The conclusion is that the taurine group of taurolithocholic acid 3-sulphate is buried within the binding cavity of LFABP when bound to the protein, whilst the 3-sulphate group of the ligand is located in the portal region.

The result of binding of the triple charge reversal mutant LFABP to DOPG vesicles was unexpected. Whilst each single mutation reduced binding of DOPG vesicles to LFABP, the triple mutation did not reduce the binding to anionic vesicles to the same extent as any of the single mutants. In fact a similar phenomenon has been seen

previously in terms of the binding of the bee venom PLA_2 to anionic vesicles. This enzyme has six cationic residues on its interfacial-binding surface and despite the mutation of five of these residues to glutamate, vesicle binding was unaffected [67]. A possible explanation for the observation is that some of the glutamate residues of the bee venom enzyme remain unionized due to the lower pH experienced at the surface of the anionic vesicles. An uncharged glutamate will promote non-polar interactions between protein and vesicle. It is possible that a similar phenomenon is occurring with LFABP.

Perhaps the most significant result of this section though is that which was obtained when DOPG was titrated into the wild type and mutant FABPs in the presence of 0.15 M NaCl. Earlier experiments had suggested that FABP did not bind to anionic vesicles at physiological salt levels [68;69]. The explanation given for this is that the salt interfered with the electrostatic interactions between the protein and the anionic vesicles. It was observed that the triple mutant was taking a long time to reach a stable fluorescence value, about 15 to 20 minutes. Upon repeating the titrations for the single mutations it was apparent that they too were taking a long time to reach a constant fluorescence value. When the entire experiment was repeated allowing for 15-minute intervals between additions of anionic vesicles that results were intriguing. There was no significant difference between the triple mutant and the single charge reversed mutants in terms of binding strength to the vesicles. However, there was a significant difference between the wild type and all of the mutants. It was found that the wild type protein displayed a much stronger binding to the anionic vesicles than the mutants (**Fig 5.9.1**). This result has physiological implications as it implies that LFABP can bind to anionic

interfaces even at the normal salt concentration present in the cell, but that such binding may have a larger contribution from non-polar interactions as a result of membrane penetration, a process operating over a large time scale.

Chapter 6 – Studies on N-terminal and Portal Region Tryptophan Mutants of LFABP

6. Studies on N-terminal and Portal Region Tryptophan Mutants of LFABP

6.1 Introduction

The binding studies reported in chapters 3-5 have relied upon a reporter molecule, DAUDA and the changes in fluorescence intensity when this ligand is released from the LFABP binding cavity. Changes in protein conformation can also be followed using tryptophan residues within the protein themselves. Tryptophan residues are intrinsically fluorescent and the fluorescence emission is sensitive to the environment of the tryptophan residue within the protein. Changes in fluorescence emission can be monitored in terms of loss of fluorescence intensity and also the wavelength at which the fluorescence intensity is maximal. LFABP wild type has no tryptophan residues in its primary sequence and therefore is an ideal candidate for tryptophan insertion mutagenesis. Site directed mutagenesis allows us to insert tryptophan molecules at specific points within the protein in order to monitor changes in protein conformation as a result of biomolecular interactions.

The tryptophan insertion mutants F3W and F18W were originally produced in this laboratory [10]. Studies using these mutants have shown a significant conformational change at the N-terminus of the protein in the presence of anionic phospholipids vesicles [25]. Fluorescence Resonance Energy Transfer (FRET) studies showed that the tryptophan at position 3 came in close proximity to the anionic interface [25]. In order to

further investigate the nature of the interaction between the N-terminal region of the protein and anionic phospholipid vesicles Tyr-7 was selected for substitution to tryptophan. The results from the Y7W mutant binding studies will determine whether the interaction with anionic phospholipid vesicles at the N-terminal region extends as far as this residue.

The second region of the protein that was selected for scrutiny by tryptophan mutagenesis was the region that has been thoroughly investigated in the previous chapters, the portal region. The significance of this region is that it is the most likely region to experience conformational changes upon ligand binding, while charge reversal mutagenesis (chapters 3-5) has highlighted the importance of cationic residues within this region in binding to anionic phospholipid vesicles as well as the binding of certain ligands to the protein. Specifically, the non-polar residues selected from the portal region to be mutated to tryptophan were Leu-28, Tyr-54 and Met-74. The Met residue at position 74 is particularly close to one of the bound oleates in the crystal structure [11]. The sulphur atom in the side chain of the methionine was found to be just 3.0 Å away from the ω terminus of oleic acid. Furthermore the side chain of this residue was found in the latter stages of refinement of the crystal structure to have a degree of ambiguity as to its position suggesting conformational instability. Leu-28 and Tyr-54 are also placed within the portal region of LFABP hence these three mutants should allow for an insight into any conformational changes within this region upon ligand binding.

The tryptophan mutants are reporting on two separate regions of LFABP, namely the N-terminal and portal region. Therefore the results of their ligand and phospholipid binding properties are dealt with separately to avoid confusion.

6.2 Expression of Tryptophan Mutants

The mutants Y7W, L28W, Y54W and M74W were produced using the Quickchange method of site directed mutagenesis [70]. They were then expressed and purified using the same method as for wild-type LFABP as described in chapter 2 of this work. The yield of the Y7W was comparable to the wild-type protein at roughly 15-20 mg per litre of culture. The yield for the three portal region tryptophan mutants (L28W, Y54W and M74W) on the other hand, was greatly enhanced to around double the wild-type yield at 40 mg per litre of culture. We do not have an explanation for this enhanced yield. Sample purity was checked on SDS-PAGE with coomassie blue staining (see **Fig 6.2.1**) and indicated that protein purity was greater than 99% for all mutants.

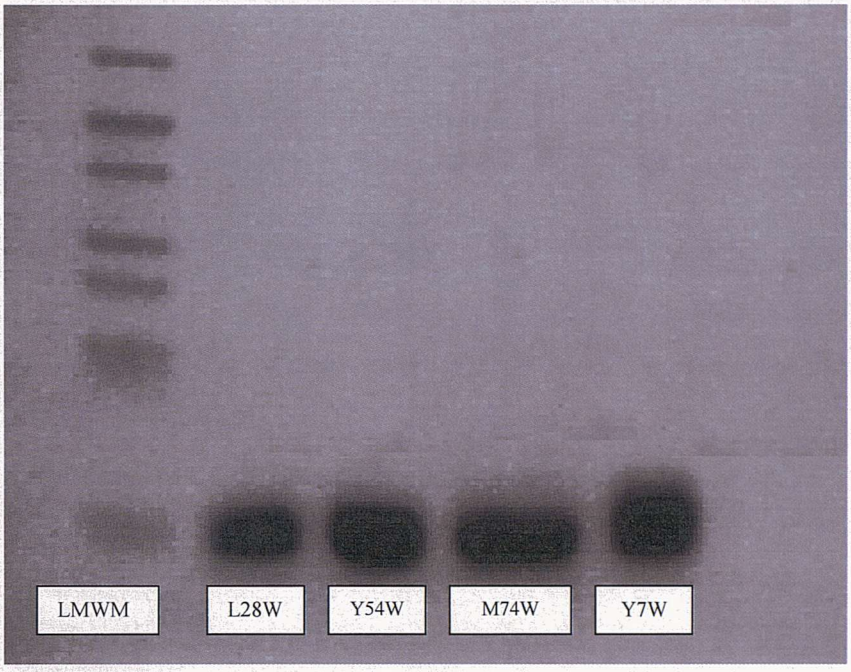

Fig 6.2.1 **SDS-PAGE of LFABP L28W, Y54W, M74W and Y7W**

Lane 1 (labeled LMWM) contains the low molecular weight markers showing, from the top of the gel, 66 kDa, 45 kDa, 36 kDa, 29 kDa, 24 kDa, 20 kDa and 14.2 kDa. Lanes 2-5 contain the tryptophan insertion mutants, as labeled from the DEAE cellulose purification.

6.3 Circular Dichroism

Circular Dichroism (CD) was used to confirm that the mutants were all correctly folded. The spectra for each of the tryptophan mutants are shown in **FIG 6.3.1**. The spectra for Y7W, L28W and M74W are essentially identical to the wild type spectrum, showing that these mutants are folded in the same way as the wild type protein. There is however a significant difference between these proteins and the Y54W mutant, suggesting that this particular mutant is not correctly folded or exists in more than one conformation. The data for the Y54W mutant is still included as the DAUDA binding data showed this mutant to have similar binding properties to the wild type protein.

However, no specific conclusions were drawn from the results of the Y54W binding data relating to LFABP structure and function.

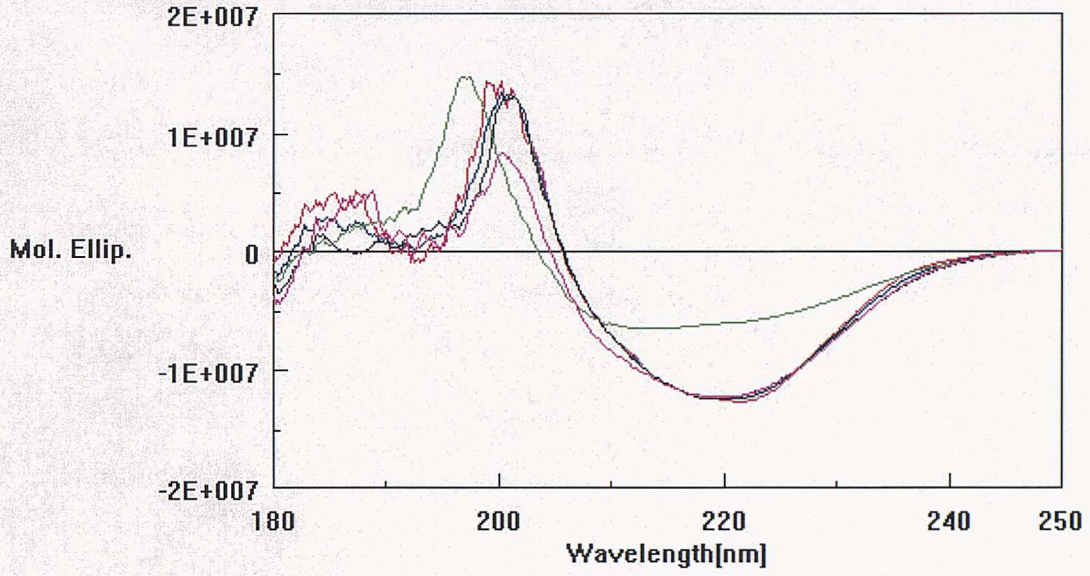

Fig 6.3.1 **Molar Ellipticity scan for FABP WT and the Tryptophan Mutants**
Scans are carried out between 180 nm and 250 nm in 10 mM KH_2PO_4. Each line represents a different protein. FABP WT (pink); FABP Y7W(red); FABP L28W (blue); FABP Y54W (green); FABP M74W (black)

6.4 DAUDA Binding to L-FABP Tryptophan Mutants

DAUDA was titrated into each of the tryptophan mutants following methods used with the charge-reversed mutants (chapters 3-5). The increase in fluorescence when DAUDA binds to LFABP was corrected for DAUDA fluorescence in buffer and the K_d values were calculated from the resultant saturation curves. The K_d values of the proteins for DAUDA are shown in **Table 6.4.1**. The results show no significant differences in the DAUDA K_d values for any of the mutants compared to the wild type. Therefore there were no apparent adverse effects of tryptophan mutagenesis on DAUDA binding. The modest increase in maximum fluorescence values for L28W, Y54W and M74W

compared to the wild type protein may be due to the tryptophan residues increasing the hydrophobicity within the binding cavity. DAUDA is a polarity sensitive probe that is more fluorescent in a non-polar environment.

	DAUDA K_d Apparent ± S.D. (μM)	Maximum Fluorescence ± S.D. (A.U.)
FABP WT	0.12 ± 0.02	469 ± 8
FABP Y7W	0.20 ± 0.06	657 ± 67
FABP L28W	0.18 ± 0.04	796 ± 82
FABP Y54W	0.09 ± 0.03	745 ± 35
FABP M74W	0.14 ± 0.03	537 ± 18

Table 6.4.1 **DAUDA binding properties of wild type and tryptophan mutant LFABPs**
DAUDA binding was determined by titrating up to 1 μM DAUDA into 0.8 μM FABP. Values given are the mean of three titrations ± S.D. The increase in fluorescence intensity was measured at 500 nm following excitation at 350 nm

6.5 Portal Region Tryptophan Mutants

Inserting tryptophan residues within the portal region of LFABP was a logical extension of the work reported in chapters 3-5. This region has been confirmed as being highly important to the binding of both ligands and anionic phospholipid vesicles in these chapters. It has been shown that lysine residues around this region at positions 31, 36 and 57 are involved in non-specific interactions with ligands and anionic phospholipid vesicles. When these positively charged residues were substituted for negatively charged glutamate residues, the affinity of LFABP for both ligands and anionic phospholipids was

reduced. Insertion of tryptophan residues in this region of the protein should give further insight into the effect of ligand and membrane binding on changes in protein conformation. The structure of LFABP highlighting the positions of the mutated residues is shown in **Fig 6.5.1**. Tryptophan residues 28 and 54 should report primarily on ligand binding at site 2 whereas tryptophan 74 is adjacent to both fatty acid binding sites 1 and 2.

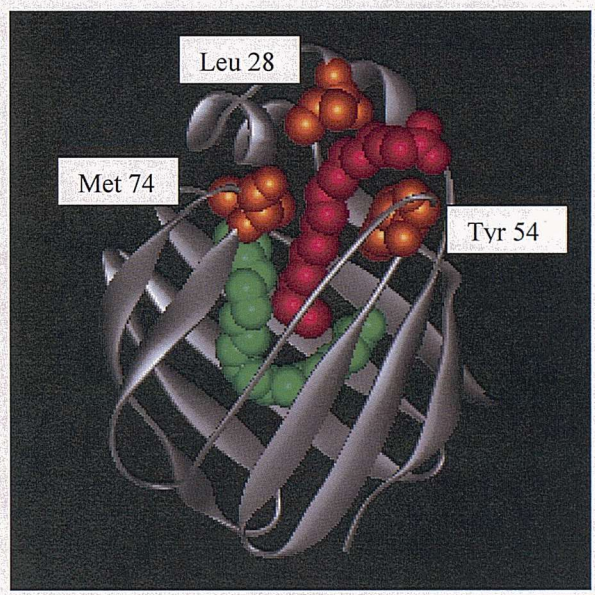

Fig 6.5.1 **LFABP showing the locations of the three residues in the portal region that are to be replaced by tryptophan**
The residues that are to be replaced by tryptophans are shown in orange. Also shown are the two oleic acid molecules that bind to LFABP, at site 1 (green) and site 2 (red).

6.5.1 Fluorescence Properties of the Portal Region Tryptophan Mutants

Each of the mutants, in the absence of oleic acid showed an emission maximum around 340nm after excitation at 280 nm, which is in line with the tryptophans being relatively solvent exposed, as would be expected around the portal region. The wavelength at which the maximum fluorescence was achieved, along with the maximum

fluorescence intensity is summarized in **Table 6.5.1.1**. The maximum fluorescence value for each of the mutants varies with the L28W mutant being the lowest, followed by Y54W and the M74W mutant has the highest maximum fluorescence value. The differences between these maximum fluorescence values could be due to the degree of solvent exposure of each of the mutants. This is considered unlikely to be the only explanation however due to the emission wavelengths at which the maximum fluorescence value is achieved for each mutant, all being similar. Another possibility is the presence of polar groups in close proximity to each of the tryptophan residues causing varying degrees of fluorescence quenching which is a common occurrence.

Tryptophan Mutant	Wavelength of Maximum Fluorescence Emission ± S.D. (nm)	Maximum Fluorescence Intensity ± S.D. (A.U.)
L28W	341 ± 1	796 ± 36
Y54W	339 ± 1	1331 ± 25
M74W	339 ± 1	2010 ± 89

Table 6.5.1.1 The fluorescence properties of tryptophan mutants of LFABP
Tryptophan fluorescence of mutants was determined in 10 mM HEPES. All proteins were at 0.8 μM. All values are the mean of measurements performed in triplicate

6.5.2 Ligand Binding Studies

The ability of liver FABP to bind a variety of physiological ligands in addition to long chain fatty acids provided an opportunity to assess the effect of ligand binding on the fluorescent properties of the tryptophan mutants. The ligands oleic acid and oleoyl

CoA were chosen together with lithocholic and the conjugated bile acids lithocholic acid 3-sulphate, taurolithocholic acid and taurolithocholic acid 3-sulphate as these bile acid derivatives show highest affinity for liver FABP [57;71] and may be physiological ligands [56;72]. Cholesterol 3-sulphate was studied because it also has a 3-sulphate group.

6.5.2.1 Oleic Acid

The fluorescence emission spectra for each of the portal tryptophan mutants were initially measured in the presence and absence of a ten times molar excess of oleic acid. This was done to ascertain whether any conformational changes in the proteins took place upon fatty acid binding. An emission wavelength scan was run at an excitation of 280nm for each of the mutants in the presence and absence of oleic acid. The results are shown in **FIGURES 6.5.2.1(a-c)** and summarized in **Table 6.5.2.1**.

Mutant	FABP L28W		FABP Y54W		FABP M74W	
Buffer only/Oleic Acid	Buffer	Oleic Acid	Buffer	Oleic Acid	Buffer	Oleic Acid
Maximum Fluorescence Intensity (A.U.)	698±25	2226±63	1213±81	1540±61	1883±73	1778±112
Ratio of Fluorescence Intensity +/- Ligand	3.2		1.3		0.94	

Table 6.5.2.1 Maximum fluorescence intensity and wavelength changes as a ten times molar excess of oleic acid is added by methanol injection to 0.8μM LFABP in 10 mM HEPES following excitation at 280 nm

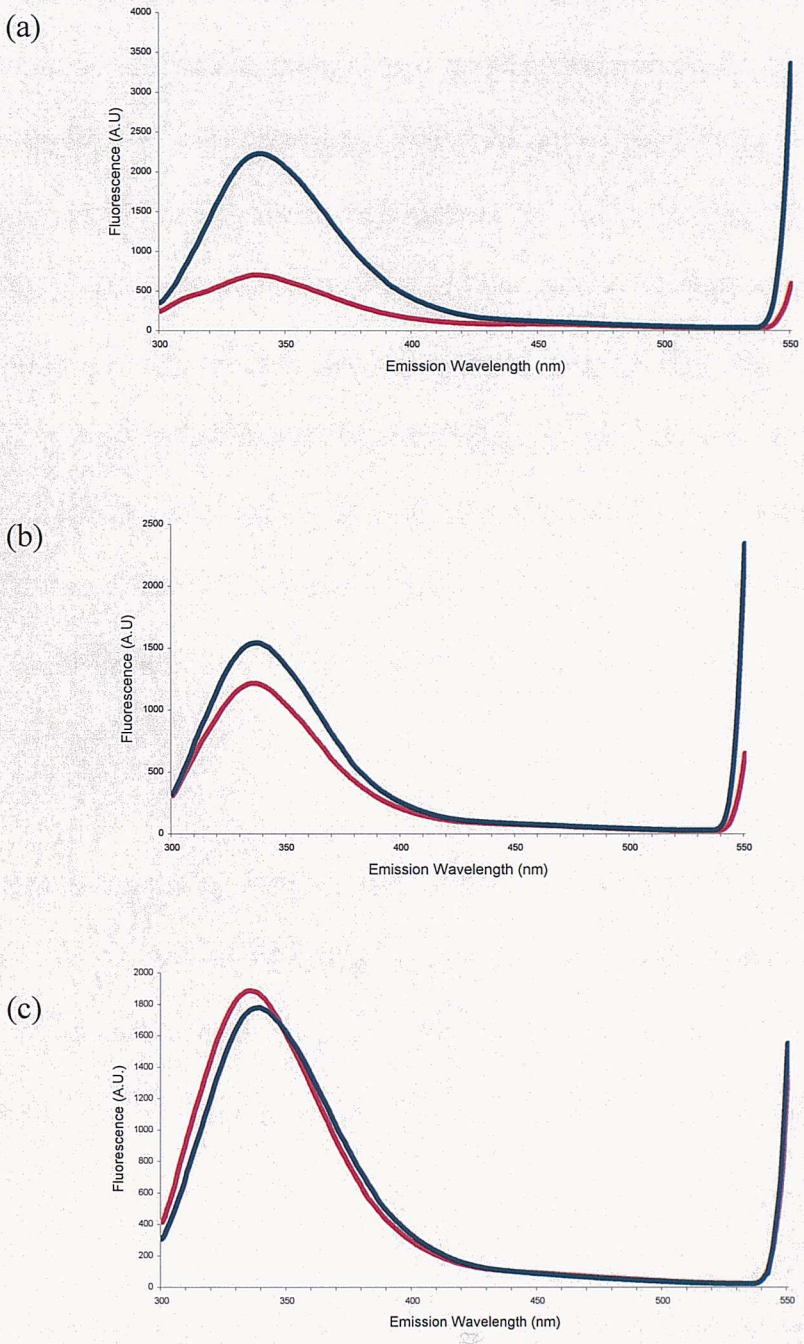

Fig 6.5.2.1 **The Effect of Oleic Acid on the Tryptophan Emission Maxima of L28W, Y54W and M74W LFABP**

Tryptophan emission of 0.8 μM FABP L28W (a), Y54W (b) or M74W (c); in 10 mM HEPES was measured between 300 nm and 550 nm following excitation at 280 nm in the absence (red) or presence (blue) of 8 μM oleic acid. Results are the mean of three titrations.

The fluorescence spectrum of FABP M74W appeared to be relatively unaffected by the addition of oleic acid, experiencing a small decrease in maximum fluorescence. As well as the small fluorescence change there was also a small change in the emission wavelength at which the maximum fluorescence was achieved (see **Fig 6.5.2.1**). FABP Y54W on the other hand did show a significant change in fluorescence, experiencing roughly a 40% increase in fluorescence upon binding to the ligand. This change in fluorescence was not accompanied by any change in the emission wavelength at which the maximum fluorescence value was achieved. By far the most interesting result was obtained when oleic acid was added to FABP L28W. When the ligand was added to the protein an increase to over 300% of the initial tryptophan fluorescence was recorded under these assay conditions.

The change in fluorescence upon binding of the ligand makes these mutants, particularly L28W, very useful tools for further studies into ligand binding. Whereas previously studies had relied upon the reporter group DAUDA, with the aid of these mutants ligand binding and even competition between ligands can be measured using the apoprotein.

Fig 6.5.2.2 shows a very large increase in fluorescence of the tryptophan as oleic acid bind is titrated into FABP L28W. The oleic acid binding curve shown in **Fig 6.5.2.2** has a distinct sigmoidal shape. This sigmoidal shape is consistent with co-operative binding of the ligand to the protein. From the crystal structure it was evident that parts of the second oleic acid binding site are not available until the first oleic acid molecule has

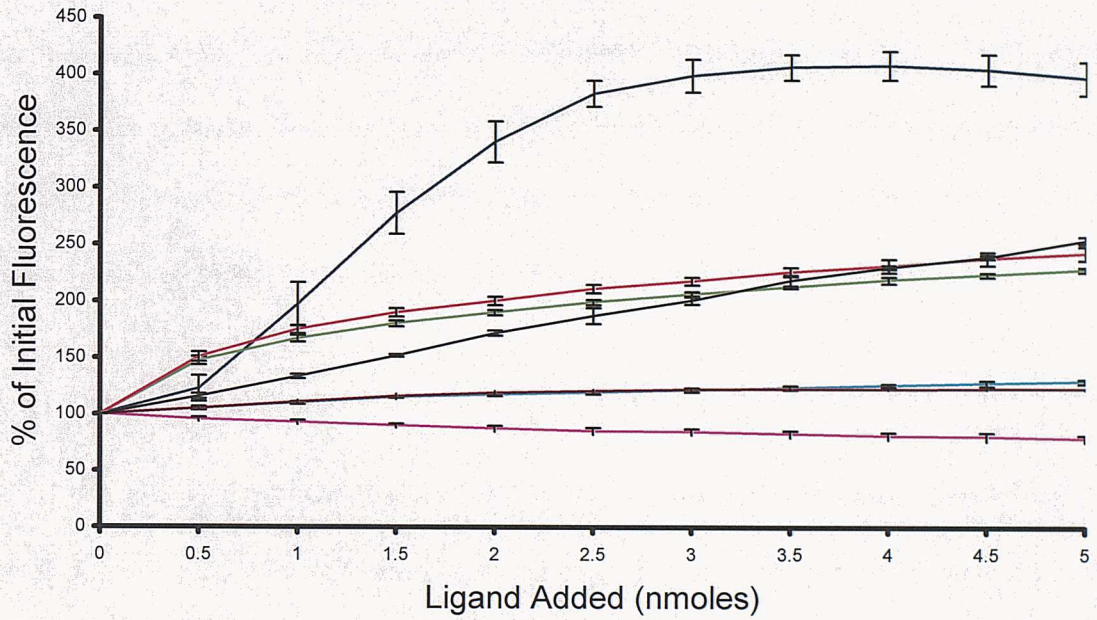

Fig 6.5.2.2 **The Effect on fluorescence intensity of the addition of ligands to the L28W mutant of liver FABP**

To a sample of FABP L28W (0.8 μM) in 10 mM HEPES was added up to 5 nmoles of ligand. The change in fluorescence intensity is plotted as % of initial fluorescence. Excitation was at 280 nm and emission was recorded at 339 nm. All values are the mean of titrations performed in triplicate ± S.D. Oleic acid (dark blue); oleoyl CoA (pink); taurolithocholic acid 3-sulphate (green); taurolithocholic acid (light blue); lithocholic acid 3-sulphate (red); lithocholic acid (brown); cholesterol 3-sulphate (black)

bound [9]. Therefore this co-operativity was not unexpected based on the crystal structure.

There are two possible explanations for this co-operativity. The first is the situation where a ligand could initially bind to either site 1 or site 2 of the apoprotein assuming the L28W mutant is reporting on site 2 ligands. Co-operativity is then achieved when a second molecule of oleic acid preferentially binds to the protein with an oleate already at site 1, rather than to apoFABP. This would be in line with evidence provided by Wang *et al* in which NMR studies using ^{13}C labeled long chain fatty acids. In these studies NMR resonance suggested exchange of fatty acid between the two binding sites [18].

The second explanation for the co-operativity relates more directly to the crystallographic data. In this model, the second binding site for oleic acid does not actually exist until the first molecule is bound. After this binding has occurred, conformational changes in the protein cavity caused by the binding of the first molecule, result in the formation of the second binding site.

The shape of the oleic acid binding curve supports the first model. A greater degree of sigmoidicty would be expected in the binding curve if co-operativity was occurring via the second model described involving sequential binding, especially if there is a major difference in affinity for fatty acid between the two sites (a 10-20 fold difference in K_d has been reported for fatty acid binding to the two sites). In this situation

it would be expected that site 1 would be over 90% saturated before binding to site 2 occurred.

The addition of oleic acid caused an increase in the tryptophan fluorescence of the Y54W mutant, by 40% confirming the results seen in the wavelength scan (**Fig 6.5.2.1**). The shape of the binding curve is also interesting as seen in **Fig 6.5.2.3**. There is no clear sign of the sigmoidicity seen with L28W, as might have been expected. It is likely that this is due to the lack of change in signal or fluorescence, compared with the L28W mutant, failing to detect the modest sigmoidal response. As had been shown with the wavelength scans, the M74W mutant experiences a loss of tryptophan fluorescence as oleic acid binds (**Fig 6.5.2.4**). This loss however, is minimal and no conclusions can be drawn from it. There is no sigmoidal binding curve as the fatty acid is titrated in, but as for Y54W this is expected as the change in fluorescence is too small for any subtle deviations from a standard hyperbola to be shown up.

6.5.2.2 Oleoyl CoA

In contrast to fatty acids, the binding of oleoyl CoA was accompanied by a fall in fluorescence of all mutants (see **Fig 6.5.2.2, Fig 6.5.2.3, Fig 6.5.2.4**). The largest fall was seen in the case of the M74W mutant while this titration curve was consistent with binding of more than one molecule of oleoyl CoA. This apparent stoichiometry contrasts with the titration curve for the L28W mutant that indicated that the binding of only a

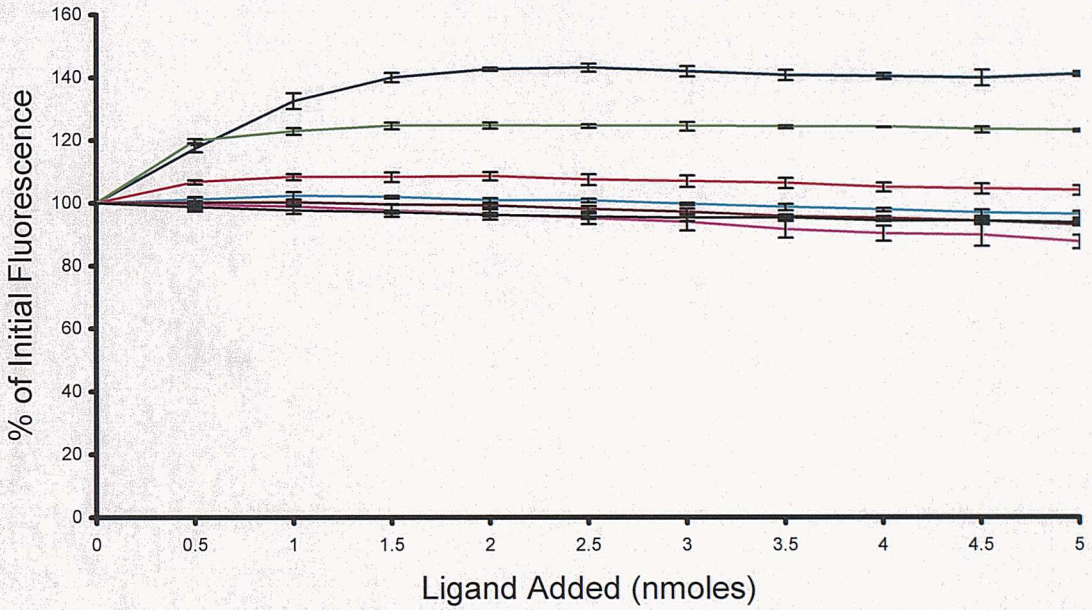

Fig 6.5.2.3 **The Effect on fluorescence intensity of the addition of ligands to the Y54W mutant of liver FABP**

To a sample of FABP Y54W (0.8 μM) in 10 mM HEPES was added up to 5 nmoles of ligand. The change in fluorescence intensity is plotted as % of initial fluorescence. Excitation was at 280 nm and emission was recorded at 339 nm. All values are the mean of titrations performed in triplicate ± S.D. Oleic acid (dark blue); oleoyl CoA (pink); taurolithocholic acid 3-sulphate (green); taurolithocholic acid (light blue); lithocholic acid 3-sulphate (red); lithocholic acid (brown); cholesterol 3-sulphate (black)

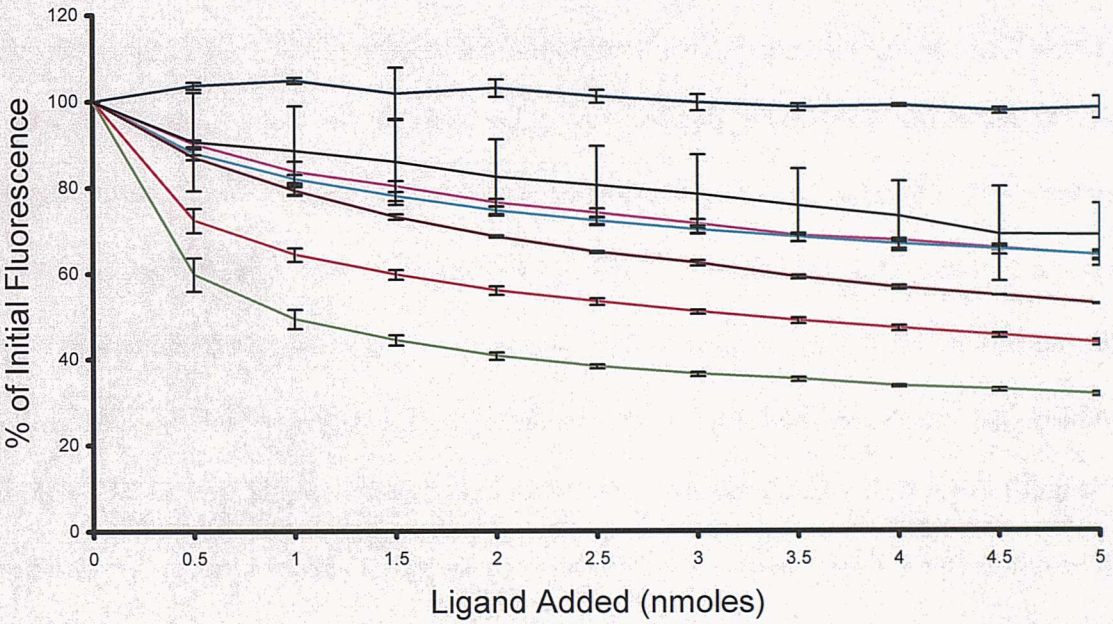

Fig 6.5.2.4 **The Effect on fluorescence intensity of the addition of ligands to the M74W mutant of liver FABP**

To a sample of FABP M74W (0.8 μM) in 10 mM HEPES was added up to 5 nmoles of ligand. The change in fluorescence intensity is plotted as % of initial fluorescence. Excitation was at 280 nm and emission was recorded at 339 nm. All values are the mean of titrations performed in triplicate ± S.D. Oleic acid (dark blue); oleoyl CoA (pink); taurolithocholic acid 3-sulphate (green); taurolithocholic acid (light blue); lithocholic acid 3-sulphate (red); lithocholic acid (brown); cholesterol 3-sulphate (black)

single molecule of oleoyl CoA was being detected by this mutation (**Fig 6.5.2.2**), which is reporting ligand binding at site 2 (see below).

The binding of oleoyl CoA has reduced the fluorescence intensity of all tryptophan containing mutants so far produced including also 3W, 18W and 69W [10] while oleoyl CoA increases the DTNB reactivity of C69 in the wild type protein [73]. These data suggest that the binding of the large and complex oleoyl CoA ligand produces an overall expansion of the protein structure, increasing solvent exposure of the tryptophan residues. The protein is known to have a degree of elasticity [4]. It is possible that this expansion generates a second oleoyl CoA binding site, previously identified using fluorescent analogues of fatty acyl CoA [74]. If there is a discrete second site for oleoyl CoA, it has been argued [9] that this site must be primarily outside the binding cavity as only one molecule of oleoyl CoA can be modelled into the cavity [9], using the published crystal structure [11]. Results from the M74W mutant suggest that a region of the protein adjacent to Met-74 may be part of this second binding site. A potential second portal, unique to liver FABP, is already recognised because of the gap between β-strands G and H. The βEβF hairpin turn (containing Met-74) has also been implicated in this portal [11]. Thus, this potential portal may be part of a second binding site for oleoyl CoA.

6.5.2.3 Bile Acids

The binding of lithocholic acid and its conjugates were accompanied by a change in fluorescence with the L28W and M74W mutants (**Fig 6.5.2.2, Fig 6.5.2.4**). In the case of the Y54W mutant (**Fig 6.5.2.3**), a small increase in fluorescence was seen with ligands containing the 3-sulphate group while negligible effects were seen with the other bile acids. This result is consistent with the sulphate group being located within the portal region of site 2. In contrast, with the M74W mutant (**Fig 6.5.2.4**), the binding of all ligands resulted in a fall in fluorescence, this being most pronounced with the sulphate-containing conjugates.

In the case of the L28W mutant, increases in fluorescence were seen with all lithocholate-derived ligands but was most dramatic with the two sulphate containing derivatives. No suggestion of co-operativity was seen for any bile acid derivative when binding to the L28W mutant, consistent with only one ligand molecule binding to the protein.

The binding of these bile acids and their conjugates could involve two possible orientations of ligands in the protein cavity. In chapter 5 it was argued that more bulky anionic groups occupy site 2 where solvent exposure allows such groups to be more readily accommodated and stabilised. We propose that the identical and small effect of lithocholic acid and taurolithocholic acid on L28W fluorescence is due to the internalisation of the bile acid side chain so that its anionic charge interacts with Site 1. In

contrast we argue that the 3-sulphate group is located at site 2 and produces the dramatic fluorescence enhancement as a result of conformational changes in the region of the tryptophan at position 28.

6.5.2.4 Cholesterol 3-Sulphate

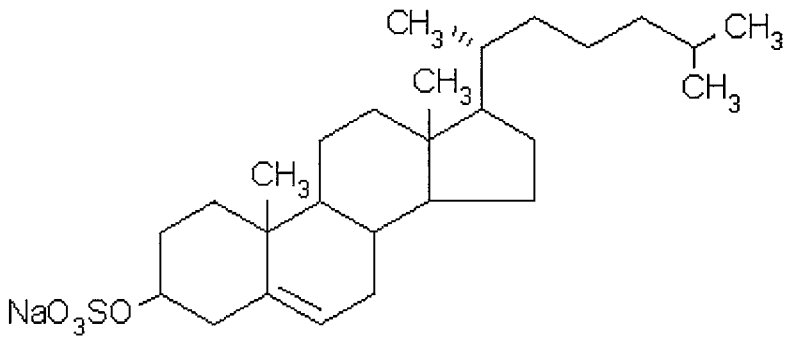

Cholesterol 3-sulphate binding generated a similar curve to that produced by lithocholic acid 3-sulphate and taurolithocholic acid 3-sulphate with no indication of sigmoidicity (**Fig 6.5.2.2**). This similarity would suggest that the 3-sulphate group is again solvent exposed as a result of a single molecule binding at site 2.

It should be noted that the changes in fluorescence with the addition of cholesterol 3-sulphate were not immediate and took several minutes to reach a maximum value. It is possible that cholesterol 3-sulphate has a very low critical micelle concentration and the slow changes in fluorescence that are observed reflect the rate of dissociation of the monomeric cholesterol 3-sulphate from the micelle.

The effect of the addition of cholesterol 3-sulphate on tryptophan fluorescence of the Y54W mutant is minimal (see **Fig 6.5.2.3**), with no significant difference in fluorescence intensity detected.

Cholesterol 3-sulphate binds to FABP M74W, producing a small but significant loss of tryptophan fluorescence (see **Fig 6.5.2.4**). This could reflect the location of the non-polar cholesterol group within the binding cavity resulting in less quenching of the tryptophan than the bile acids that contain a second polar group.

6.5.2.5 Competition For Binding Between Oleic Acid and Oleoyl CoA

The tryptophan fluorescence changes upon ligand binding to L28W make it a useful tool in measuring competition between ligands for the protein. Previously ligand binding was measured using DAUDA displacement. As this method for measuring binding relied upon displacement by any one ligand, there was no way of making direct comparisons between ligands. The opposing fluorescence changes upon ligand binding to apoFABP L28W had now made this possible in the case of oleic acid and oleoyl CoA. Oleic acid causes the most dramatic increase in tryptophan fluorescence upon binding to the protein while oleoyl CoA causes a decrease in tryptophan fluorescence. There is insufficient space within the cavity for both ligands to bind simultaneously and so titrating in one ligand then the other will cause competition between the ligands for the protein. This competition is measurable using the intrinsic fluorescence of the tryptophan residue. This is an important study as there is some controversy about the relative affinity

of fatty acids and fatty acyl CoAs for LFABP and if fatty acyl CoAs are able to regulate LFABP function in vivo.

Oleic acid was titrated into the liver FABP to achieve a ratio of ligand : protein of 2 : 1. After the 2 : 1 stoichiometry had been achieved, an excess of oleoyl CoA was then titrated into the same solution. As can be seen in **Fig 6.5.2.5** the addition of oleic acid caused the same sigmoidal shaped titration curve that was seen and discussed earlier. Upon addition of oleoyl CoA there is a dramatic fall in tryptophan fluorescence indicating that the oleoyl CoA is binding with similar affinity to the fatty acid. With the addition of the first 0.5 nmoles of oleoyl CoA there is a 40% fall in the tryptophan fluorescence. Given that there are only 0.8 nmoles of FABP L28W, this would suggest that just over half of the oleoyl CoA added is binding and in doing so is displacing oleic acid.

When the order of ligand addition is reversed, the resulting graph is effectively a reverse of the first, as seen in **Fig 6.5.2.6**. Initially there is the loss of tryptophan fluorescence that had been recorded earlier, as the oleoyl CoA is added. Oleoyl CoA is titrated in here to achieve a 2 : 1 stoichiometry. It is important to remember that only one molecule of oleoyl CoA is likely to bind to Liver FABP. As oleic acid is added, there is a corresponding large increase in fluorescence. The sigmoidal shape is no longer apparent and the overall steepness of the binding curve is less pronounced as we might expect given that the oleic acid is now competing with oleoyl CoA for the LFABP binding site. The addition of the first 0.5 nmoles of oleic acid results in a tryptophan fluorescence

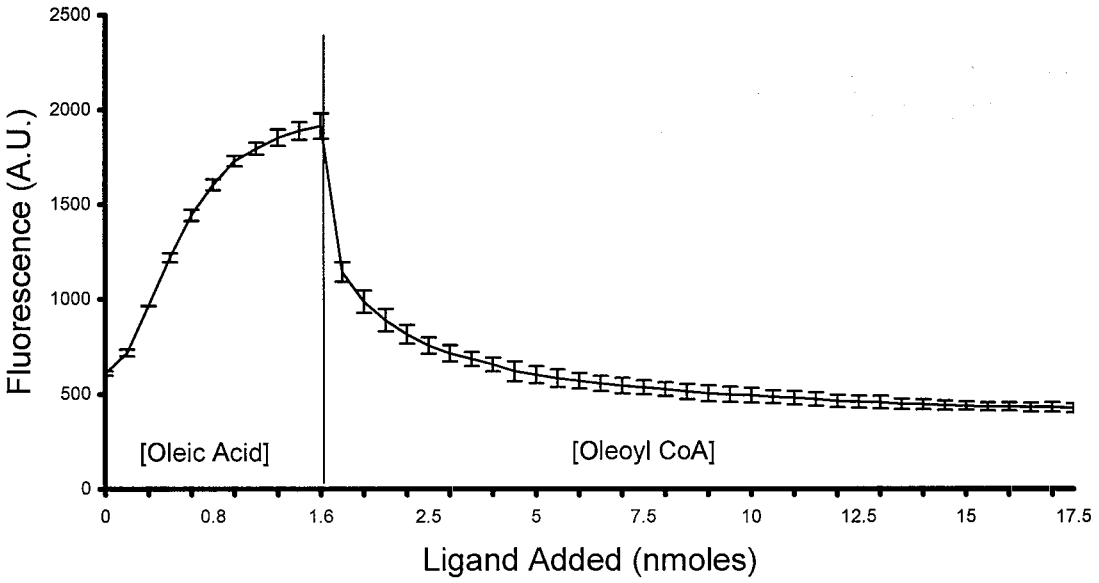

Fig 6.5.2.5 **The effect on fluorescence intensity of the sequential addition of oleic acid and oleoyl CoA to the L28W mutant of LFABP**

To 0.8 μM FABP L28W in 10 mM HEPES was added oleic acid (up to 1.6 μM) followed by oleoyl CoA and the percentage change in fluorescence intensity was recorded. The oleic acid concentration is on an exaggerated scale. Three separate titrations are shown.

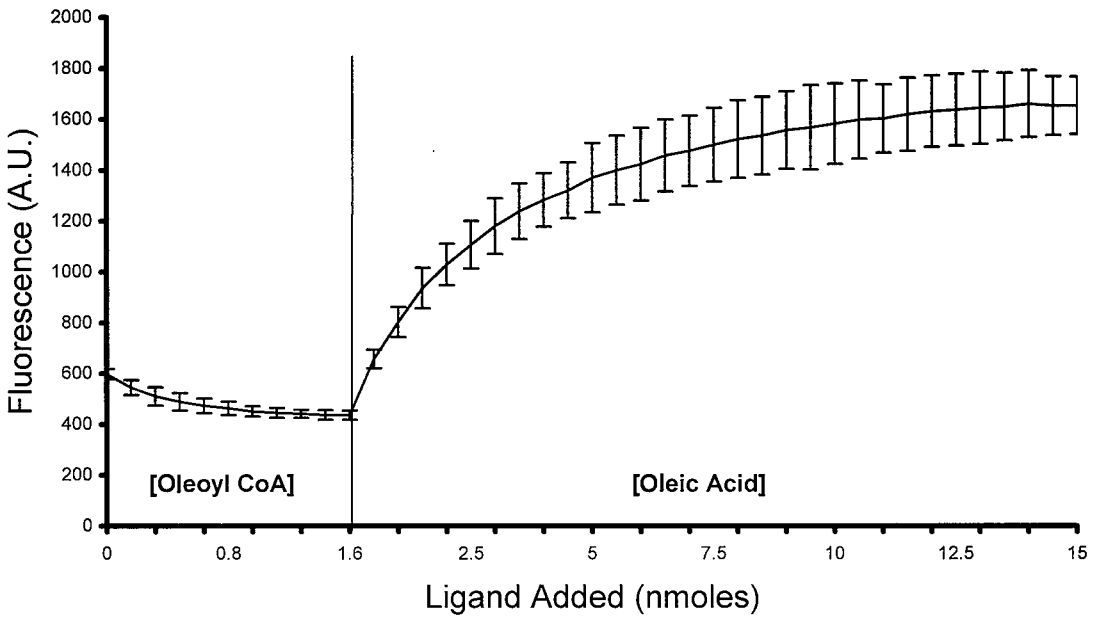

Fig 6.5.2.6 **The effect on fluorescence intensity of the sequential addition of oleoyi CoA and oleic acid to the L28W mutant of LFABP**

To 0.8 μM FABP L28W in 10 mM HEPES was added oleoyl CoA (up to 1.6 μM) followed by oleic acid and the percentage change in fluorescence intensity was recorded. The oleoyl CoA concentration is on an exaggerated scale. Three separate titrations are shown.

increase equivalent to about 0.2 nmoles of oleic acid binding and 0.1 nmoles of oleoyl CoA being displaced. Again the shapes of the titration curves are consistent with oleic acid and oleoyl CoA binding with similar affinities.

Previous results had quoted the K_i values for oleic acid and oleoyl CoA as 0.04 μM and 0.81 μM respectively, see chapter 3. A 20-fold difference in K_i values should have a very dramatic effect on the titration curves and does not appear to match the results that have been obtained in this section. It would be expected, given the K_i values that addition of oleoyl CoA to FABP L28W with oleic acid bound to it would produce little change in fluorescence. Following the reverse logic, addition of oleic acid to FABP L28W with oleoyl CoA already bound to it should produce a large increase in fluorescence as the oleoyl CoA is displaced. Neither of these predictions match the results obtained. The results in this section suggest that the protein has very similar affinities for these two ligands, contradicting the previously recorded K_i values. The reason for this discrepancy is most likely related to DAUDA in FABP wild type and the tryptophan residue in FABP L28W reporting on different parts of the protein. FABP L28W is reporting on oleic acid binding site 2, which has a lower fatty acid affinity (reported K_d range 0.06 to 4.0 μM) than site 1 (reported K_d range 0.009 to 0.2 μM) [13;19;75] where DAUDA is proposed to bind. These reported values confirm that site 1 has been a 10 and 20 fold higher affinity for fatty acids than site 2.

It is worth reiterating the point made earlier that for oleoyl CoA to bind, it is presumably displacing the oleic acid molecule at site 1 as well as the oleic acid at site 2,

so that the bulky acyl chain of oleoyl CoA can be accommodated in the binding cavity. Thus although the oleoyl CoA binding at site 2 reflects the binding properties at that site, displacement of a ligand (fatty acid or DAUDA) from site 1 will follow.

6.5.3 Interaction Between Tryptophan Mutants of LFABP and Phospholipid Vesicles

The tryptophan insertion mutants L28W, Y54W and M74W are located in the portal region of liver FABP. It has also been shown in previous chapters that phospholipid vesicles interact with lysine residues also located within the portal region. Therefore it was expected that as the mutant proteins bind to the phospholipid vesicles there would be detectable changes in the tryptophan fluorescence as a result of conformational changes. Such conformational changes were predicted because of the release of DAUDA when the LFABP-DAUDA complex binds to such vesicles.

Wavelength scans were carried out at an excitation of 280 nm in the presence and absence of 12.5 μM DOPG. The scan for FABP L28W is shown in **Fig 6.5.3.1(a)**. As can be seen from **Fig 6.5.3.1(a)** the addition of DOPG causes a large increase in tryptophan fluorescence to a maximum emission value that is over twice the maximum emission value achieved in buffer alone. There is a significant change in the wavelength that the maximum emission fluorescence value is reached. In buffer this maximum is at an emission of 338 nm and when DOPG is added the wavelength at which this maximum is reached shifts to 333 nm. These changes in the maximum fluorescence and the

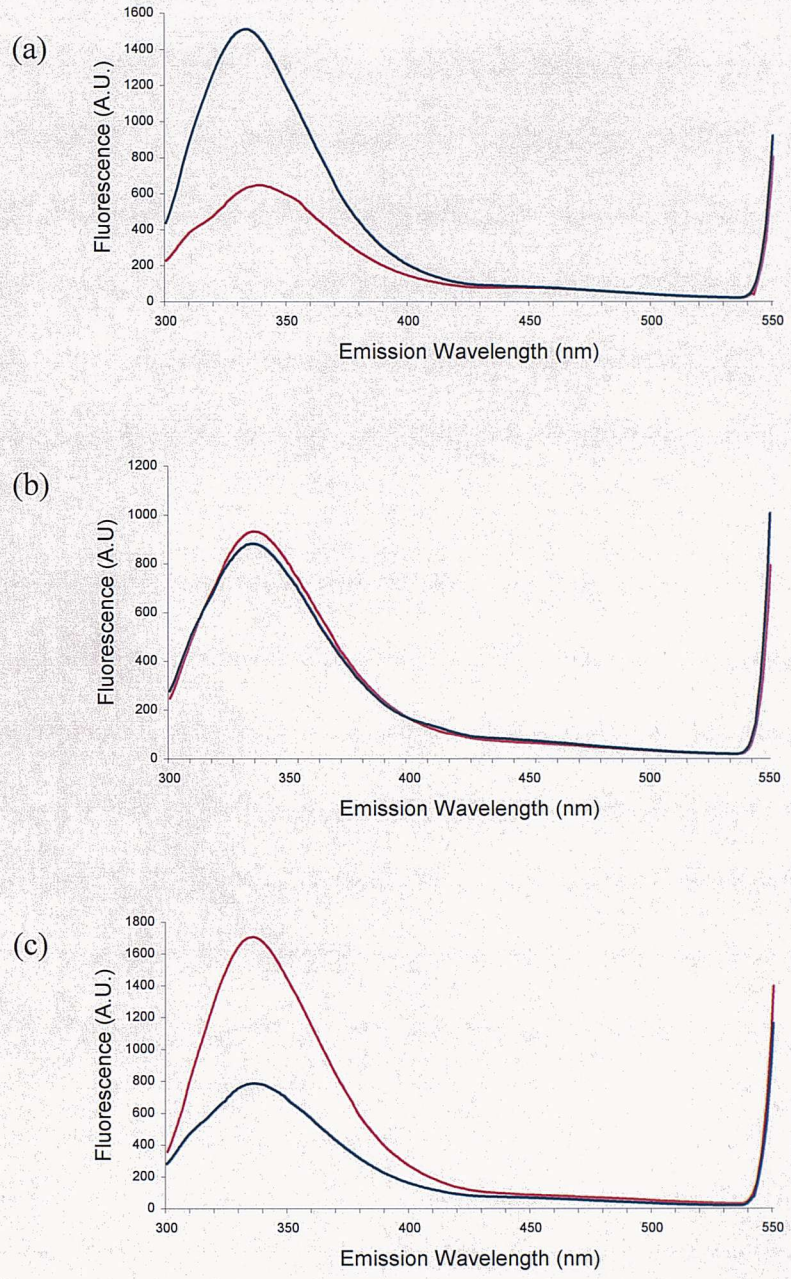

Fig 6.5.3.1 **The Effect of DOPG on the Tryptophan Emission Maxima of L28W, Y54W and M74W LFABP**

Tryptophan emission of 0.8 μM FABP of either L28W (a), Y54W (b) or M74W (c); in 10 mM HEPES was measured between 300 nm and 550 nm following excitation at 280 nm in the absence (red) or presence (blue) of 12.5 μM DOPG. Results are the mean of three titrations.

wavelength at which this new maximum is reached suggest a conformational change as the protein binds to the DOPG vesicles. This large change in fluorescence also makes it possible to investigate in more detail the interaction between liver FABP and phospholipids. Moreover, monitoring tryptophan changes on binding to DOPG vesicles provides an alternative assay to monitoring DAUDA release (chapters 3-5). Assays using DAUDA had to be corrected for the released DAUDA partitioning into phospholipids vesicles, no such problem exists when monitoring tryptophan fluorescence.

The wavelength scan for FABP Y54W is shown in **Fig 6.5.3.1 (b)**. There is no significant difference in the wavelength scans carried out in the presence and absence of DOPG. The emission wavelength at which the maximum fluorescence value was measured was 336 nm in buffer alone and 335 nm in the presence of DOPG. Such a change is regarded as negligible. The maximum fluorescence value itself falls by just 5% when DOPG is added. This small change indicates no significant effect on the environment surrounding the tryptophan residue as the protein binds to phospholipids vesicles.

The wavelength scan for the final mutant under investigation in this section, FABP M74W, can be seen in **Fig 6.5.3.1 (c)**. With the M74W mutant, addition of DOPG results in a large loss of fluorescence with no corresponding wavelength shift. The maximum fluorescence drops by roughly 50% in the presence of 12.5 μM DOPG. The emission wavelength for the maximum fluorescence value also remains unchanged at 336 nm in the presence and absence of DOPG. Thus the conformational change on binding to

DOPG vesicles produces very different effects in terms of the changing environment of 28W and 74W.

Fig 6.5.3.2 acts as a summary and gives a more direct comparison between the mutants. The results as recorded and discussed above are supported by the titration curves for DOPG in **Fig 6.5.3.2**. The titration curves show a smooth gradation from 0 μM levelling out to a peak close to 12.5 μM. The changes in fluorescence also support the values given above. At 12.5 μM DOPG L28W has increased in fluorescence by just over double, Y54W remains relatively unaffected but displays a small loss of fluorescence and M74W has lost 50% of its starting fluorescence at this DOPG concentration.

The release of DAUDA from LFABP in the presence of DOPG vesicles involves non-specific electrostatic interactions between the protein and the phospholipid interface (chapters 3 and 4). No such interactions were seen with DOPC vesicles. Therefore it was an important control to confirm that the changes in tryptophan fluorescence were also dependent on the presence of anionic phospholipid vesicles. The result of titrating DOPC vesicles into all three tryptophan containing mutants is shown in **Fig 6.5.3.3**. No change in tryptophan fluorescence is observed, consistent with a lack of interaction between the protein and the zwitterionic DOPC vesicles.

With phospholipids studies it is important that results can be replicated at more physiological levels of negatively charged phospholipid. Therefore the experimental approach was repeated with 20mol% DOPG in DOPC. The results shown in **Fig 6.5.3.4**,

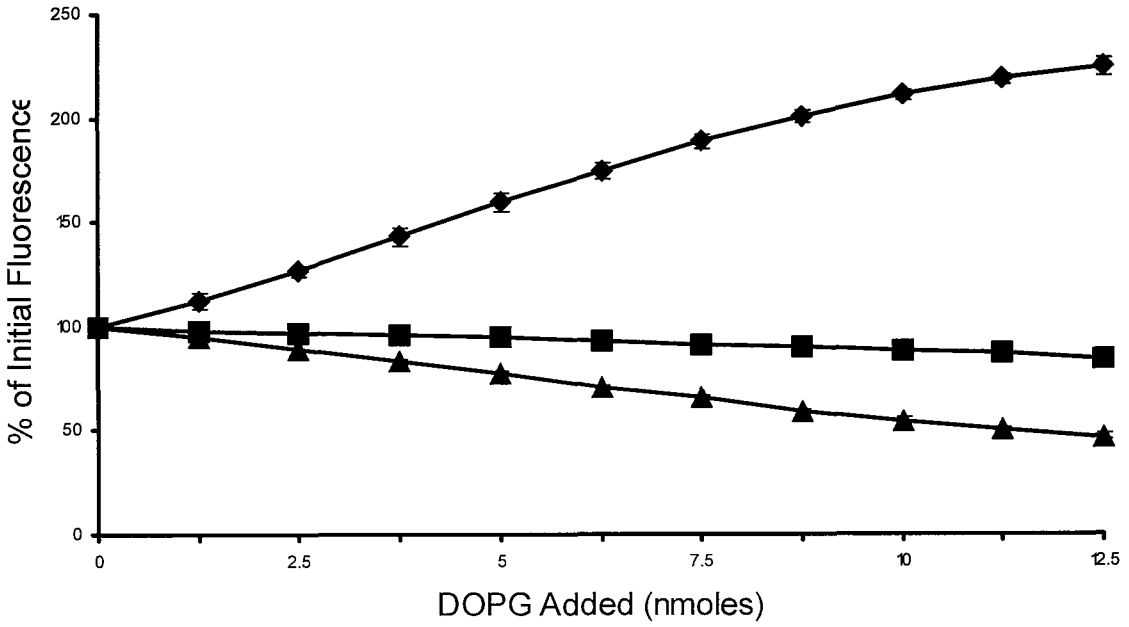

Fig 6.5.3.2 **The Effect on the Tryptophan Fluorescence of the Titration of 100% DOPG SUVs into L28W, Y54W and M74W LFABP**

100% DOPG SUVs were titrated by methanol injection into 0.8 μM LFABP L28W (♦), Y54W (■) or M74W (▲) in 10 mM HEPES. Tryptophan fluorescence was measured at 339 nm following excitation at 280 nm. All data points shown are the mean of three titrations ± S.D.

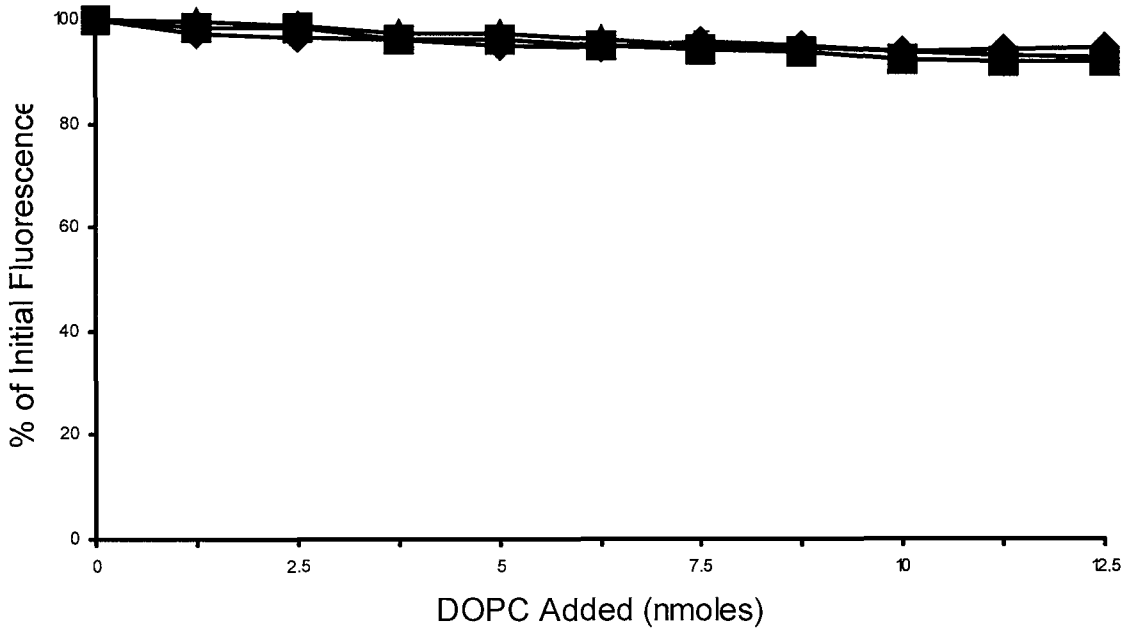

Fig 6.5.3.3 **The Effect on the Tryptophan Fluorescence of the Titration of 100% DOPC SUVs into L28W, Y54W and M74W LFABP**

100% DOPC SUVs were titrated by methanol injection into 0.8 μM LFABP L28W (♦), Y54W (■) or M74W (▲) in 10 mM HEPES. Tryptophan fluorescence was measured at 339 nm following excitation at 280 nm. All data points shown are the mean of three titrations ± S.D.

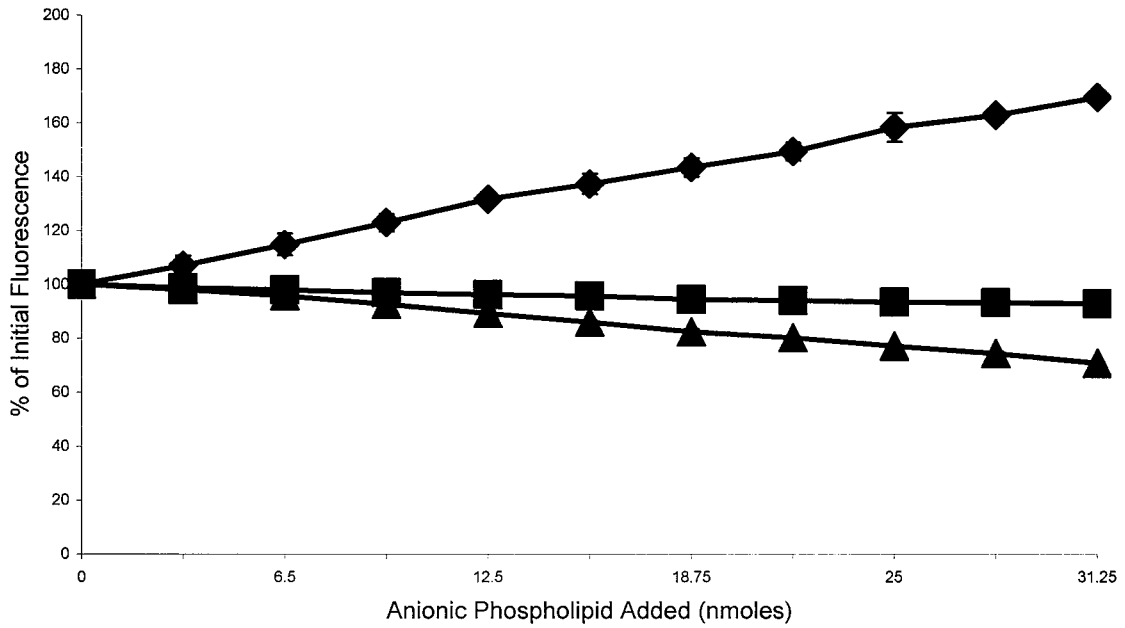

Fig 6.5.3.4 **The Effect on the Tryptophan Fluorescence of Titration of 20 mol% DOPG in DOPC into L28W, Y54W and M74W LFABP**

20 mol% DOPG in DOPC was titrated by methanol injection into 0.8 μM LFABP L28W (♦), Y54W (■) or M74W (▲) in 10 mM HEPES. Tryptophan fluorescence was measured at 339 nm following excitation at 280 nm. All data points shown are the mean of three titrations ± S.D.

are clearly very similar to those produced with 100% DOPG. Again there is a large significant increase in the tryptophan fluorescence of L28W as the mixed phospholipids are added. There is also a large significant loss of tryptophan fluorescence from M74W as seen previously. Y54W experiences no significant change in fluorescence as predicted. The M74W result and to a greater degree, the L28W result indicate that these mutants lend themselves to further studies involving interaction of the protein with phospholipids and this is discussed in detail under 'Future Work'.

The large increase in fluorescence intensity that occurs as FABP L28W interacts with the anionic phospholipids interface can be used to confirm the observation in chapter 5 that a high salt concentration reduces the rate of this interaction, rather than preventing it. To test this wavelength scans of 0.8 μM FABP L28W in 10 mM HEPES and 12.5 μM DOPG were carried out in the presence and absence of 0.15 M NaCl. A scan was carried out immediately after the additions were made, the result of which can be seen in **Fig 6.5.3.5**. In **Fig 6.5.3.5** the large increase in fluorescence intensity with L28W that accompanies interaction with DOPG vesicles is not seen in the presence of NaCl. However, when these scans are repeated with the same solutions after three hours the wavelength scans for the two assays containing 12.5 μM DOPG, both in the presence and absence of 0.15 M NaCl, are essentially identical (see **Fig 6.5.3.6**). These scans confirm the observation in chapter 5 that NaCl slows the rate of interaction between FABP and anionic phospholipid vesicles, rather than preventing it. It is the subsequent hydrophobic interaction of LFABP with DOPG that produces the observed fluorescence changes. These results have implications with respect to the mechanism of lipid binding

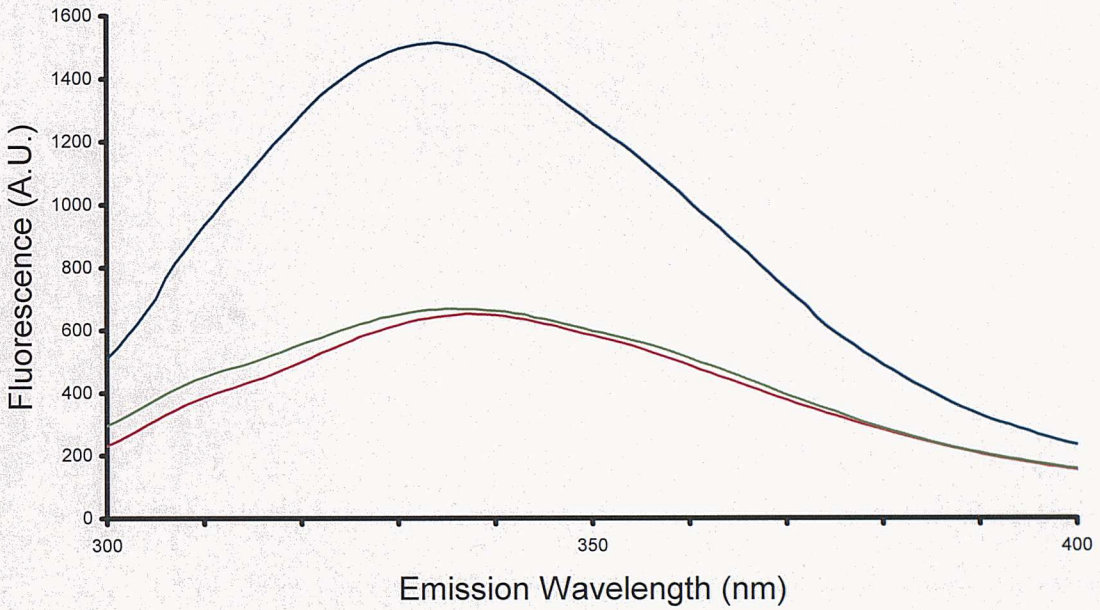

Fig 6.5.3.5 **The Immediate Effect of DOPG on the Tryptophan Emission Maxima of FABP L28W in the presence and absence of NaCl**

Tryptophan emission of 0.8 μM FABP L28W in 10 mM HEPES was measured between 300 nm and 400 nm following excitation at 280 nm in the absence (red) or presence (blue) of 12.5 μM DOPG and in the presence of both 12.5 μM DOPG and 0.15 M NaCl (green). Results are the mean of three titrations.

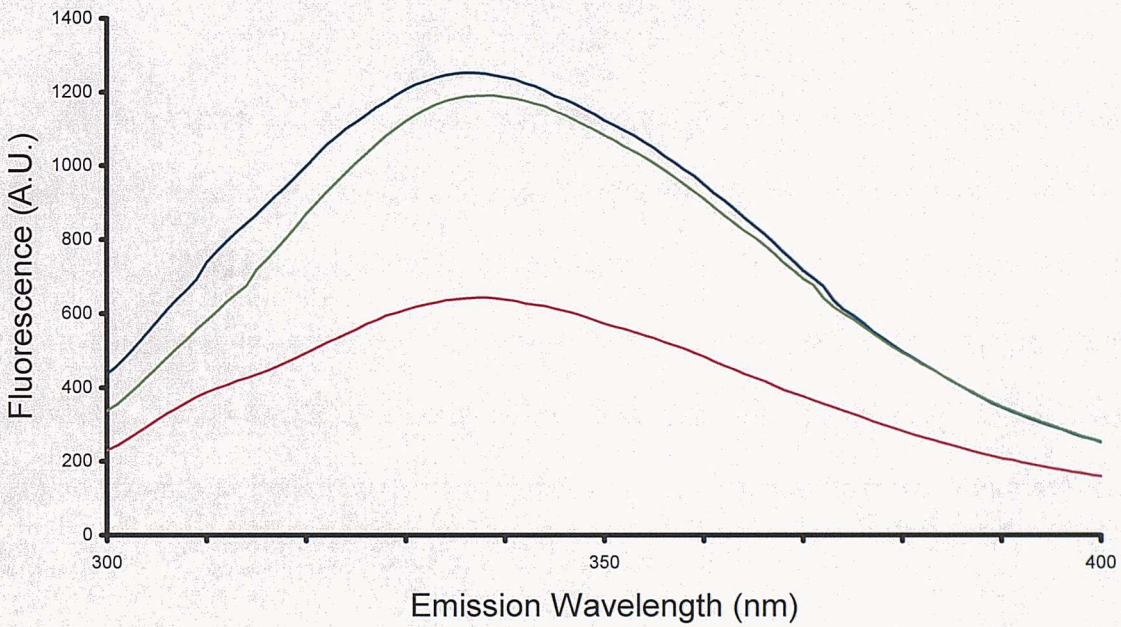

Fig 6.5.3.6 **The Immediate Effect of DOPG on the Tryptophan Emission Maxima of FABP L28W in the presence and absence of NaCl After Incubation For Three Hours**

Tryptophan emission of 0.8 μM FABP L28W in 10 mM HEPES was measured between 300 nm and 400 nm following excitation at 280 nm in the absence (red) or presence (blue) of 12.5 μM DOPG and in the presence of both 12.5 μM DOPG and 0.15 M NaCl (green). Results are the mean of three titrations.

to the FABP family. It shows that the initial electrostatic interaction with the portal region of FABP is a catalytic step rather than an essential step in the binding of fatty acids. This initial interaction is likely to aid orientation of the protein and lipid prior to binding.

6.6 N-terminal Region Tryptophan Mutants

The N-terminal tryptophan containing mutants have previously been prepared and analysed [10;25]. Mutation of residues at the N-terminal region had already been carried out by Dr. Joanne Davies who produced the F3W and F18W mutants of liver FABP. Previous studies on these residues had shown that the N-terminal region was in close proximity to the phospholipid vesicle as it interacted with the protein. In order to determine the extent of the interaction of the N-terminal with the phospholipids interface a further tryptophan-containing mutant, Y7W, was prepared.

The structure of liver FABP highlighting the positions of the F3W, Y7W and F18W is shown below in **Fig 6.6.1**. It can be seen that the Phe-3 on the protein is at the opposite end of the β-barrel to the portal and α-helical regions. The Tyr-7 is positioned half way down the β-barrel on the same β-strand as Phe 3. The Phe-18 is located within the α-helical region on helix 1 that forms the top of the proposed portal region of the protein.

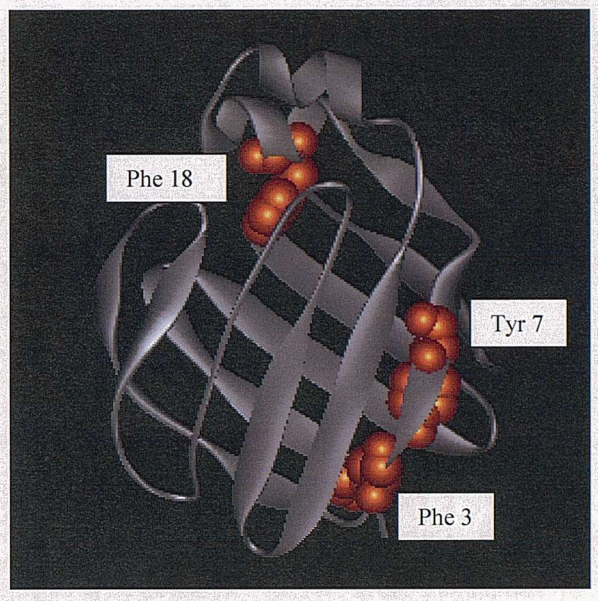

Fig 6.6.1 LFABP showing the three residues that are replaced by tryptophan

6.6.1 Interaction Between the N-terminal Region and DOPG Vesicles

DOPG vesicles were titrated into the three tryptophan containing mutants and the change in fluorescence intensity was monitored at an emission wavelength of 330 nm after excitation at 280 nm. The results are shown in **Fig 6.6.1.1**.

A significant loss of fluorescence was seen with the F3W mutant, to approximately 50% of its starting value. This loss of fluorescence intensity was in line with previous studies [25]. There was no significant change in the tryptophan fluorescence of F18W as DOPG SUVs were titrated in, again this result matches data obtained previously. Of particular interest was the effect that the DOPG SUVs would have on the tryptophan fluorescence of the Y7W mutant. The Y7W mutant experienced a 25% fall in tryptophan fluorescence as DOPG SUVs were added. It would be tempting to

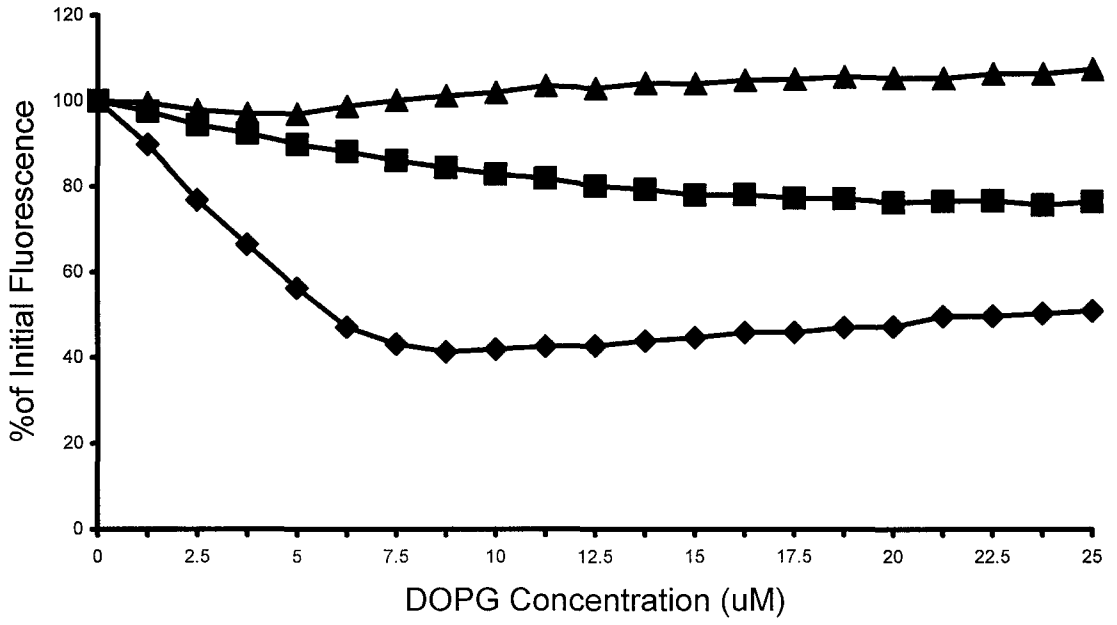

Fig 6.6.1.1 **The Effect on the Tryptophan Fluorescence of Titration of 100% DOPG SUVs into F3W, Y7W and F18W LFABP**

100% DOPG SUVs were titrated by methanol injection into 0.8 μM LFABP F3W (♦), Y7W (■) or F18W (▲) in 10 mM HEPES. Tryptophan fluorescence was measured at 330 nm following excitation at 280 nm. All data points shown are the mean of three titrations ± S.D.

speculate that this change in fluorescence represents partial insertion of the tryptophan at position 7 into the phospholipids interface, but it does not appear to be inserted as deeply as the tryptophan residue in the F3W mutant. However, what can be concluded is that the environment of the tryptophan at position 7 changes when the protein binds to DOPG vesicles, possibly due to this residue coming in close proximity to the phospholipids interface.

Wavelength scans were carried out for Y7W in 12.5 μM DOPG in the presence and absence of 0.15 M NaCl, the results are shown in **Fig 6.6.1.2**. The same 25% loss of tryptophan fluorescence is seen in the wavelength scan as had been seen in the titration. This loss of tryptophan fluorescence is accompanied by a shift in the emission wavelength at which the maximum fluorescence value is reached from 329 nm to 331 nm. This red-shift, that has also been recorded with F3W [25], is characteristic of the movement of the residue into a more polar environment. As had been seen in earlier chapters, the presence of NaCl inhibits the interaction between phospholipid SUVs and LFABP. In the presence of NaCl there is no change in the wavelength scan for FABP Y7W when DOPG is added. This shows that the loss of tryptophan fluorescence observed from Y7W LFABP requires an initial electrostatic interaction between the protein and anionic phospholipid vesicles.

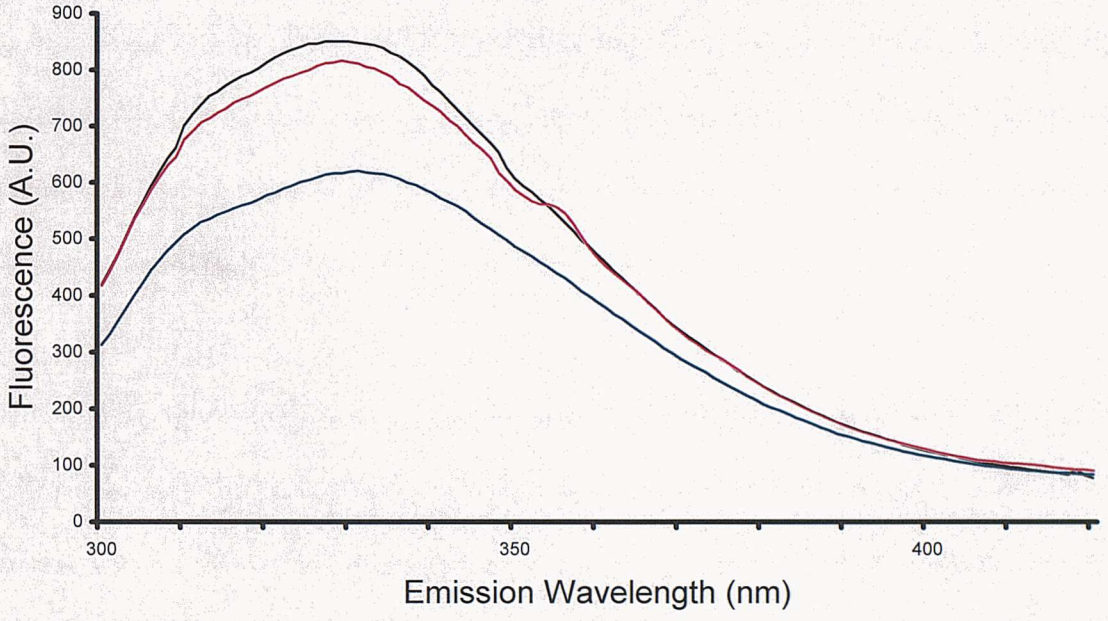

Fig 6.6.1.2 **The Effect of DOPG on the Tryptophan Emission Maxima of Y7W LFABP in the presence and absence of 0.15 M NaCl**
Tryptophan emission of 0.8 μM FABP of Y7W in 10 mM HEPES was measured between 300 nm and 420 nm following excitation at 280 nm in buffer only (black) and in 12.5 μM DOPG in the absence (blue) or presence (red) of 0.15 M NaCl. Results are the mean of three titrations.

6.6.2 Fluorescence Resonance Energy Transfer (FRET) Studies Using Tryptophan Mutants of LFABP

FRET is a more direct measure of the proximity of a tryptophan residue to an appropriate receptor such as a dansyl group. FRET is not dependent on any conformational changes in the tryptophan donor to report changes in fluorescence intensity of dansyl emission. FRET instead is dependent on the distance between the tryptophan residue and the dansyl group [76]. After exciting at 280 nm fluorescence enhancement was monitored at 500 nm due to dansyl fluorescence, as a result of FRET, to follow the binding of F3W, Y7W and F18W to phospholipids.

DOPG vesicles containing 5mol% dansyl DHPE were titrated into F3W, Y7W and F18W LFABP. The results can be seen in **Fig 6.6.2.1**. There was significant FRET recorded with LFABP F3W as had been seen previously [25]. This suggests that the tryptophan residue in LFABP F3W is in close proximity to the dansyl DHPE in the phospholipid vesicles. This further supports the conclusion from **section 6.6.1** that the tryptophan residue at position 3 on this protein is present at the phospholipid interface.

Although no major differences in FRET were observed comparing these three mutants, at higher concentrations of DOPG greatest FRET was seen with the F3W mutant see **Fig 6.6.2.1**. In contrast, the FRET value was least for the F18W mutant while the Y7W value was intermediate. Overall the results are consistent with residue 7 at the N-terminal being closer to the interface than residue 18, but not as close as residue 3.

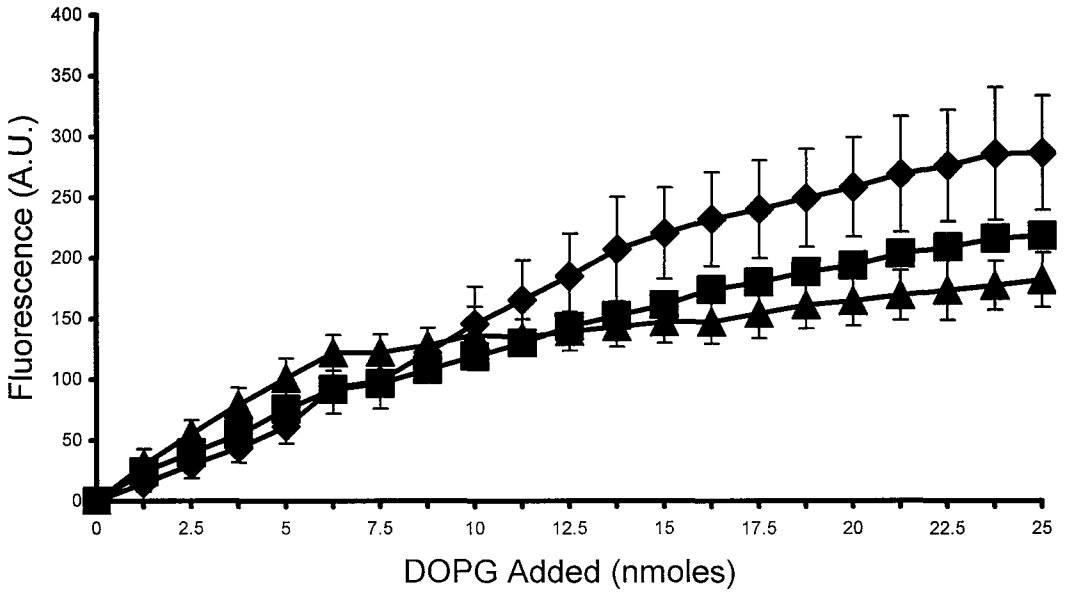

Fig 6.6.2.1 **The Effect of DOPG Containing 5 mol% Dansyl DHPE Vesicles on Tryptophan Fluorescence of F3W, Y7W and F18W LFABP Mutants**
DOPG containing 5 mol% dansyl DHPE was titrated as a methanol solution into 0.8 μM LFABP F3W (♦), Y7W (■) or F18W (▲) in 10 mM HEPES. Dansyl fluorescence was measured at 500 nm following excitation at 280 nm. All data points are the mean of three titrations ± S.D.

Again this result follows the data from **section 6.6.1**, suggesting that the tryptophan residue in Y7W is close to the interface, but not buried within it.

6.6.3 Succinimide Quenching of F3W, Y7W and F18W

Succinimide is a fluorescence quencher that has been used in studies, including a related FABP (Sj-cFABP [77]), to measure the solvent exposure of tryptophan residues. A tryptophan residue that is highly solvent exposed will undergo a significant loss of tryptophan fluorescence in the presence of succinimide. On the other hand the fluorescence of a tryptophan residue that is not solvent exposed will be unaffected by the addition of succinimide. Succinimide is used in preference to the more commonly used quencher, acrylamide, due to succinimide being larger and hence more sensitive to the structural location of the tryptophan residue [78].

The succinimide quenching studies were carried out using 0.8 μM FABP in 10 mM HEPES buffer in the presence and absence of 25 μM DOPG vesicles. The results are shown in **Fig 6.6.3.1** where the reduction in fluorescence intensity is plotted as a function of succinimide concentration. All three mutants experienced quenching in the presence of succinimide. F18W, which underwent the largest degree of quenching, is most likely the mutant with the most solvent exposed tryptophan residue. Applying the reverse logic F3W, which shows the least quenching in the presence of succinimide, is the mutant with the least solvent exposed tryptophan residue. These results standing alone only confirm

(a)

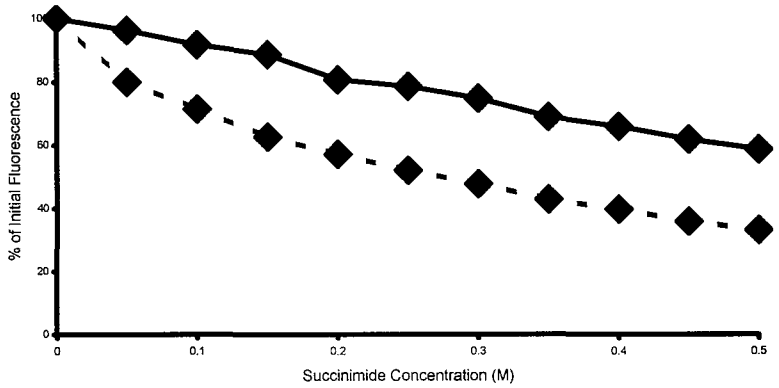

(b)

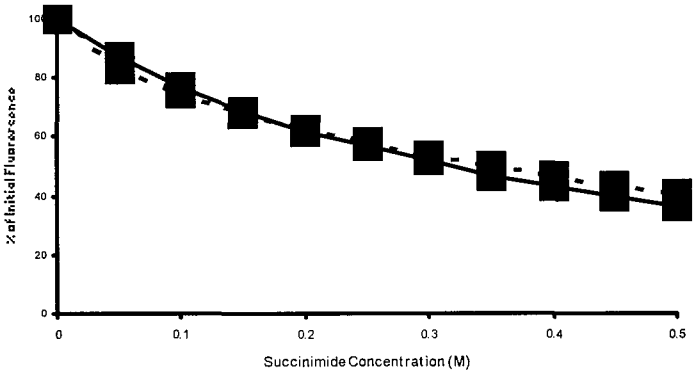

(c)

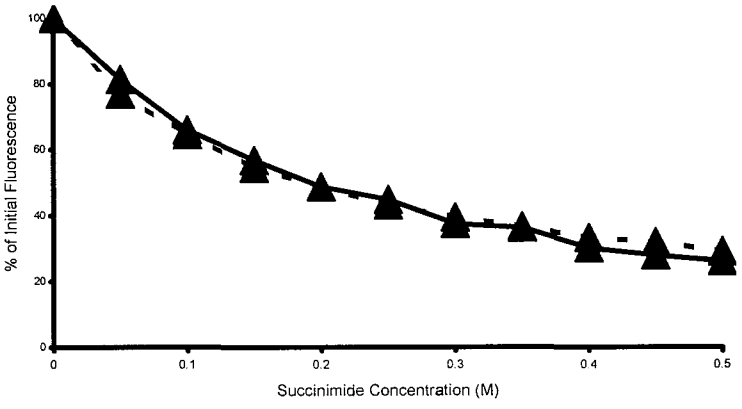

Fig 6.6.3.1 **The Effect of Succinimide on the Tryptophan Fluorescence of F3W, Y7W and F18W LFABP Mutants in the Presence and Absence of DOPG**
Succinimide was titrated into 0.8 μM LFABP F3W (a), Y7W (b) or F18W (c) in 10 mM HEPES , in the presence (continuous line) or absence (broken line) of 25 μM DOPG. Tryptophan fluorescence was measured at 330 nm following excitation at 280 nm. All data points are the mean of three titrations.

what is already known from the crystal structure. Far more significant was the effect that the presence of DOPG vesicles had on this quenching.

It is clear from **Fig 6.6.3.1 (a)** that the effects of succinimide quenching on the F3W mutant are prevented in the presence of DOPG vesicles. There are two explanations for this. The first is that the tryptophan residue is undergoing a conformational change and being internalized by the protein in the presence of DOPG. The second is that the tryptophan residue is becoming sufficiently embedded in the surface of the vesicles so as to become inaccessible to the succinimide. **Fig 6.6.3.1** does not tell us which explanation is correct, however the results of the previous FRET studies support the second model. The ability of the F3W mutant to undergo FRET with dansyl DHPE containing anionic phospholipids means that the tryptophan in this mutant must be in close proximity to the phospholipid interface. If this residue was being internalized in the presence of anionic phospholipid vesicles, the enhanced FRET compared with the Y7W and F18W would not have been anticipated.

Fig 6.6.3.1 (b) and **Fig 6.6.3.1 (c)** show that this protection from quenching by the addition of DOPG that is found in the F3W mutant is not apparent in the Y7W or the F18W mutant. Such findings mean that even in the presence of DOPG the tryptophan residues in these mutants remain sufficiently solvent exposed to be accessible to succinimide.

6.7 Discussion

In chapters 3-5 of this work the importance of the portal region in the interaction of LFABP in binding to anionic phospholipid vesicles and in ligands binding to the protein has been established and discussed. It is believed that ligand binding to LFABP and interaction of the protein with anionic phospholipids result in conformational changes within LFABP. In order to investigate this further, tryptophan residues were inserted into LFABP (which has no tryptophan residues in its native state), both at the portal region (L28, Y54 and M74) and also at the N-terminal (Y7) region of the protein which is known to undergo a conformational change when LFABP interacts with anionic phospholipid vesicles [25]. The intrinsic fluorescence of tryptophan allows for studies to be carried out on the apo protein, as apposed to studies in chapters 3-5 which relied upon a fluorescent reporter group (either DAUDA or ANS).

The use of tryptophan insertion mutagenesis to produce three portal mutants, L28W, Y54W and M74W, has clarified three important ligand binding properties of liver FABP.

Firstly, ligand binding studies with the L28W mutant demonstrated co-operativity between sites 1 and 2 when binding fatty acids, a co-operativity that was originally proposed based on the crystal structure with bound oleic acid [11]. These binding results suggest that the first bound fatty acid can exchange between the two sites, while occupancy of site 2 is accompanied by a dramatic increase in fluorescence.

Secondly, changes in fluorescence of tryptophan mutants on binding of oleoyl CoA highlighted a number of important properties of liver FABP with respect to this ligand. In particular, the fluorescent changes seen with the L28W mutant allowed a direct measurement of the competition of fatty acid and fatty acyl CoA binding to liver FABP. It is apparent that these two ligands bind with similar affinities when assessed using ligand competition for this mutant. This is a very important observation because it will reflect the situation in vivo and hence modulation of fatty acid metabolism by mechanisms involving ligand-bound liver FABP will be effected by both fatty acids and fatty acyl CoA concentrations within the cell.

Liver FABP with bound fatty acyl CoA will probably have different structural properties compared to the apoprotein or with fatty acid as the ligand. This is because the highly anionic phosphopanthenyl part of the molecule is surface exposed within the portal region [9] and should dramatically effect potential protein : protein or protein : membrane interactions. It remains to be established if these structural differences in properties effect ligand targeting or if the holo-protein has more specific regulatory effects on lipid metabolism such as interacting with PPAR α [36]. A recent study involving liver FABP knockout mice has highlighted the significant role of this protein in binding fatty acyl CoA in vivo, while the relative contributions of liver FABP and ACBP under varying conditions were discussed [35].

In another liver FABP gene deletion study [79] no significant differences were seen when comparing wild type and liver FABP -/- chow fed mice. However, dramatic differences were observed between +/+ and -/- mice after 48 hour fasting [79]. In particular, a 10-fold increase in hepatic triglyceride content in normal mice was only 2-fold in liver FABP-/-mice. Overall it would appear that in fasting, liver FABP is involved in targeting fatty acids to triglyceride biosynthesis relative to other pathways. Whether this targeting involves liver FABP-bound fatty acid per se or FABP-bound fatty acyl CoA remains to be determined. Most recently, fluorescence studies have demonstrated the ability of liver FABP to colocalise with PPAR α in the nucleus while the nuclear concentration of the FABP was estimated to be similar to that in the cytoplasm [28]. Moreover, over-expression enhanced the targeting of both fluorescent fatty acids and acyl CoAs to the nucleus.

Thirdly, bile acids derived from lithocholic acid are good ligands for FABP and lack of co-operativity is consistent with liver FABP binding only one molecule of ligand. When the 3-sulphate derivatives of lithocholic acid were employed, the fluorescence changes were consistent with these ligands binding at site 2 with the sulphate group accommodated within the portal region. Lithocholic acid derivatives lacking the 3-sulphate appear to bind at site 1 or may exchange between the two sites.

In summary, tryptophan insertion mutagenesis has highlighted conformation changes in liver FABP as a result of ligand binding that provide more details as to how specific ligands, particularly fatty acids and acyl CoAs, interact with the protein. It is

proposed that competition between fatty acids and fatty acyl CoAs for liver FABP should play an important role in ligand targeting within the cell.

The three portal mutants each undergo different fluorescence changes upon ligand binding. The fluorescence intensity of LFABP L28W changes from having the lowest tryptophan fluorescence of the three mutants in buffer, to having the highest fluorescence upon vesicle or ligand binding. For LFABP M74W the reverse is true, this mutant has the highest tryptophan fluorescence in buffer and after ligand or vesicle binding it has the lowest. The increase in fluorescence intensity for the Trp-28 mutant may be explained by loss of quenching on ligand binding, protein fluorescence thus approaching that seen with the other tryptophan mutants (**Table 6.5.1.1**). We suggest that the tryptophan in the apoprotein is quenched by another group within the protein that is in close proximity to Trp-28. The ligand binding at site 2 produces a conformational change that removes the quenching group, possibly the ligand inserts between the tryptophan and the quenching group. (It has been proposed that quenching of tryptophan by nearby amino acid residues is a common occurrence in folded proteins [80]). Inspection of the structure (**Fig 6.5.1**) suggests that residues in the vicinity of Tyr-54 at the βCβD turn are appropriately placed.

If the low fluorescence of the apo form of L28W is the result of internal quenching by an adjacent amino acid, then loss of protein structure as a result of unfolding should, at least in terms of partial unfolding, result in an increase in fluorescence. This was tested by Jane Worner-Gibbs within this laboratory. When the three tryptophan mutants were equilibrated in a range of urea concentrations, the M74W

demonstrated the typical loss of fluorescence previously seen with F3W, F18W and C69W [10]. In marked contrast, the L28W mutant demonstrated a significant increase in fluorescence when exposed to up to 8 M urea (**Fig 6.7.1**). The Y54W mutant demonstrated an overall fall in fluorescence but with somewhat anomalous fluorescence behaviour with increasing urea. Recall that this mutant also showed anomalous CD behaviour (**Fig 6.3.1**) consistent with more than one conformation of the protein.

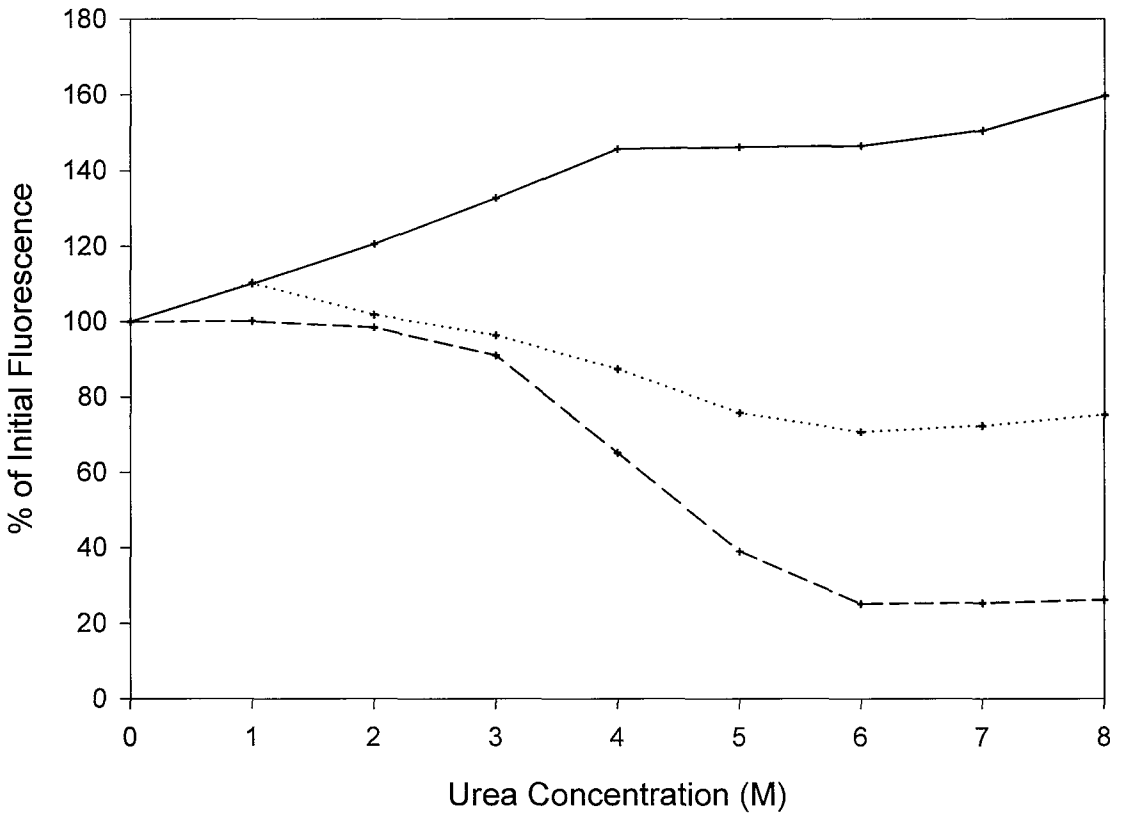

Fig. 6.7.1 **The effect of urea concentration on the tryptophan fluorescence of L28W, Y54W and M74W mutants of liver FABP**
1nmole of LFABP L28W (—), Y54W (·····) or M74 W (----) in 50mM Hepes buffer was equilibrated with up to 8M urea for 2 hours. The fluorescence intensity was measured and plotted as a % of fluorescence in the absence of urea. The values are the mean of three separate incubations at each concentration of urea. Data provided by Jane Worner-Gibbs

The study of the F3W, Y7W and F18W tryptophan mutants of LFABP has extended our knowledge of the conformational change at the N-terminal region of the protein. Fluorescence resonance energy transfer studies have shown the tryptophan residues at positions 3 and 7 come in close proximity to the anionic interface. This was supported by the titration of DOPG SUVs causing a loss of tryptophan fluorescence from Y7W. It is proposed that Tyr-7 and Phe-3 both interact with phospholipids vesicles. The fluorescence quenching studies however showed that the tryptophan fluorescence of Y7W was not protected from quenching by DOPG vesicles. Hence Trp-7 is sufficiently distant from the phospholipid interface to allow for quenching by succinimide. Overall then Trp-7 is close to the anionic phospholipid interface, but its properties are not perturbed by interfacial binding to the extent seen with Trp-3.

It is possible that a conformational change at the N-terminal region of the protein opens up a second portal region for ligand exit. Investigation of the crystal structure (**Fig 6.7.2)** shows that the N-terminal region of the protein occludes a large gap region at the base of the protein that might provide a second portal for ligand release. Inspection of the crystal structure of IFABP [81] also highlighted a potential portal in the equivalent region of IFABP, but significant conformational changes would again be required to remove amino acid side chains obstructing this portal before ligand could exit.

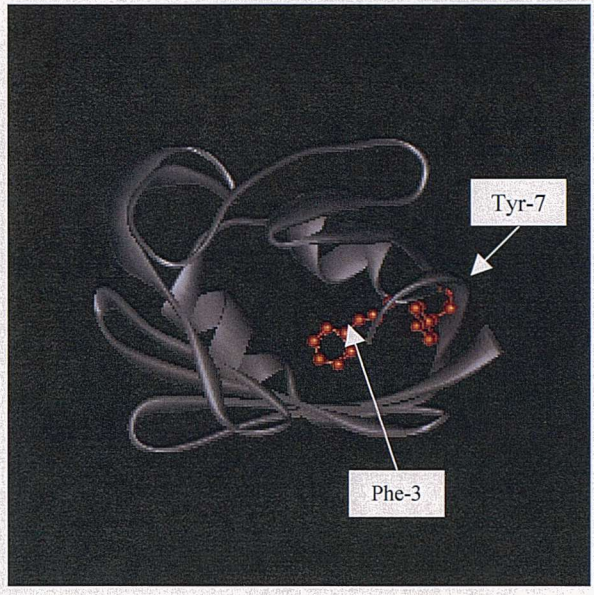

Fig 6.7.2 **View of LFABP looking through the binding cavity from the N-terminal region to the α-helical region**
Phe3 and Tyr7 are shown in CPK representation (orange)

Chapter 7 – General Summary and Future Work

7. General Summary and Future Work

Liver fatty acid binding protein has been extensively studied and its precise physiological role and its mechanism of ligand binding are slowly being elucidated.

Within this investigation the molecular interactions involved in binding of ligands to the protein and in the interaction of the protein with phospholipid vesicles have been explored. The hypothesized portal region has been shown to be of major importance to both ligand binding and the interaction with anionic phospholipids.

Charge reversal mutagenesis studies have highlighted residues specific cationic lysine residues as being of significant importance in ligand binding. K31, positioned within α-helix II, was the only cationic residue within the α-helical region that when mutated to E31 lowered the protein's affinity for each of a broad range of ligands investigated in this work. The K33E mutation had a lesser effect on the affinity for some of the ligands studied, whilst the K20E mutation reported no significant effect on the binding of any of the ligands. The K31E mutation also had a detrimental effect on the interaction of the protein with anionic phospholipid vesicles, whilst the K20E and K33E mutations reported no differences in binding to these vesicles.

Three further cationic residues, which along with K31 contribute to the surface charge of the protein have also been studied, namely K36, K47 and K57. Using charge reversal mutagenesis once again, K57 and to a lesser extent K36 have been shown to play

a role in ligand binding to LFABP. The mutant proteins K36E and K57E both reported reduced K_i values for ligand binding compared to the wild type LFABP, whilst the K47E mutation appeared to have minimal effect.

The significance of the results of the two sets of charge reversal mutagenesis investigations becomes clear when the three residues K31, K36 and K57 are viewed on the structure of LFABP (**Fig 7.1**).

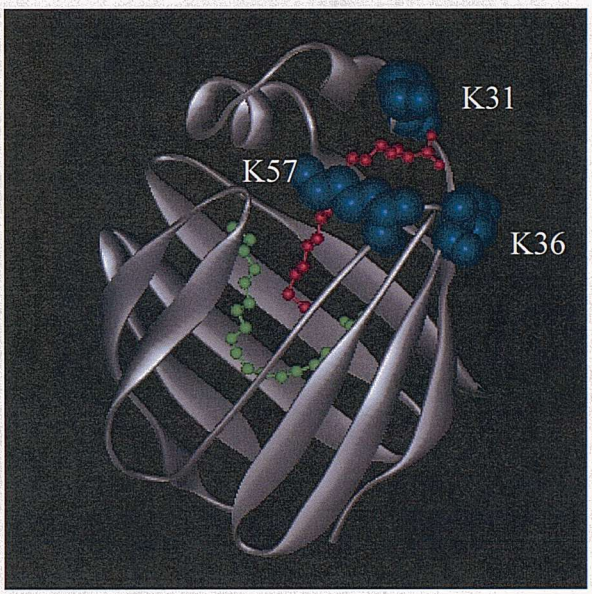

Fig 7.1 3-D ribbon diagram of LFABP highlighting the three lysine residues (shown in blue CPK representation) that are determined as having a significant effect on binding of the protein to phospholipid vesicles and the greatest effect overall on ligand binding. The positions of the two oleic acid molecules found in the crystal structure are also included in scaled ball-and-stick representation. The first oleic acid to bind (at site 1) is shown in green and the second (at site 2) is shown in red

K31, K36 and K57 are positioned within the portal region of LFABP. This is the region of the protein through which ligands are believed to enter the binding cavity. It is also the region through which numerous bulky ligands are believed to protrude. These

results strongly also implicate this region in the initial interaction between phospholipids and the protein.

The triple charge reversal mutant K31E,K36E,K57E, produced the predicted cumulative effect of the single mutations with regard to ligand binding. All of the ligands investigated reported a greater reduction in the proteins affinity for them, than the single charge reversal mutants. The lower affinity of the triple charge reversal mutant was equivalent to the combined effect of each of the single charge reversal mutations.

The charge reversal mutation also allowed for investigation of the orientation of lithocholic acid derivatives. It was apparent with the single charge reversal mutants that taurolithocholic acid was affected to a greater extent by charge reversal mutagenesis than lithocholic acid. This was consistent with either the taurine group or the 3-sulphate group of taurolithocholic acid 3-sulphate being positioned at the portal region. Using the triple charge reversal mutant and a selection of lithocholic acid derivatives, it was possible to determine that the presence of a 3-sulphate group on a derivative of lithocholic acid enhanced the effect of charge reversal mutagenesis in the portal region. This result is consistent with the 3-sulphate group of taurolithocholic acid 3-sulphate being positioned in the portal region of LFABP.

The triple charge reversal mutation did not have the expected effect on the binding of anionic phospholipids to the protein. The triple charge reversal mutant had a lesser effect on the interaction between the protein and the anionic vesicles than any of

the single mutations. A similar anomalous result was reported with a multiple charge reversal mutant of bee venom $sPLA_2$ binding to anionic vesicles [67] as discussed in **section 5.10**. It was suggested that some of the glutamate residues of the bee venom enzyme remain unionized due to the lower pH experienced at the surface of the anionic vesicles. An uncharged glutamate may promote non-polar interactions between the protein and the vesicle. Another possible explanation is that the combined charge reversal mutagenesis lowers the stability of the protein resulting in the ligand being more easily released from the protein. The stability of the triple charge reversal mutant compared to the wild type protein remains undetermined and should be measured as a next step in determining the cause of this unexpected result. It would also be of interest to produce double mutants of this protein using different pairings of K31E, K36E and K57E, to see whether these double mutants have a greater or lesser effect than the single mutations. A K31E,K57E double mutant is already available, produced as an intermediate step in preparing the triple mutant.

Binding of LFABP to anionic phospholipid vesicles at physiological ionic strength has been reported for the first time within this work. Previous studies had reported that such binding does not occur in the presence of such salt concentrations [68;82]. The interaction of LFABP with anionic phospholipid vesicles has now been recorded, but at a much slower rate than at low ionic strength. This result suggests that LFABP can undergo ligand transfer by a collisional mechanism under physiological conditions. This observation is worthy of further investigation. A more precise rate of binding of LFABP to anionic vesicles should be determined in the first instance. The

effect of ionic concentration on the rate of this interaction should also be investigated. Currently the binding of the protein to anionic phospholipids at higher salt concentration has only been determined with 100% anionic phospholipids and so the experiment should be repeated at 20 mol% DOPG to more accurately reflect the conditions *in vivo*.

The LFABP Y7W mutation allowed for an extension of previous work on the N-terminal region of LFABP [25]. FRET studies reported that Trp-7 comes in close contact with phospholipid vesicles, a finding that was supported by the loss of tryptophan fluorescence from Trp-7 as the protein bound to phospholipid vesicles. In contrast the presence of phospholipids failed to prevent fluorescence quenching by succinimide. The conclusion then is that Trp-7 is close to the phospholipid interface, but that its properties are not perturbed by interfacial binding to the same extent as seen with Trp-3. Conformational changes in this region could open up a ligand exit portal. Phe-3 is one of several amino acid residues that has amino acid side chains occluding an opening at the base of LFABP (**Fig 6.7.2**). A conformational change in this region, such as that observed with the LFABP F3W mutant [25] may allow for a portal region through which ligand can exit (**Fig 7.2**)

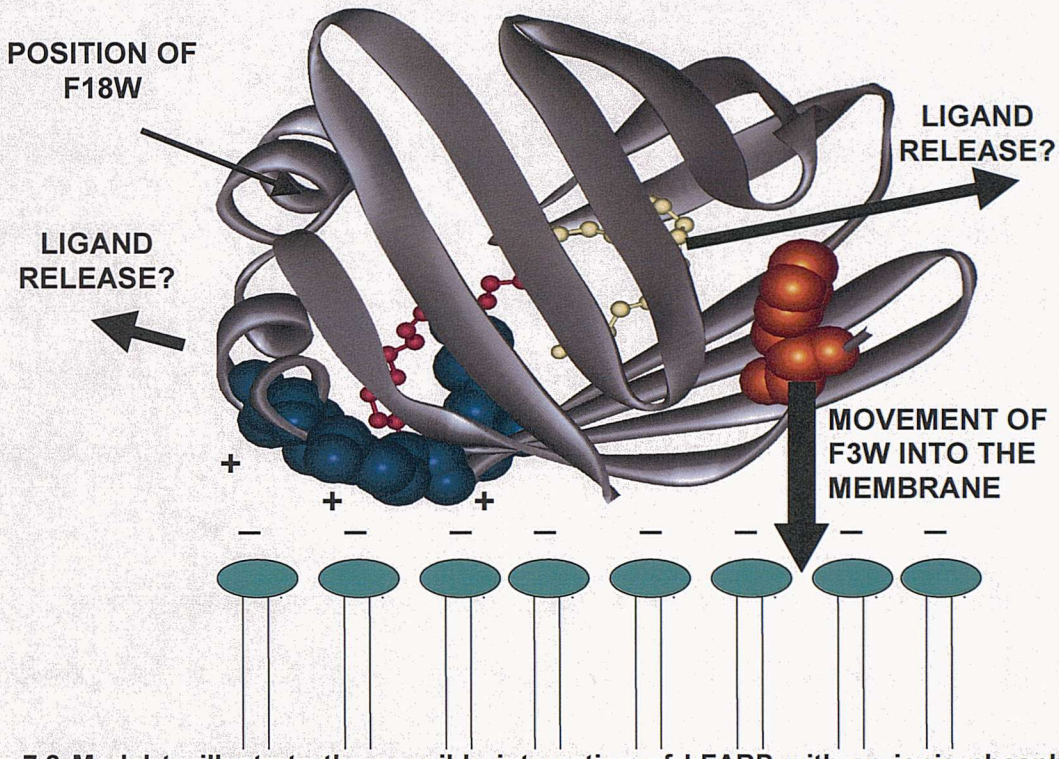

Fig 7.2 Model to illustrate the possible interaction of LFABP with an ionic phospholipid interface

The initial interaction of the cationic residues Lys-31, Lys-36 and Lys-57 (shown in CPK representation) results in protein unfolding and the N-terminal moves into the phospholipid interface. The conformational change disrupts the ligand binding cavity of LFABP resulting in release of ligand. The precise route of ligand release is not known, however, in addition to the normal ligand portal, movement of the N-terminal may expose a second portal for ligand exit in this region. The position of F3W is shown in CPK representation. The two oleic acid molecules in this crystal structure [11] are shown in ball-and-stick representation.

The large increase in tryptophan fluorescence upon ligand binding to the L28W mutant of LFABP makes this mutant a very useful tool for studying ligand binding to the protein.

The L28W mutant was able to report co-operativity between the two oleic acid binding sites when binding fatty acids, as demonstrated by the sigmoidal binding curve (**Fig 6.5.2.2**). These results suggest that the first fatty acid to bind can exchange between the two sites and that binding to the second fatty acid binding site is accompanied by a large increase in tryptophan fluorescence of LFABP L28W.

The fluorescence changes upon ligand binding to the LFABP L28W mutant makes it possible to study ligand binding in the absence of a reporter molecule. This in turn provides an opportunity for studying the competition between ligands for the protein. This has already been made use of to investigate the competition between oleoyl CoA and oleic acid. The relative affinities of these ligands for LFABP is controversial. This study showed that oleic acid and oleoyl CoA have similar affinities for LFABP, contradicting the K_i values calculated using the fluorescent probe DAUDA in chapters 3 and 4 (a contradiction that is discussed in **section 6.5.2.5**). Such a result is significant in terms of assigning the role of LFABP in the cell. If the two ligands bind with similar affinity then they will compete within the cell for the protein. Therefore modulation of fatty acid metabolism by mechanisms involving LFABP will be affected by both fatty acid and fatty acyl CoA concentrations within the cell.

It is unfortunate that ligands for LFABP, when free in solution, partition into phospholipid vesicles. This makes it difficult to show ligand release from the protein occurs in the presence of anionic phospholipid vesicles using the L28W mutant. It is hard to distinguish between ligand being released from LFABP as a result of a conformational change and ligand release to compensate for the shift in equilibrium as a result of partitioning of free ligands into phospholipids. However, two controls do exist for confirming ligand release is due to the interaction between the protein and anionic phospholipid vesicles. Firstly, a comparison could be made between the loss of fluorescence from holo-LFABP L28W upon addition of DOPG vesicles and upon addition of DOPC vesicles. The partitioning effect will be greater with DOPC, but only the anionic DOPG vesicles will interact with LFABP and cause a conformational change in the protein. Hence if tryptophan fluorescence loss is greater with DOPG, this can be attributed to the anionic phospholipid causing a conformational change in the protein. A similar control would be to titrate in DOPG vesicles in the presence of a high salt concentration and take an immediate fluorescence reading. In the presence of a high salt concentration LFABP will not bind immediately to anionic phospholipid vesicles. Hence, differences between tryptophan fluorescence changes in low and high ionic concentrations can be attributed to LFABP binding to anionic phospholipid vesicles, resulting in a conformational change that causes ligand release from the protein.

In summary this investigation has highlighted the importance of cationic lysine residues in the portal region of the LFABP in ligand binding and in the interaction between anionic phospholipid vesicles and the protein. For the first time binding has been

recorded between LFABP and anionic phospholipid vesicles at physiological salt concentrations. Furthermore, direct competition assays between fatty acids and fatty acyl CoAs has shown these two groups to bind with similar affinity to the protein, indicating that they compete for LFABP within the cell.

Reference List

1. Ockner,R.K., J.A.Manning, R.B.Poppenhausen, and W.K.Ho. 1972. A binding protein for fatty acids in cytosol of intestinal mucosa, liver, myocardium, and other tissues. Science 177: 56-58.

2. Cordoba,O.L., E.I.Sanchez, and J.A.Santome. 1999. The main fatty acid-binding protein in the liver of the shark (Halaetunus bivius) belongs to the liver basic type - Isolation, amino acid sequence determination and characterization. Eur. J. Biochem. 265: 832-838.

3. Schievano,E., S.Mammi, and E.Peggion. 1999. Determination of the secondary structural elements of chicken liver fatty acid binding protein by two-dimensional homonuclear NMR. Biopolymers 50: 1-11.

4. Banaszak,L., N.Winter, Z.H.Xu, D.A.Bernlohr, S.Cowan, and T.A.Jones. 1994. Lipid-Binding Proteins - A Family Of Fatty-Acid And Retinoid Transport Proteins. Advances In Protein Chemistry, Vol 45 45: 89-151.

5. Coe,N.R. and D.A.Bernlohr. 1998. Physiological properties and functions of intracellular fatty acid-binding proteins. Biochimica Et Biophysica Acta-Lipids And Lipid Metabolism 1391: 287-306.

6. Murphy,E.J., R.D.Edmondson, D.H.Russell, S.Colles, and F.Schroeder. 1999. Isolation and characterization of two distinct forms of liver fatty acid binding protein from the rat. Biochim. Biophys. Acta-Mol. Cell Biol. Lipids 1436: 413-425.

7. Glatz,J.C. and G.J.VanderVusse. 1996. Cellular fatty acid-binding proteins: Their function and physiological significance. Prog. Lipid Res. 35: 243-282.

8. Thompson,J., J.Ory, A.ReeseWagoner, and L.Banaszak. 1999. The liver fatty acid binding protein - comparison of cavity properties of intracellular lipid binding proteins. Molecular And Cellular Biochemistry 192: 9-16.

9. Thompson,J., A.Reese-Wagoner, and L.Banaszak. 1999. Liver fatty acid binding protein: species variation and the accommodation of different ligands. Biochim. Biophys. Acta-Mol. Cell Biol. Lipids 1441: 117-130.

10. Thumser,A.A. and D.C.Wilton. 1994. Characterization Of Binding And Structural-Properties Of Rat-Liver Fatty-Acid-Binding Protein Using Tryptophan Mutants. Biochem. J. 300: 827-833.

11. Thompson,J., N.WINTER, D.Terwey, J.Bratt, and L.Banaszak. 1997. The crystal structure of the liver fatty acid-binding protein - A complex with two bound oleates. J. Biol. Chem. 272: 7140-7150.

12. Thumser,A.A., C.Evans, A.F.Worrall, and D.C.Wilton. 1994. Effect On Ligand-Binding Of Arginine Mutations In Recombinant Rat- Liver Fatty-Acid-Binding Protein. Biochem. J. 297: 103-107.

13. Rolf,B., E.OudenampsenKruger, T.Borchers, N.J.Faergeman, J.Knudsen, A.Lezius, and F.Spener. 1995. Analysis of the ligand binding properties of recombinant bovine liver-type fatty acid binding protein. Biochimica Et Biophysica Acta-Lipids And Lipid Metabolism 1259: 245-253.

14. Thumser,A.A., J.E.Voysey, and D.C.Wilton. 1994. The Binding Of Lysophospholipids To Rat-Liver Fatty-Acid-Binding Protein And Albumin. Biochem. J. 301: 801-806.

15. Cistola,D.P., M.T.Walsh, R.P.Corey, J.A.Hamilton, and P.Brecher. 1988. Interactions Of Oleic-Acid With Liver Fatty-Acid Binding- Protein - A C-13 NMR-Study. Biochemistry 27: 711-717.

16. Richieri,G.V., R.T.Ogata, and A.M.Kleinfeld. 1996. Thermodynamic and kinetic properties of fatty acid interactions with rat liver fatty acid-binding protein. J. Biol. Chem. 271: 31068-31074.

17. Cistola,D.P., J.C.Sacchettini, L.J.Banaszak, M.T.Walsh, and J.I.Gordon. 1989. Fatty-Acid Interactions With Rat Intestinal And Liver Fatty Acid-Binding Proteins Expressed In Escherichia-Coli - A Comparative C-13 NMR-Study. J. Biol. Chem. 264: 2700-2710.

18. Wang,H., Y.He, C.D.Kroenke, S.Kodukula, J.Storch, A.G.Palmer, and R.E.Stark. 2002. Titration and exchange studies of liver fatty acid-binding protein with C-13-labeled long-chain fatty acids. Biochemistry 41: 5453-5461.

19. Miller,K.R. and D.P.Cistola. 1993. Titration Calorimetry As A Binding Assay For Lipid-Binding Proteins. Molecular And Cellular Biochemistry 123: 29-37.

20. Guinto,E.R. and E.Di Cera. 1996. Large heat capacity change in a protein-monovalent cation interaction. Biochemistry 35: 8800-8804.

21. Sacchettini,J.C. and J.I.Gordon. 1993. Rat Intestinal Fatty-Acid-Binding Protein - A Model System For Analyzing The Forces That Can Bind Fatty-Acids To Proteins. J. Biol. Chem. 268: 18399-18402.

22. Kaikaus,R.M., Z.H.Sui, N.Lysenko, N.Y.Wu, P.O.Demontellano, R.K.Ockner, and N.M.Bass. 1993. Regulation Of Pathways Of Extramitochondrial Fatty-Acid Oxidation And Liver Fatty-Acid-Binding Protein By Long-Chain Monocarboxylic Fatty-Acids In Hepatocytes - Effect Of Inhibition Of Carnitine Palmitoyl Transferase-I. J. Biol. Chem. 268: 26866-26871.

23. Storch,J. and A.A.Thumser. 2000. The fatty acid transport function of fatty acid-binding proteins. Biochim. Biophys. Acta-Mol. Cell Biol. Lipids 1486: 28-44.

24. Thumser,A.A. and J.Storch. 2000. Liver and intestinal fatty acid-binding proteins obtain fatty acids from phospholipid membranes by different mechanisms. J. Lipid Res. 41: 647-656.

25. Davies,J.K., A.A.Thumser, and D.C.Wilton. 1999. Binding of recombinant rat liver fatty acid-binding protein to small anionic phospholipid vesicles results in ligand release: A model for interfacial binding and fatty acid targeting. Biochemistry 38: 16932-16940.

26. Nolan,V., M.Perduca, H.L.Monaco, B.Maggio, and G.G.Montich. 2003. Interactions of chicken liver basic fatty acid-binding protein with lipid membranes. Biochimica Et Biophysica Acta-Biomembranes 1611: 98-106.

27. Huang,H., O.Starodub, A.McIntosh, A.B.Kier, and F.Schroeder. 2002. Liver fatty acid-binding protein targets fatty acids to the nucleus - Real time confocal and multiphoton fluorescence imaging in living cells. J. Biol. Chem. 277: 29139-29151.

28. Huang,H., O.Starodub, A.McIntosh, B.Atshaves, G.Woldegiorgis, A.B.Kier, and F.Schroeder. 2004. Liver Fatty Acid-Binding Protein Colocalizes with Peroxisome Proliferator Activated Receptor and Enhances Ligand Distribution to Nuclei of Living Cells. Biochemistry 43: 2484-2500.

29. Cistola,D.P., K.Kim, H.Rogl, and C.Frieden. 1996. Fatty acid interactions with a helix-less variant of intestinal fatty acid-binding protein. Biochemistry 35: 7559-7565.

30. Corsico,B., H.L.Liou, and J.Storch. 2004. The α-Helical Domain of Liver Fatty Acid Binding Protein Is Responsible for the Diffusion-Mediated Transfer of Fatty Acids to Phospholipid Membranes. Biochemistry 43: 3600-3607.

31. Nemecz,G. and F.Schroeder. 1991. Selective Binding Of Cholesterol By Recombinant Fatty-Acid Binding-Proteins. J. Biol. Chem. 266: 17180-17186.

32. McCormack,M. and P.Brecher. 1987. Effect of liver fatty acid binding protein on fatty acid movement between liposomes and rat liver microsomes. Biochem. J. 244: 717-723.

33. Noy,N. and D.Zakim. 1985. Fatty Acids Bound to Unilamellar Lipid Vesicles as Substrates for Microsomal Acyl-CoA Ligase. Biochemistry 24: 3521-3525.

34. Glatz,J.C. and J.H.Veerkamp. 1985. Intracellular Fatty Acid-Binding Proteins. International Journal Of Biochemistry 17: 13-22.

35. Martin,G.G., H.Huang, B.P.Atshaves, B.Binas, and F.Schroeder. 2003. Ablation of the liver fatty acid binding protein gene decreases fatty acyl CoA binding capacity and alters fatty acyl CoA pool distribution in mouse liver. Biochemistry 42: 11520-11532.

36. Wolfrum,C., C.M.Borrmann, T.Borchers, and F.Spener. 2001. Fatty acids and hypolipidemic drugs regulate peroxisome proliferator-activated receptors alpha- and gamma-mediated gene expression via liver fatty acid binding protein: A signaling path to the nucleus. Proc. Nat. Acad. Sci. 98: 2323-2328.

37. Erol,E., L.S.Kumar, G.W.Cline, G.I.Shulman, D.P.Kelly, and B.Binas. 2004. Liver fatty acid binding protein is required for high rates of hepatic fatty acid oxidation but not for the action of PPARα in fasting mice. Faseb Journal 18: 347-349.

38. Wolfrum,C., C.Buhlmann, B.Rolf, T.Borchers, and F.Spener. 1999. Variation of liver-type fatty acid binding protein content in the human hepatoma cell line HepG2 by peroxisome proliferators and antisense RNA affects the rate of fatty acid uptake. Biochim. Biophys. Acta-Mol. Cell Biol. Lipids 1437: 194-201.

39. Zimmerman,A.W. and J.H.Veerkamp. 2001. Fatty-acid-binding proteins do not protect against induced cytotoxicity in a kidney cell model. Biochem. J. 360: 159-165.

40. Myers-Payne,S.C., R.N.Fontaine, A.Loeffler, L.Pu, A.M.Rao, A.B.Kier, W.G.Wood, and F.Schroeder. 1996. Effects of chronic ethanol consumption on sterol transfer proteins in mouse brain. J Neurochem 66: 313-320.

41. Engels,W., M.Van Bilsen, B.H.Wolffenbuttel, G.J.Van der Vusse, and J.F.C.Glatz. 1999. Cytochrome P450, peroxisome proliferation, and cytoplasmic fatty acid-binding protein content in liver, heart and kidney in the diabetic rat. Mol Cell Biochem 192: 53-61.

42. Vergani,L., M.Fanin, A.Martinuzzi, A.Galassi, A.Appi, R.Carrozzo, M.Rosa, and C.Angelini. 1990. Liver fatty acid-binding protein in two cases of human lipid storage. Mol Cell Biochem 98: 225-230.

43. Lawrie,L.C., D.R.Dundas, S.Curran, and Murray G.I. 2004. Liver fatty acid binding protein expression in colorectal neoplasia. Br. J. Cancer 90: 1955-1960.

44. Hashimoto, T., Kusakabe, T., Watanabe, K., Sugino, T., Fukuda, T., Nashimoto, A., Honma, K., Sato, Y., Kimura, H., Fujii, H., and Suzuki, T. Liver-type fatty acid-binding protein is highly expressed in intestinal metaplasia and in a subset of carcinomas of the stomach without association

with the fatty acid synthase status in the carcinoma. Pathobiology 71[3], 115-122. 2001.

45. Kunkel,T.A. 1985. Rapid And Efficient Site-Specific Mutagenesis Without Phenotypic Selection. Proc. Nat. Acad. Sci. 82: 488-492.

46. Kunkel,T.A., J.D.Roberts, and R.A.Zakour. 2004. Rapid and efficient site-specific mutagenesis without phenotypic selection. Meth. Enzym. 154: 367-382.

47. Nelson,M. and M.McClelland. 1992. Use of DNA methyl transferase/endonuclese enzyme combinations for megabase mapping of chromosomes. Meth. Enzym. 216: 279-303.

48. Stratagene. 2003. QuickChange Site-Directed Mutagenesis Kit. Stratagene Pamphlet 2: 1-27.

49. Worrall,A.F., C.Evans, and D.C.Wilton. 1991. Synthesis Of A Gene For Rat-Liver Fatty-Acid-Binding Protein And Its Expression In Escherichia-Coli. Biochem. J. 278: 365-368.

50. Laemmli,U.K. 1970. Cleavage of structural proteins during the assembly of the head of bacteriophage T4. Nature 227: 680-685.

51. Smith,P.K., R.I.Krohn, G.T.Hermanson, A.K.Mallia, F.H.Gartner, M.D.Provenzano, E.K.Fujimoto, N.M.Goeke, B.J.Olson, and D.C.Klenk. 1985. Measurement of protein using bicinchoninic acid. Anal. Biochem. 157: 169-180.

52. PerkinsS.J. 1986. Protein Volumes And Hydration Effects - The Calculations Of Partial Specific Volumes, Neutron-Scattering Matchpoints And 280-nm Absorption-Coefficients For Proteins And Glycoproteins From Amino-Acid-Sequences. Eur. J. Biochem. 157: 169-180.

53. Kane,C.D. and D.A.Bernlohr. 1996. A simple assay for intracellular lipid-binding proteins using displacement of 1-anilinonaphthalene 8-sulfonic acid. Analytical Biochemistry 233: 197-204.

54. Epps,D.E., T.J.Raub, and F.J.Kezdy. 1995. A General, Wide-Range Spectrofluorimetric Method For Measuring The Site-Specific Affinities Of Drugs Toward Human Serum- Albumin. Analytical Biochemistry 227: 342-350.

55. Higuchi,R., B.Krummel, and R.K.Saiki. 1988. A General-Method Of Invitro Preparation And Specific Mutagenesis Of DNA Fragments - Study Of Protein And DNA Interactions. Nucleic Acids Research 16: 7351-7367.

56. Stolz,A., H.Takikawa, M.Ookhtens, and N.Kaplowitz. 1989. The role of cytoplasmic proteins in hepatic bile acid transport. Annual Review of Physiology 51: 161-176.

57. Thumser,A.A. and D.C.Wilton. 1996. The binding of cholesterol and bile salts to recombinant rat liver fatty acid-binding protein. Biochem. J. 320: 729-733.

58. Jain,M.K. and O.G.Berg. 1989. The kinetics of interfacial catalysis by phospholipase-a2 and regulation of interfacial activation - hopping versus scooting. Biochim. Biophys. Acta 1002: 127-156.

59. Baier,L.J., C.Bogardus, and J.C.Sacchettini. 1996. A polymorphism in the human intestinal fatty acid binding protein alters fatty acid transport across Caco-2 cells. J. Biol. Chem. 271: 10892-10896.

60. Baier,L.J., J.C.Sacchettini, W.C.Knowler, J.Eads, G.Paolisso, P.A.Tataranni, H.Mochizuki, P.H.Bennett, C.Bogardus, and M.Prochazka. 1995. An Amino-Acid Substitution In The Human Intestinal Fatty-Acid- Binding Protein Is Associated With Increased Fatty-Acid- Binding, Increased Fat Oxidation, And Insulin-Resistance. J. Clin. Inves. 95: 1281-1287.

61. Chiu,K.C., L.M.Chuang, A.Chu, and C.Yoon. 2001. Fatty acid binding protein 2 and insulin resistance. European Journal Of Clinical Investigation 31: 521-527.

62. Mitchell,B.D., C.M.Kammerer, P.O'Connell, C.Harrison, M.Manire, P.Shipman, M.P.Moyer, M.P.Stern, and M.C.Frazier. 1995. Evidence for linkage of postchallenge insulin levels with intestinal fatty acid-binding protein (FABP2) in Mexican-Americans. Diabetes 44: 1046-1053.

63. Yamada,K., X.Yuan, S.Ishiyama, K.Koyama, F.Ichikawa, A.Koyanagi, W.Koyama, and K.Nonaka. 1997. Association between Ala54Thr substitution of the fatty acid-binding protein 2 gene with insulin resistance and intra-abdominal fat thickness in Japanes men. Diabetologica 40: 706-710.

64. Kim,C.-H., S.-K.Yun, D.-W.Byun, M.-H.Yoo, K.-U.Lee, and K.I.Suh. 2001. Codon 54 polymorphism of the fatty acid binding protein 2 gene is associated with increased fat oxidation and hyperinsulinemia, but not with intestinal fatty acid absorption in Korean men. Metabolism 50: 473-476.

65. Hodsdon,M.E. and D.P.Cistola. 1997. Ligand binding alters the backbone mobility of intestinal fatty acid-binding protein as monitored by N-15 NMR relaxation and H- 1 exchange. Biochemistry 36: 2278-2290.

66. Hodsdon,M.E. and D.P.Cistola. 1997. Discrete backbone disorder in the nuclear magnetic resonance structure of apo intestinal fatty acid-binding

protein: Implications for the mechanism of ligand entry. Biochemistry 36: 1450-1460.

67. Ghomashchi,F., Y.Lin, M.S.Hixon, B.Z.Yu, R.Annand, M.K.Jain, and M.H.Gelb. 1998. Interfacial recognition by bee venom phospholipase A(2): Insights into nonelectrostatic molecular determinants by charge reversal mutagenesis. Biochemistry 37: 6697-6710.

68. Hsu,K.T. and J.Storch. 1996. Fatty acid transfer from liver and intestinal fatty acid- binding proteins to membranes occurs by different mechanisms. J. Biol. Chem. 271: 13317-13323.

69. Kim,H.K. and J.Storch. 1992. Free Fatty-Acid Transfer From Rat-Liver Fatty Acid-Binding Protein To Phospholipid-Vesicles - Effect Of Ligand And Solution Properties. J. Biol. Chem. 267: 77-82.

70. Braman,J., C.Papworth, and A.Greener. 1996. Site-directed mutagenesis using double-stranded plasmid DNA templates. Methods Mol. Biol. 57: 31-44.

71. Takikawa,H. and N.Kaplowitz. 1986. Binding Of Bile-Acids, Oleic-Acid, And Organic-Anions By Rat And Human Hepatic Z-Protein. Archives Of Biochemistry And Biophysics 251: 385-392.

72. Dietrich,A., W.Dieminger, K.Fuchte, G.H.Stoll, E.Schlitz, W.Gerok, and G.Kurz. 1995. Functional-Significance Of Interactions Of H-FABP With Sulfated And Nonsulfated Taurine-Conjugated Bile-Salts In Rat-Liver. J. Lipid Res. 36: 1745-1755.

73. Wilton,D.C. 1989. Studies On Fatty-Acid-Binding Proteins - The Purification Of Rat- Liver Fatty-Acid-Binding Protein And The Role Of Cysteine-69 In Fatty-Acid Binding. Biochem. J. 261: 273-276.

74. Frolov,A., T.H.Cho, E.J.Murphy, and F.Schroeder. 1997. Isoforms of rat liver fatty acid binding protein differ in structure and affinity for fatty acids and fatty acyl CoAs. Biochemistry 36: 6545-6555.

75. Richieri,G.V., R.T.Ogata, and A.M.Kleinfeld. 1994. Equilibrium-Constants For The Binding Of Fatty-Acids With Fatty-Acid-Binding Proteins From Adipocyte, Intestine, Heart, And Liver Measured With The Fluorescent Probe ADIFAB. J. Biol. Chem. 269: 23918-23930.

76. Selvin,P.R. 1995. Fluorescence Resonance Energy-Transfer. Meth. Enzym. 246: 300-334.

77. Kennedy,M.W., J.C.Scott, S.Lo, J.Beauchamp, and D.P.McManus. 2000. Sj-FABPc fatty-acid-binding protein of the human blood fluke Schistosoma

japonicum: structural and functional characterization and unusual solvent exposure of a portal- proximal tryptophan residue. Biochem. J. 349: 377-384.

78. Eftink,M.R. and C.A.Ghiron. 1984. Indole Fluorescence Quenching Studies On Proteins And Model Systems - Use Of The Inefficient Quencher Succinimide. Biochemistry 23: 3891-3899.

79. Newberry,E.P., Y.Xie, S.Kennedy, X.L.Han, K.K.Buhman, J.Y.Luo, R.W.Gross, and N.O.Davidson. 2003. Decreased hepatic triglyceride accumulation and altered fatty acid uptake in mice with deletion of the liver fatty acid- binding protein gene. J. Biol. Chem. 278: 51664-51672.

80. Lakowicz,J.R. 1999. Principles of Fluorescence Spectroscopy, 2nd. Edition ed. Kluwer Academic/Plenum, New York.

81. Sacchettini,J.C., J.I.Gordon, and L.J.Banaszak. 1989. Refined Apoprotein Structure Of Rat Intestinal Fatty-Acid Binding-Protein Produced In Escherichia-Coli - (Protein- Structure X-Ray Crystallography Fatty Acid-Protein Interactions). Proc. Nat. Acad. Sci. 86: 7736-7740.

82. Herr,F.M., V.Matarese, D.A.Bernlohr, and J.Storch. 1995. Surface Lysine Residues Modulate The Collisional Transfer Of Fatty-Acid From Adipocyte Fatty-Acid-Binding Protein To Membranes. Biochemistry 34: 11840-11845.

83. Di Pietro,S.M. and Santome,J.A. 2000. Isolation, characterization and binding properties of two rat liver fatty acid-binding protein isoforms. Biochimica Et Biophysica Acta-Protein Structure And Molecular Enzymology 1478: 186-200

84. Liou,H.L., Kahn,P.C. and Storch,J. 2002. Role of the helical domain in fatty acid transfer from adipocyte and heart fatty acid-binding proteins to membranes - Analysis of chimeric proteins. J. Biol. Chem. 277: 1806-1815

85. Liou,H.L. and Storch,J. 2001. Role of surface lysine residues of adipocyte fatty acid-binding protein in fatty acid transfer to phospholipid vesicles. Biochemistry 40: 6475-6485